

Current and emerging trends in polymeric 3D printed microfluidic devices

*Original*

Current and emerging trends in polymeric 3D printed microfluidic devices / Gonzalez, G., Roppolo, I., Pirri, C.F., Chiappone, A.. - In: ADDITIVE MANUFACTURING. - ISSN 2214-8604. - ELETTRONICO. - 55:(2022), p. 102867. [10.1016/j.addma.2022.102867]

*Availability:*

This version is available at: 11583/2968086 since: 2022-06-16T15:49:20Z

*Publisher:*

Elsevier B.V.

*Published*

DOI:10.1016/j.addma.2022.102867

*Terms of use:*

This article is made available under terms and conditions as specified in the corresponding bibliographic description in the repository

*Publisher copyright*

Elsevier postprint/Author's Accepted Manuscript

© 2022. This manuscript version is made available under the CC-BY-NC-ND 4.0 license  
<http://creativecommons.org/licenses/by-nc-nd/4.0/>. The final authenticated version is available online at:  
<http://dx.doi.org/10.1016/j.addma.2022.102867>

(Article begins on next page)

# 1 Current and emerging trends in polymeric 3D printed microfluidic 2 devices

3 Gustavo Gonzalez <sup>a</sup>, Ignazio Roppolo <sup>a,b,c\*</sup>, Candido Fabrizio Pirri <sup>a,b,c</sup>, Annalisa Chiappone <sup>d</sup>

4 <sup>a</sup> Department of Applied Science and Technology, Politecnico di Torino, C.so Duca Degli Abruzzi 24, 10129, Turin, Italy

5 <sup>b</sup> Center for Sustainable Future Technology @Polito, Italian Institute of Technology, Via Livorno 60, 10144, Turin, Italy

6 <sup>c</sup> PolitoBIOMed Lab, Politecnico di Torino, C.so Castelfidardo 30/A, 10129, Turin, Italy

7 <sup>d</sup> Dipartimento di Scienze Chimiche e Geologiche, Università di Cagliari, Complesso Universitario di Monserrato, S.S.  
8 554 bivio Sestu, 09042 Monserrato, Italy

9

10

11 \* email: ignazio.roppolo@polito.it

12

## 13 Abstract

14 During the last two decades, 3D printing technology has emerged as a valid alternative for  
15 producing microfluidic devices. 3D printing introduces new strategies to obtain high precision  
16 microfluidic parts without complex tooling and equipment, making the production of microfluidic  
17 devices cheaper, faster, and easier than conventional fabrication methods such as soft lithography.  
18 Among the main 3D techniques used for this purpose, fused filament manufacturing (FFF), inkjet  
19 3D printing (i3Dp) and vat polymerization (VP) are of the greatest interest since they are well-  
20 established techniques in the field and are cost-affordable both in equipment and material.  
21 However, there are still some barriers in terms of technology and materials to overtake for  
22 definitively establishing 3D printing as a truly microfluidic production method. For example, the  
23 level of resolution and precision of 3D printed microfluidic parts still does not reach the level of  
24 conventional fabrication techniques, and, from a materialistic point of view, few materials present  
25 the desired characteristics (e.g., biocompatibility, optical transparency, and mechanical properties)  
26 for target areas such as medicine, analytical chemistry, and pharmaceuticals. This review intends  
27 to evaluate and analyze the current state of polymeric 3D printing techniques and materials to  
28 manufacture microfluidic chips. The article will show and discuss the latest innovations, materials,  
29 and applications of such 3D printed microstructures. The focus of this review is to provide an  
30 overview of recent and future developments in 3D printing and materials in the branch of  
31 microfluidics fabrications, showing that the selection of the right materials together with the design  
32 freedom afforded by 3D printing will be the cornerstone for microfluidic development.

33

34 **Keywords: 3D printing; polymer; microfluidic; additive manufacturing; lab on a chip**

35

36

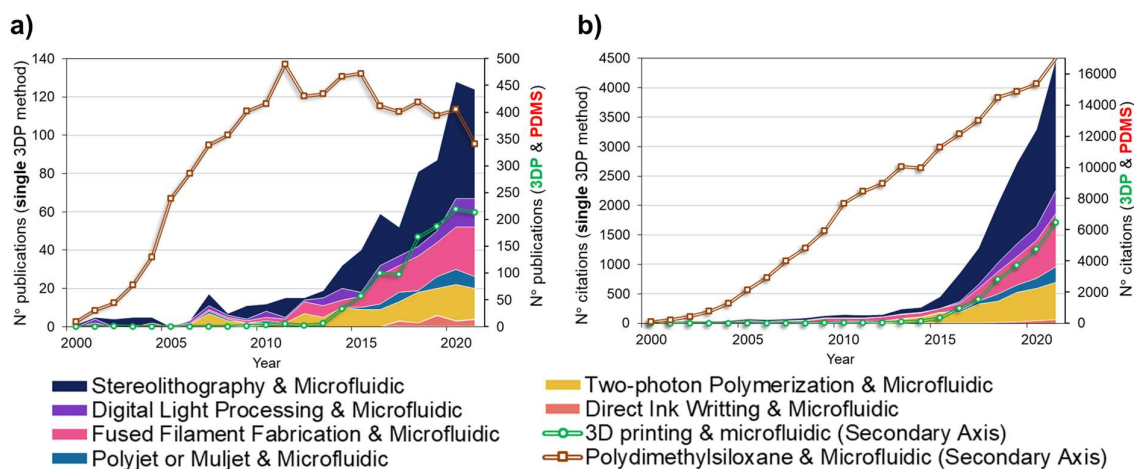
## 37 1. Introduction

38 Over the last decades, microfluidic devices have been used for different applications, especially  
39 in chemistry and biology, introducing new analytical and laboratory procedures [1–3]. For  
40 instance, these microdevices have been applied to study cancer cells' growth and metastasis, for  
41 analyzing the interaction of such carcinogenic entities with other cells, or test and screen new types  
42 of drugs [4–7]. The interest in microfluidics lies mainly in the possibility of performing laboratory  
43 analyses on a micrometer scale, allowing savings in sample consumption, and reducing the overall  
44 costs compared to conventional laboratory procedures [8–10]. The application of these devices  
45 owed a series of benefits: high spatial resolution and sensitivity, low volume consumption, fast  
46 processing, and easiness of integration with electronic elements. Microfluidic chips are assembled  
47 with a series of sub-millimeter channels, specifically designed to achieve the desired features, e.g.,  
48 mixing, pumping, or sorting the liquid passing through them [3,11–13]. By connecting such  
49 microfluidics with a few electronic elements, the devices (known as lab-on-a-chip) might be used  
50 in different biochemical applications for controlling/monitoring the behavior of specific analytical  
51 solutions, useful for rapid DNA sequencing, electrophoretic separation, wearable sensors, organ-  
52 on-chip development and disease diagnosis in point-of-care settings with a high level of precision  
53 [14–17]. The rapid deployment of microfluidic devices in laboratories and industries was marked  
54 by the introduction of polymeric materials, such as poly(methyl methacrylate) (PMMA),  
55 polycarbonate, polystyrene, polyethylene terephthalate (PET), and especially  
56 polydimethylsiloxane (PDMS). Today, PDMS elastomer is frequently used for fabricating  
57 microfluidic chips since it is an inexpensive, biocompatible, transparent, and deformable material,  
58 very suitable for molding production. For these reasons PDMS can be considered the standard  
59 material to produce microfluidic chips [18–21]. Nevertheless, PDMS presents some drawbacks,  
60 such as the non-specific adsorption of biological and chemical analytes as well as high  
61 hydrophobicity, which can be addressed with specific surface modification methods, e.g., plasma  
62 treatment, physical or chemical deposition or microwave radiation [22–30]. PDMS-based  
63 microfluidic chips are often fabricated through Soft Lithography and mold replica, a fabrication  
64 technique that involves multiple, manual, and labor-intensive steps for fabricating microfluidic  
65 devices. [31]. Other methods are micromachining, (hot)-embossing, injection molding, and laser  
66 ablation, among the principals [32–34]. Most of these methods to work properly require controlled  
67 environments or cleanroom facilities, which might not be compatible with mass production. Hence,  
68 microfluidic devices' potential growth is somehow limited to research laboratories due to the  
69 tedious and expensive fabrications methods, limiting their diffusion [35]. Therefore, more and  
70 more efforts are currently devoted to produce microfluidic devices with the right materials  
71 properties and features, by employing easier and cheaper fabrication methods, with the final goal  
72 of establishing and expanding their use and applications.

73 3D printing (3DP) technologies emerged as valid methods to produce fluidic devices with  
74 satisfactory results, supported by recent technological advancements in the field. 3D printing can  
75 overcome microfluidics limitations associated with mass production by enabling lower-cost and  
76 simplest fabrication of such devices in fewer steps [36–43]. 3DP, in fact, enables the on-demand  
77 production of parts from different materials that can be used in numerous industrial and research  
78 applications [44–47]. The principle behind this technology is the fabrication of three-dimensional  
79 objects from a digital model design through a single machine. The digital model (commonly in  
80 Computer-Aided Design or CAD format) is cross-sectioned by dedicated computer software. The  
81 objects are then fabricated by the selective and successive addition of material until the part is

82 completed. With 3DP, complex-shaped structures can be easily obtained, requiring minutes (or a  
83 few hours) without using tools, molds or complicated equipment, leading to savings in materials  
84 utilization and consumption, overall production costs, and energy, among others benefits [48–50].  
85 Today, many different 3D printing technologies have been developed. They can be classified based  
86 on the type of material used, how materials are joined, and the working principle; each brings  
87 unique characteristics [51]. The different 3DP techniques have been extensively evaluated in  
88 multiple literature reviews, based on the type of printable material used, application areas,  
89 benefits, and drawbacks [44,51–57].

90 Among the different materials employed, polymeric 3DP offers multiple advantages for the  
91 medical and biomedical fields, e.g., automation, personalization, keeping relatively fast printing  
92 times, cost-affordable materials and equipment, accessibility, and high printing resolutions [58–  
93 65]. These features make polymeric 3DP a promising method for numerous biomedical  
94 applications, e.g., prototyping organ models, producing *in-vitro* platforms for cell culturing, scaffold  
95 structures for tissue engineering, on-demand fabrication of medical implants and prostheses, and  
96 multiple medical situations where it is required a fast production of customized parts [58,60,65–  
97 71]. Indeed, during the recent pandemic crisis, polymeric 3D printing demonstrated that it could  
98 be used in hospitals for the fast production of plastic valves and connectors for addressing the  
99 shortage of respiratory tools during the coronavirus disease (COVID-19) caused by the novel  
100 coronavirus (Sars-CoV-2) [72–75]. For microfluidic fabrications, not all 3D printing techniques are  
101 appropriate. Microfluidic devices should gather some essential criteria for their correct operation,  
102 such as flexibility, biocompatibility, precise design and geometry, and optical transparency, which  
103 only a few polymeric 3D printing techniques can meet. Different studies have reported the 3D  
104 printing of polymeric microfluidic devices for various *in-vitro* studies, such as bioreactors for real-  
105 time biological analysis or analytical systems [39–43]. Most of these studies are mainly focused on  
106 using methods such as (see Fig. 1) fused filament fabrication (FFF), inkjet-based 3DP, e.g., PolyJet  
107 and MultiJet, and vat polymerization methods, e.g., stereolithography (SL) and digital light  
108 processing (DLP). Several review papers have been published in the last years describing the  
109 advancements done in the development of polymeric 3D printed microfluidic chips: most of these  
110 papers analyse the literature referred to the advancements in the healthcare/biomedical field [76–  
111 78], but also different applications were reviewed[79–82]. The approach used in the most of the  
112 this literature show a technological or application-driven point of view, focusing on the different  
113 3D printing technologies [77,83–85]. Differently, this review intends to present the updated state-  
114 of-the-art, focusing particularly on the material development, 3D printed part features such as  
115 optical transparency, printing resolution and biocompatibility, and the technological 3D printing  
116 trends considering the afore-mentioned methods. This work aims to give tools for researchers  
117 involved in microfluidic to approach more consciously to 3DP and, at the same time, for the  
118 operators of 3DP to understand the requirements of microfluidic. The most relevant applications  
119 of 3D-printed microfluidic devices are examined, highlighting the main barriers to adopt this  
120 technology in microfluidics scenarios, such as personalized medicine systems and point-of-care  
121 devices.



122

123 Fig. 1. Statistics data of the (a) Publications and (b) citations per year (from 2001 to 2021) searching by  
 124 the keywords: "Stereolithography," "Digital Light Processing," "Fused Filament Fabrication," "PolyJet"  
 125 or "MultiJet," and "two-photon polymerization" together with "microfluidic." The terms "3D printing" &  
 126 "microfluidic" and "Polydimethylsiloxane" & "Microfluidic" were also considered as a point of  
 127 comparison. Data obtained from the Scopus database, accessed January 12th, 2022.

## 128 2. 3D printing of polymeric microfluidic devices

129 Numerous studies have reported the use of polymeric 3DP for microfluidic devices fabrication  
 130 (see Fig. 1), showing the vast number of publications and citations per year over the last two  
 131 decades using the keywords "microfluidic" and the name of a single 3D printing method [39–43,86–  
 132 88]. Fig. 1.b also considers the term 3D printing to include other not well-known terms in the area of  
 133 microfluidic fabrication. The acceptance of polymeric 3DP for microfluidic fabrication is evident.  
 134 The number of publications in 2021 has increased more than ten times compared to 2010 and  
 135 nearly four times compared to 2015. Such observation is also witnessed by the number of citations  
 136 per year, which increased with  $\times 20$  and  $\times 6$  in 2020 compared to 2010 and 2015, respectively.

137 Interestingly, while the diagram of 3D printing and Microfluidic (both N° publications and  
 138 citations per year) increases, the graph of Polydimethylsiloxane (PDMS), one of the most used  
 139 materials for microfluidic fabrication start to decrease from 2010 forward. This trend is probably  
 140 not only due to the appearance of 3D printing for microfluidic chip fabrication, as other  
 141 microfabrication technologies and materials have appeared in recent years; however, such a trend  
 142 shows that the scientific community has been searching for alternatives to conventional  
 143 microfabrication methods. Most of these published works about 3D printing and microfluidic are  
 144 focused on using mainly fused filament fabrication (FFF), Polyjet/MultiJet, and vat polymerization  
 145 techniques, i.e., stereolithography and digital light processing, since they are well-established  
 146 techniques that present a good compromise between printing resolution/accuracy, printing speed  
 147 and material availability [59,89–91]. Each of the 3D printing methods offers different  
 148 characteristics that can be beneficial according to the microfluidic system and its application, as  
 149 summarized in Table 1. The most requested characteristics of 3D printed polymeric microfluidics  
 150 are biocompatibility, optical transparency, and microchannels' reliability. The following section  
 151 will present an overview of current trends and strategies to fabricate microfluidic chips by  
 152 polymeric 3D printing.

153

154 **2.1. Fused Filament Fabrication methods for microfluidic devices fabrication**

155 Fused deposition modelling (FDM), also known as fused filament fabrication (FFF), is probably  
156 the most recognized 3D printing method [59,92,93]. As schematized in Fig. 2.a, in these 3D printing  
157 techniques, the material (filament) is extruded through a nozzle by thermal effect. Other extrusion-  
158 based 3D printing techniques (known as Direct Ink Writing –DIW) follow a similar extrusion-  
159 processing principle, although they use a screw, piston, or pneumatic force (pressurized air or gas)  
160 to deposit the material [52]. In general, extrusion-based 3D printing consists of a motorized system  
161 with a three-axis motion that allows material deposition selectively. The material is first deposited  
162 at the preferred position in the *XY* plane to achieve the first layer. Then a second layer is deposited  
163 onto the prior one by either the building platform moving down or the extrusion nozzle moving up;  
164 the process is repeated until the final part is obtained [94]. The fused deposition modeling (FDM)  
165 technique was invented by Scott Crump in 1989 [54,95], and after the patent expired in 2009,  
166 people started to fabricate FDM printers independently without compensating *Stratasys* (the  
167 company that branded the FDM technique), decreasing equipment and materials costs. However,  
168 *Stratasys* is still proprietary to the FDM acronym, so these methods are generally recognized as  
169 Fused Filament Fabrication (FFF) [96]. The success of FFF methods lies in their larger palette of  
170 available printable materials (see Table 1), their relatively lower cost and their more user-friendly  
171 systems and software. FFF works by heating thermoplastic filaments (linear macromolecules)  
172 through a heated nozzle above their softening point (glass transition/melting point according to  
173 the material). The softened material is deposited onto the build platform, following the computer  
174 specifications, and then cooled down [97].

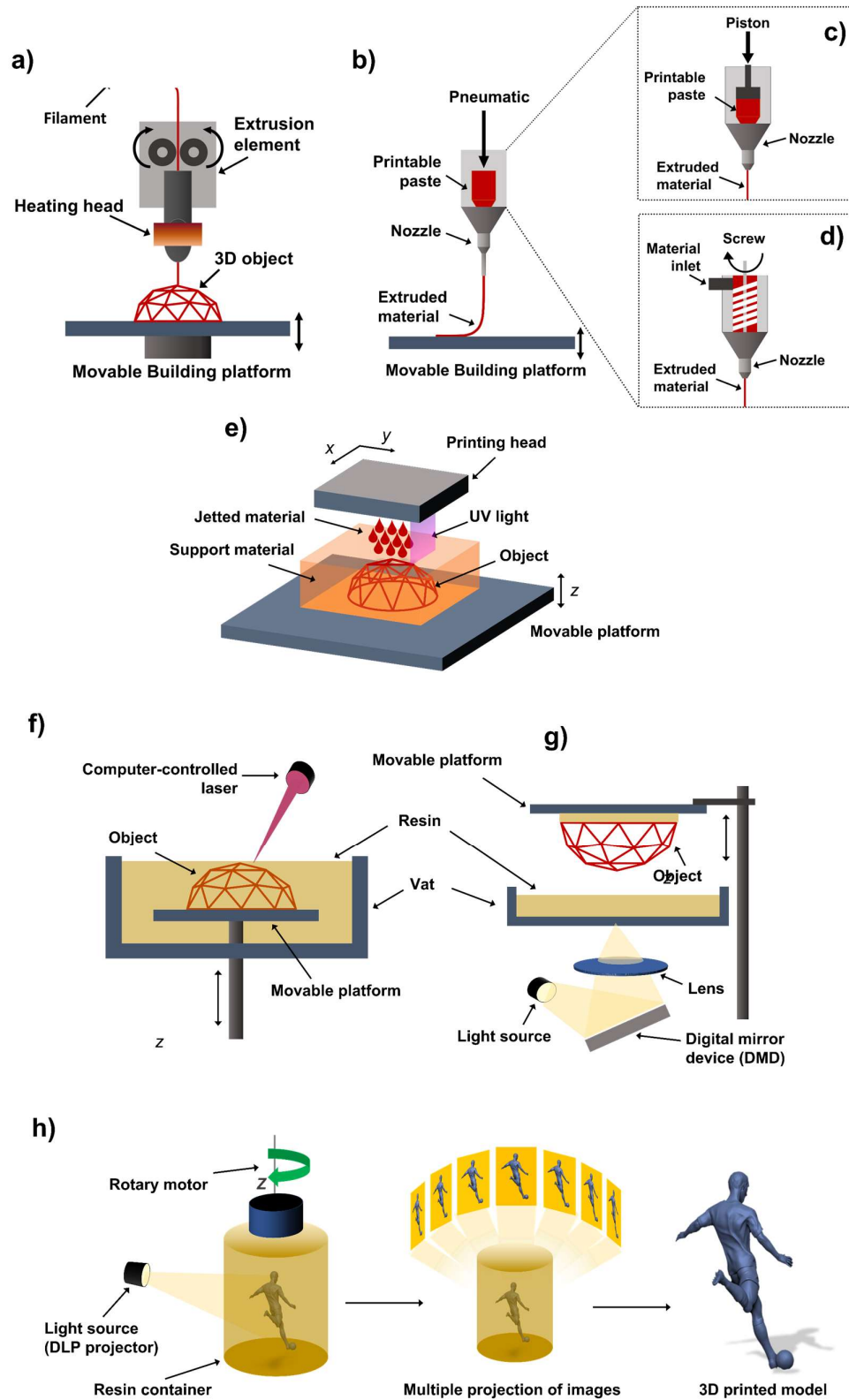
Table 1. Comparison of the Fused Filament Fabrication (FFF), Polyjet/Multijet and Vat-Polymerization (VP) 3D printing in terms of microfluidic chips fabrication. The table compares the different methods of energy required to join materials (energy source), materials used, minimal printing features, smallest channel achieved, building speed, multi-material ability and pros/cons [52,69,98].

3D printing technique	General characteristics				For microfluidic manufacturing			
	Printing principle	Material	Finest machine resolution	Advantages	Disadvantages	Smallest channel achieved	Benefits	Drawbacks
Fused Filament Fabrication (FFF)	A nozzle gun builds objects by layering softened/melted wires; the objects are then hardened by cooling down	Poly(lactic acid) (PLA), Acrylonitrile-butadiene-styrene (ABS), Polycaprolactone (PCL), Polymethylmethacrylate (PMMA), Polyurethane (PU), Polystyrene (PS), Polycarbonate (PC), Polyether ether ketone (PEEK), cyclic olefin copolymer (COC), polypropylene (PP), polyglycolic acid (PGA), polyethylene terephthalate (PET), Polyamide, polyurethane (TPU)	10-20 $\mu\text{m}$ [99,100]	Low cost; A vast range of processable thermoplastics; simplicity; open-source machines; inexpensive materials; functional objects from common plastics; high printing speed	Low level of precision; Nozzle clogging; anisotropy of the printed parts; only thermoplastics materials; weak mechanical properties; rough finish; weak interlayer bonding	40 $\mu\text{m}$ [101]	Cost-affordable material per printed chip. Some materials present good biocompatibility	Limited printing precision; resolution limited by nozzle diameter; Limited optical transparency; surface roughness might alter fluid flow
Polyjet/Multijet	Jetting of photopolymerizable inks and subsequent curing of the material	Photocurable resins/photopolymers. (meth)acrylate-based; liquid suspensions; elastomers and ceramic-based inks	25 $\mu\text{m}$ [102]	High accuracy, precision, and surface finishing Multi-material/color objects can be obtained	Materials are not so durable in time Sacrificial materials are difficult to recycle Post-processing might damage small features Low mechanical strength	54 $\mu\text{m}$ [103]	Fast printing times, multi-material objects.	Laborious material removal from the microchannels; No transparency parts; rough surface
Vat polymerization (VP)	Selective curing of liquid resins contained in a vat.	Photocurable resins/photopolymer. (meth)acrylate-based; epoxy; pristine acrylic resins; elastomers and ceramic-based formulations; composites and hybrid photopolymers	0.6-2 $\mu\text{m}$ [104,105]	High accuracy and resolution; using flexible resins; smooth surface finish; versatility on raw material preparation; processing complex nanocomposites	High costs; low printing times; Require support; post-processing to remove support; require post-curing; limited choice of materials; difficult to produce multi-material parts	18 $\mu\text{m}$ [43]	High printing resolution, fast printing chip times, good surface finishing; direct printing of fluidic channels	Post-treatment to remove unreacted material from channels and supports Cytotoxicity Limited materials

179 The resolution and performance of FFF methods depend on various parameters, such as  
180 temperature, the viscosity of the extruded filament, layer height, layer density, shear force, nozzle  
181 diameter printing velocity and type of material. Hence, it is essential to balance these printing  
182 parameters to reach reliable printing resolutions and accuracy and avoid defects during the 3D  
183 printing step. Today, FFF-based 3D printers can be found with a printing resolution of 10  $\mu\text{m}$ , a  
184 building size as large as 200 x 200 x 400  $\text{mm}^3$ , and a building speed as high as 500  $\text{mm/s}$  [99,106].  
185 The most common issue between FFF users is the inadequate adhesion between layers, leading to  
186 objects with poor mechanical properties. Such phenomenon occurs when some printing variables,  
187 such as the temperature of the processing, the temperature of the build platform (creating thermal  
188 shrinkage), and physicochemical properties of the material (e.g., heat transfer), are not well  
189 balanced [94]. Another common shortcoming of FFF methods is the lack of mechanical strength of  
190 the molten thermoplastic (it might not support itself during slow cooling) [52]. Indeed, some FFF  
191 machines use a secondary filament to support the object temporarily. This support material can be  
192 later removed by immersion in water or other types of solvents. Other drawbacks of FFF-based 3D  
193 printing are the vertical anisotropy, step structured surface (meaning low superficial resolution),  
194 layer adhesion between layers, porosities or air trapped between layers and nozzle clogging [97].

195 In FFF-3D printing methods, more than one nozzle can be used in the same printing process.  
196 Each nozzle can be loaded with different materials, enabling the manufacture of multi-material  
197 structures that display different properties and features in a single 3D printed object [107]. The  
198 printable filaments can also be loaded with fillers, fibers, dyes, and other additives (e.g., carbon  
199 black, glass fiber, carbon fiber and metallic powders), looking to impart specific characteristics.  
200 Various thermoplastic polymers with different features can be used in FFF-based 3D printing. The  
201 most common thermoplastics materials are polystyrene (PS), polycarbonate (PC), acrylonitrile-  
202 butadiene-styrene copolymers (ABS), polymethylmethacrylate (PMMA), polylactic acid (PLA),  
203 polyetheretherketone (PEEK), poly- $\epsilon$ -caprolactone (PCL), and Polyamide or Nylon; few of them  
204 with biocompatible properties [94,96,108–111]. Fig. 3 shows the chemical structure of commonly  
205 used thermoplastics for FFF-3D printing. An alternative method to FFF printing is Direct Ink  
206 Writing or DIW, in which a paste is printed (Fig. 2.b-d) [112,113]. This technique can use air  
207 pressure, a piston, or a screw to extrude the material onto the build platform. In this case, the  
208 solidification of the material can be achieved by thermal effect, photopolymerization, chemical  
209 crosslinking, rapid phase transition, and fast solvent evaporation rate, and instead of printable  
210 filaments, the DIW technique uses viscoelastic materials (or inks) with suitable rheological  
211 properties. The rheological properties of the printable ink should guarantee continuity of extrusion  
212 and be self-consistent to ensure the correct piece formation during the layer-by-layer step [114].  
213 Typical DIW inks are made of polymers mixed with suitable organic solvents or water to adjust the  
214 viscosity of the printable material. Besides, inks of high-molecular-weight oligomers or pastes with  
215 high inorganic material content can be used [115]. DIW can process various materials since many  
216 available polymers exhibit good rheological properties. In addition, DIW can be set with multiple  
217 dispensers and composite inks, allowing multi-material and functional structures fabrication. The  
218 most used materials for DIW are silicone elastomers, polyurethane, fluorinated polymers, cellulose  
219 and gelatin-based (see Fig. 3), hydrogels polymer-based colloids, nanocomposite (e.g., graphene  
220 oxide, carbon nanotubes, silver nanowires or MXenes) and even biological material (in this case,  
221 the printing techniques are better referred to as bioprinting) [116–122].

222

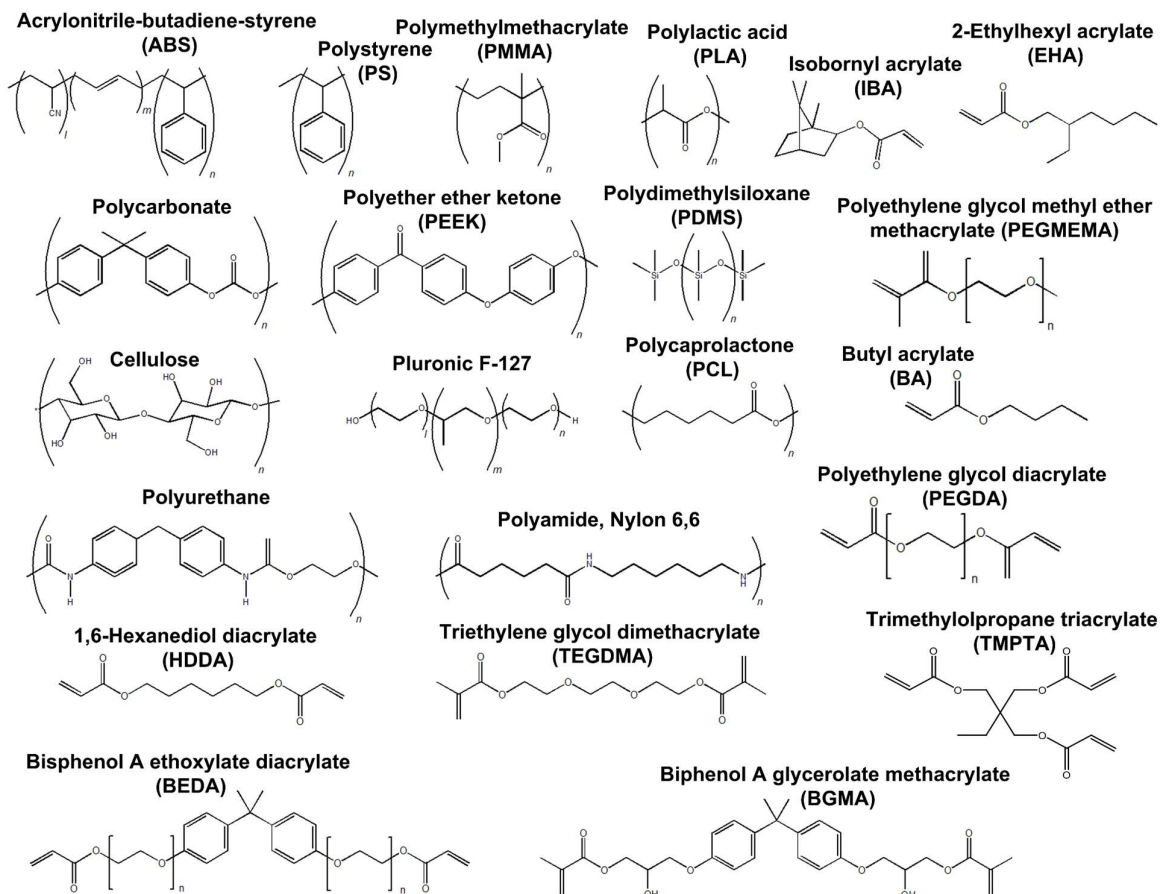


223

224 Fig. 2. Representation of (a) Fused filament fabrication (FFF), Direct ink writing based on (b) pneumatic  
 225 force, (c) a piston and (d) a screw to extrude the material, (e) Photopolymerization-based inkjet 3D  
 226 printing, (f) Stereolithography (SL), (g) Digital light processing (DLP) and (h) Computed axial  
 227 lithography (CAL) methods.

228 One of the main disadvantages of DIW is the low printing velocity and resolution. In optimized  
229 conditions, the DIW can reach a printing resolution in the order of micrometers, but on the other  
230 hand, the printing time increases [118]. The highest DIW printing speed reported to date is 100  
231 mm/s, far below the speed of other printing techniques for polymers [54]. FFF methods offer  
232 microfluidic chip fabrication benefits, such as cost-affordable materials and equipment, high  
233 printing speed, and standardized and user-friendly apparatus. Moreover, many commercially  
234 available and biocompatible filaments can be processed for microfluidic chip fabrications. The first  
235 approach involves the use of 3D printing of filaments to build the negative molds to fabricate  
236 microfluidics by casting of PDMS. In this context, it is worthy to mention the pioneering work of  
237 Saggiomo and Velders [123]. Although this method was widely explored by researchers, this is out  
238 of the scope of this review, which aims at reporting direct 3D printing of microfluidics. Through  
239 FFF methods, interesting fluidic devices have been created with satisfactory results in  
240 transparency, resolution, and biocompatibility. For example, Bressan et al. developed 3D-printed  
241 microfluidic chips based on polylactic acid (PLA) to synthesize silver and gold nanoparticles  
242 [124,125]. By optimizing the printing parameter, the chips were fabricated with channels as small  
243 as  $260\ \mu\text{m} \times 260\ \mu\text{m}$  employed to well-control the fluid flow behavior for obtaining particles with  
244 the desired features. These particles were then used for biological applications such as crystal  
245 violet (CV) through SERS analysis or to improve the electrocatalytic capability of carbon paste  
246 electrode (CPE) for the electrochemical determination of gallic acid (GA) and thiocyanate ions.  
247 During FFF printing processes, the wall surfaces of the printed parts can be rough due to the  
248 deposition of melted filaments. Therefore, channels with a well-established sidewall dimension are  
249 quite challenging to produce with such a 3D printing technique.

250



251

252  
253

Fig. 3. Chemical structure of some commercially available polymers (thermoplastics and thermosets) used for polymeric 3D printing.

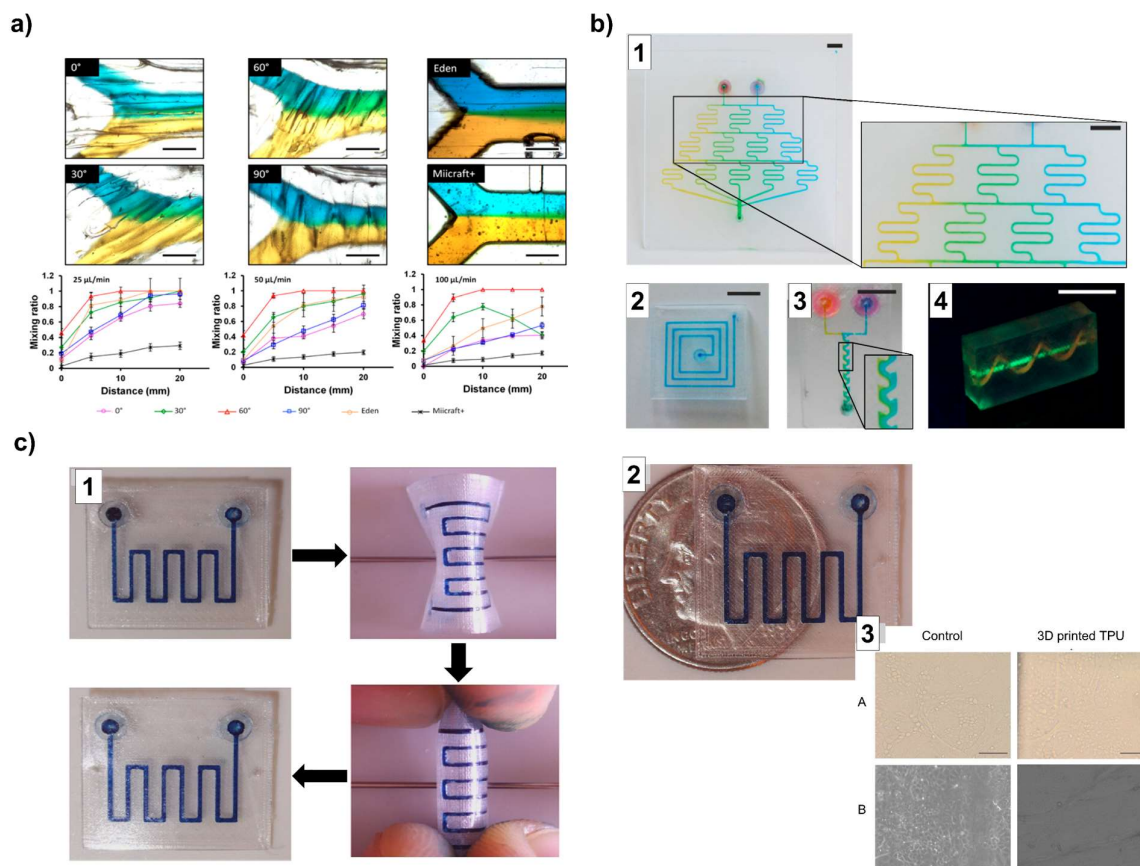
254  
255  
256  
257  
258  
259  
260  
261  
262  
263  
264  
265  
266  
267  
268  
269

During FFF printing processes, the filament deposition can influence the walls' features, producing uneven surfaces. Therefore, channels with a well-established sidewall dimension are quite challenging to produce with FFF printing technique. Though, such surface characteristics might be used as an advantage for fluid mixing, since the surface roughness can alter the fluid behavior during the flow [126]. For example, Li et al. demonstrated how the extruded filament orientation could enhance fluidic behavior control [127]. They developed various microfluidic chips (channels of 500  $\mu\text{m}$  x 500  $\mu\text{m}$ ) with different printing orientations of the filament (0°, 30°, 60°, and 90°) respecting the fluid flow direction to examine the fluid mixing performance (Fig. 4.a). These chips were produced with good optical transparency using a commercial filament, Crystal Clear acrylonitrile-butadiene-styrene (ABS) from 3D Systems. Li and coworkers showed that in microfluidic chips, where the extruded filament was oriented at 60° to the flow direction, the mixing of fluids in laminar flow was achieved without any complex channel geometry or other passive mixers. Moreover, the authors demonstrated that chips' mixing performance could be adjusted by changing the filament orientation at 0° and 90°. The researchers performed simple colorimetric assays to measure the content of iron in environmental water samples, where is desired a mixing property.

270  
271

The fabrication of truly microfluidic devices (<100  $\mu\text{m}$ ) is still challenging using FFF-3D printing. The typically requested microchannel dimensions are much smaller than most extruded filaments

272 and nozzles available today. Moreover, another shortcoming of FFF-3D printing is that only a few  
273 thermoplastic filaments might be used to produce optically transparent structures, which is one of  
274 the most requested characteristics of microfluidic devices for allowing the correct real-time  
275 visualization of the fluids. Some interesting strategies have been followed in this sense. For  
276 example, Kotz and coworkers produced transparent chips using commercially available  
277 polymethylmethacrylate (PMMA) filament, one of the most used materials for microfluidic chip  
278 fabrication [128]. With PMMA filaments (from *Material4print*), the authors created chips with a  
279 minimum channel width of about 300  $\mu\text{m}$  x 300  $\mu\text{m}$ . The chips' bottom transparency (the region of  
280 interest for proteins patterning) was significantly improved by directly printing onto PMMA sheets  
281 (not created by FFF 3d printing). These chips were used for mixing dyed water. The chip's surface  
282 was then selectively photopatterned with fluorescently labeled biotin (F5B), showing the easy  
283 biofunctionalization of 3D printed closed PMMA chips (Fig. 4.b). Similar work was presented by  
284 Bressan et al. by directly printing PLA filaments onto PMMA sheets, obtaining 3D printed  
285 microdevices with transparent bottoms [129]. The authors produced complex-shaped microfluidic  
286 devices with microchannels dimensions as narrow as 200  $\mu\text{m}$  x 200  $\mu\text{m}$  and with an optically  
287 transparent window in a single printing step that can be applied to perform a series of chemical  
288 measurements and visualize *Saccharomyces cerevisiae* microorganisms. Transparent microfluidic  
289 chips were also obtained from Nelson et al. using a commercial thermoplastic polyurethane  
290 filament (SainSmart Clear flexible TPU) [101]. They developed microfluidic chips with optical  
291 transparency (up to 85 % of transmission), chemical solvent stability, high-pressure resistance,  
292 and flexibility (see Fig. 4.c). The printed chips' biocompatibility was demonstrated by culturing  
293 mouse inner medullary collecting duct cells (mIMCD3). The researchers produced microfluidic  
294 chips with channel features as small as 50  $\mu\text{m}$  x 50  $\mu\text{m}$  (the smallest one by FFF to date) in less than  
295 25 minutes. Other researchers developed transparent and sealed microfluidic chips with PLA as an  
296 alternative to conventional polydimethylsiloxane material (PDMS), acting as an electronic tongue  
297 (e-tongue). These flexible and interdigitated microfluidic chips could distinguish tastes below the  
298 human threshold. The chips were built within less than one hour, using a homemade 3D printer  
299 [130]. In addition to PLA, other types of cost-affordable materials can also be used. As reported in  
300 2018 by Romanov and coworkers, 3D printed microfluidic chips with a channel dimension of about  
301 400  $\mu\text{m}$  were produced with either polylactic acid (PLA) or polyethylene terephthalate glycol  
302 (PETg) through two different types of commercially available low-cost FDM-3D printers: Prusa i3  
303 (\$ 600) and LulzBot (\$ 2500) [131]. Such devices presented high-pressure, heat resistance, and  
304 glass-like layer characteristics, features that were useful for DNA melting analysis and facilitated  
305 the optical visualization of fluids in droplet generation and tracking and identifying DNA. Direct ink  
306 writing (DIW) methods have also been used for fabrication microstructures or microfluidic devices.



307

308 Fig. 4. 3D printed microfluidic chips fabricated by Fused Filament Fabrication (FFF)-3D printing. (a)  
 309 Microscopic photographs of the laminar fluid flow inside  $500\mu\text{m}\times 500\mu\text{m}$  channel toward a  
 310  $750\mu\text{m}\times 500\mu\text{m}$  channel, where yellow/blue dyed water is passed through microfluidic channels  
 311 fabricated by FFF methods at  $0^\circ, 30^\circ, 60^\circ$ , and  $90^\circ$  of filament orientation. The results were compared  
 312 with chips produced using Eden (Polyjet) and Miicraft+ (DLP-SL) printers. Plots of distance vs. mixing  
 313 ratio demonstrated the diffusion through the laminar flow channel at 25, 50, and  $100\mu\text{L}/\text{min}$ . Reprinted  
 314 with permission from Ref. [127] (b) 3D printed chips in PMMA: 1) Microchip cascade for mixing  
 315 yellow/blue-dyed water, 2) chip with a square channel of  $600\mu\text{m}\times 600\mu\text{m}$ , 3) improved mixer  
 316 structure of  $600\mu\text{m}\times 600\mu\text{m}$  channel, and 4) 3D printed serpentine-like channel produced around a  
 317 straight channel, containing an aqueous fluorescent dye. Images with a scale bar of 10 mm. Ref. [128].  
 318 (c) Transparent 3D printed microfluidic chips made of polyurethane (TPU) images showing 1) the  
 319 flexibility, 2) the chip transparency, and 3) mIMCD3 cells behavior where a characteristic cobblestone  
 320 appearance was observed in both, control wells, and 3D printed TPU (scale bars =  $100\mu\text{m}$ ). Reprinted  
 321 with permission from Ref. [101].

322 Ching et al. introduced a method for fabricating microfluidic devices by directly depositing the  
 323 extruded filament material onto a flat substrate using a commercial desktop DIW-3D printer [132].  
 324 The material used was a commercial silicone elastomer (Silicone sealant, Wet Area Speedseal®)  
 325 patterned onto a sheet of polymethylmethacrylate (PMMA). Once the machine sketched the  
 326 microchannel features, a second PMMA was used to close the device; then, a laser created the inlets  
 327 and outlets elements. By intercalating multiple PMMA sheets between each printed silicone  
 328 microstructure, the authors produced 3D networks of microchannels. Through such DIW method,  
 329 the researchers could select the substrate (i.e., PMMA) with the required characteristics such as  
 330 optical transparency and biocompatibility. Additionally, Ching and coworkers were able to willfully  
 331 deform the microchannel to control the channel dimension (owing the elastomeric characteristics

332 of the material), reaching features as small as near 32  $\mu\text{m}$  (in width) and 20  $\mu\text{m}$  (in height). Through  
333 this approach, the authors pointed out three key beneficial points for the manufacturing of  
334 microfluidic chips: (1) the possibility of tuning channel dimensions, (2) the possibility of  
335 incorporating diverse types of substrates, according to the looked-for characteristic, and (3) the  
336 possibility of integrating fluid-handling and functional components such as valve and pumps in the  
337 same 3D printing process. However, the method proposed by Ching et al. requires certain manual  
338 labor to thread the PMMA sheets during 3D printing. On the other side, this method does not  
339 require removing supporting material from the microchannels, which could be a great advantage  
340 when handling fragile or delicate microfluidic systems. Athanasiadis et al. developed a DIW-based  
341 strategy to produce filaments with an internal microfluidic channel [133]. They used the 3D printer  
342 (3D discovery bioprinter, Regen HU) to first deposit a filament made of silicone elastomer  
343 (polydimethylsiloxane, SE1700 from Dow Corning) and then modify the just deposited filament  
344 with the same printing nozzle, used as a “pencil,” to remove part of the material. The authors set  
345 the correct printing parameters (i.e., pneumatic pressure, nozzle diameter, nozzle height, and  
346 extrusion speed) to perform the post-extrusion modification and create groove-shaped filaments.  
347 Programming the stylus nozzle position above the substrate, the groove depth increase making  
348 collapse the groove walls, closing it and producing the channel. The width of the groove depends  
349 on the external diameter of the printing nozzle, which in the case of the authors was 430  $\mu\text{m}$ . Even  
350 though such a strategy allowed the creation of fibers with microfluid channels), the channel  
351 dimension depended on the external diameter of the nozzle. Hu et al. described an easy way to  
352 produce PDMS-based microfluidic chips using a 3D printed sacrificial microstructure [134]. The  
353 researchers used a 3D-plotter (EnvisionTEC) to pattern the material on a PDMS substrate in a petri  
354 dish, creating fugitive or sacrificial microstructures for PDMS casting. The material was the water-  
355 soluble Pluronic F-127 ink that, once is plotted on the substrate surface, the microstructure was  
356 encapsulated with PDMS by casting. By this strategy, microdevices with channel widths varying  
357 from 300 to 570  $\mu\text{m}$  were obtained by setting the right printing parameters. The Pluronic F-127  
358 material contained inside the channels was removed, after the PDMS curing, by constantly flushing  
359 cold water and ethanol. Such a hybrid manufacturing approach allowed the authors to produce  
360 flexible, transparent, and low-cost microfluidic devices used to acetylate various amines through  
361 microwave irradiation, obtaining acetamides in shorter reaction times and good yields than  
362 conventional chemical methods. Looking for an easier integration of microfluidic devices in  
363 laboratory analysis and applications, some researchers have focused their work on creating  
364 polymeric micropumps through 3D printing [135]. Alvarez-Braña et al. created a set of polymeric  
365 micropumps using different materials, geometry, and 3D printing fabrication techniques. The  
366 authors presented the production of different self-powered modular micropumps using FFF (and  
367 other techniques such as SLA, DLP) printing techniques, studying their performance when  
368 integrated into a portable and low-cost microfluidic cartridge. In the works, the authors showed  
369 the great benefits of 3D printing in developing modular micropumps (with cylindrical cavities of  
370 800  $\mu\text{m}$  in diameter and 4 mm in depth), especially when these microparts are designed with a  
371 geometry that cannot be produced by conventional techniques. The micropumps were designed  
372 and fabricated to create autonomous flow microsystems when these are assembled with common  
373 microfluidic devices. The researchers also demonstrated that the 3D printed micropumps were  
374 responsible for the movement of the liquid through the microchannels by generating a negative  
375 pressure in the channel. Such pressure from the micropumps can be tuned according to suction  
376 properties and air absorption surfaces of the microfluidic material. The authors demonstrated the  
377 potentiality of their 3D printed micropumps by assembling them into a polymeric microfluidic  
378 cartridge to carry out a self-powered microfluidic device for colorimetric starch detection,

379 introducing innovative elements for the development of integrated microsystems for applications  
380 such as rapid analysis at the point-of-care.

## 381 **2.2. Inkjet-based 3D printing method (i3Dp)**

382 Inkjet-based 3D printing, i.e., Polyjet and MultiJet, is a method that employs photocurable resins  
383 deposited selectively on a platform drop-by-drop, as schematized in Fig. 2.e [136]. After the  
384 deposition of the first layer, a UV lamp, located inside the machine chamber, rapidly cures it. The  
385 platform stage is lowered, and the next film is built, repeating the process until obtaining the final  
386 structure. During the i3Dp, a blade can be used to smooth the surface of the just printed layer to  
387 guarantee a clean and uniform layer before the light-curing phase.

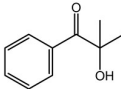
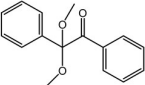
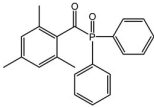
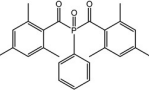
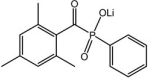
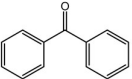
388 Polyjet 3D printing technique was invented in the latest '90s by Object Ltd (now Stratasys),  
389 being nowadays one the most commercially available 3DP methods. While in 1996, 3D Systems  
390 presented their material jetting method commercialized as MultiJet printing [137,138]. A common  
391 configuration of these printing techniques consists of various jetting heads, a three-axis motion  
392 platform, and the UV-curing device. In most of the Inkjet-based 3D printing methods, the jetting of  
393 material can be achieved by two modalities: continuous inkjet (CIJ) and drop-on-demand (DOD)  
394 [139,140]. In the CIJ-based methods, the photopolymer is continuously jetted through the nozzle  
395 by pressure action, generating a stream of droplets according to the Rayleigh-Plateau instability  
396 phenomenon of the liquid column, as described by others works [141,142]. In the DOD-based  
397 methods, the pressures pulse generates the droplets, and when this pulse exceeds the threshold at  
398 the nozzle, the droplets are ejected. Commonly, the velocity of droplets generation with CIJ-based  
399 3D printing methods is higher than DOD-based ones with >10 m/s and 5–8 m/s, respectively [141].  
400 The printing resolution of the inkjet-based technique is limited to hundreds of micrometers,  
401 depending on factors such as droplet diameter, the impact of the droplets onto the platform, the  
402 contact angle between the droplet and the substrate [137,141]. During a typical i3D printing  
403 condition, the printer heads spray two different materials: the building and support/sacrificial  
404 materials (used to maintain the just deposited and still liquid building material) [139,143]. In  
405 Polyjet, this sacrificial material combines acrylate monomers and other elements such as  
406 polyethylene and propylene that can be removed after the printing step by high-pressure waterjet  
407 or solvent dissolution. In MultiJet, the sacrificial material is a wax composition that is melted in a  
408 dedicated post-printing process. Both building and sacrificial material should present two crucial  
409 requirements for i3Dp use: (i) appropriate fluid properties to guarantee droplets' correct  
410 formation and precise deposition (low-viscosity materials are preferred) and (ii) high  
411 photopolymerization (curing) rate to polymerize the deposited material fast, avoiding losing the  
412 structure shape [54].

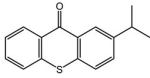
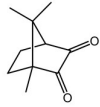
413 In general, i3Dp formulations are made of a mix of monomers and oligomers, photoinitiators,  
414 dyes and other additives. Monomers and oligomers are reactive polymers with functional groups  
415 (unsaturated functional groups or C=C) necessary to create the polymeric network. The chemical  
416 structures of the most common monomers and oligomers used are depicted in Fig. 3. The backbone  
417 of these reagents defines the polymerized part's final physical and mechanical properties (together  
418 with the appropriate adhesion between cured layers). Photoinitiators are compounds that absorb  
419 part of the incident light, generating reactive species or radicals through chemical transformations.  
420 These species interact with monomers and oligomers, enabling the photopolymerization  
421 mechanism [144,145]. Table 2 shows the most typical photoinitiators used for 3D printable  
422 photopolymers preparation. Dyes or pigments are organic or organometallic molecules used to

423 control the light's penetration during 3D printing (*Z-axis*) to enhance the printing resolution (*X-Y*  
 424 *plane*) [146]. Other additives can be combined with printable ink, such as reactive diluents used to  
 425 adjust the material's viscosity or enhance the solubility of other components such as  
 426 photoinitiators or dyes [147,148]. Nano-fillers such as silica or clay fillers can also be combined  
 427 with the printable ink (according to the nozzle diameter and final viscosity of the ink) to enhance  
 428 the specific characteristic of the final parts, such as the mechanical properties [149].

429 For microfluidic chips fabrication, photopolymer-based i3Dp is preferred over other material  
 430 jetting techniques such as thermal-curing-based since they combine the benefits of lithographic  
 431 methods (e.g., high spatial resolution, high feature definition and good surface quality) and high  
 432 build speed, material versatilities and large build volume from material jetting techniques [102].  
 433 Using Polyjet or Multijet-based printing methods, the printed microchips' surface features could be  
 434 significantly enhanced compared to FFF-3D printing (although the prices are typically higher than  
 435 FFF methods). Moreover, with these i3Dp methods, the printing speed and the microfluidic chips'  
 436 accuracy can be higher in all axes to the extrusion-based techniques [150]. Lee et al. reported  
 437 microfluidic chips by Polyjet with a nominal *X-Y* plane and *z* dimensions of 500  $\mu\text{m}$  and 100  $\mu\text{m}$ ,  
 438 respectively, with an average deviation (between the printed part and the CAD design) of 25.2  $\mu\text{m}$   
 439 and with smoother features (surface roughness of 0.47  $\mu\text{m}$ ) compared to 67.8  $\mu\text{m}$  of average  
 440 deviation and 42.97  $\mu\text{m}$  of surface roughness of FFF-3D printed parts (Fig. 5.a) [151]. These  
 441 microfluidic chips, made from commercial material (FullCure, *Stratasys*), presented high cell  
 442 viability toward C2C12 cells as a function of an appropriate post-printing sterilization step.

443 Table 2. Most common type I and II free radical photoinitiators for photopolymerization-based 3D  
 444 printing.

Compound name	Type <sup>a)</sup>	Structure	Range of absorption (nm)
2-hydroxy-2-methyl propiophenone (HMMP)	I		(320-360) [152]
2,2-dimethoxy-2-phenylacetophenone (DMPA)	I		(310-370) [153]
Diphenyl(2,4,6-trimethylbenzoyl)-phosphine oxide (TPO)	I		(350-410) [154,155]
phenyl bis (2,4,6-trimethylbenzoyl)-phosphine oxide (BAPO)	I		(360-440) [154]
lithium phenyl-2,4,6-trimethylbenzoyl phosphinate (LAP)	I		(340-400) [156]
Benzophenone	II		(230-280) [157]

2-Isopropylthioxanthone (ITX)	II		(320-400) [158]
Camphorquinone (CQ)	II		(420-490) [159]

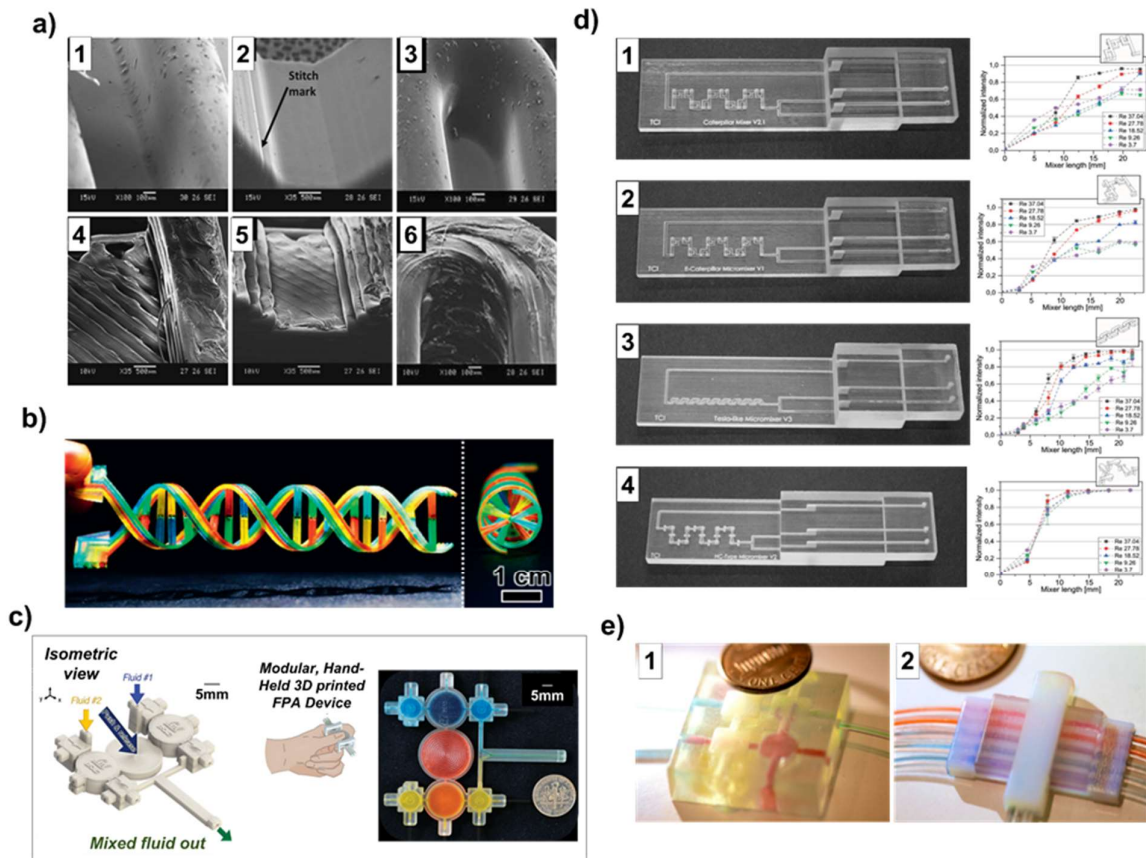
445 <sup>a)</sup> Type I photoinitiators are compounds that undergo homolytic bond cleavage when absorbing photons, generating two  
 446 free radicals from Norrish type I reactions and inducing the polymerization process. Type II photoinitiators are  
 447 uncleavable organic molecules that have a more complex initiating mechanism. These bimolecular photoinitiators, upon  
 448 light irradiation, can abstract hydrogen atoms from a hydrogen donor to produce excited complexes for initiating the  
 449 polymerization.

450 Sochol et al. developed advanced components used as fluidic capacitors, diodes, and transistors  
 451 to construct integrated fluidic circuits (IFC) [160]. The components were fabricated using a  
 452 commercial material, Visijet M3 Crystal from 3D Systems (see Fig. 5.b), presenting limited  
 453 biocompatibility. Indeed, the investigators evidenced that further works are required using more  
 454 biocompatible material for Multijet printing, such as MED610, or performing the appropriate post-  
 455 processing steps to provide higher biocompatibility to the chips. The authors produced reliable and  
 456 sophisticated chips in which the functionalities could be customized by modifying the geometric  
 457 parameters. Sweet and coworkers' work produced a series of finger-powered actuator (FPA)  
 458 prototypes using Visijet material through Polyjet 3D printing [161]. The pulsatile fluid motion  
 459 capability of the fabricated devices was used as modular models for microfluidic actuation and  
 460 mixing purposes in an integrated fluidic platform; see Fig. 5.c. A further advantage of inkjet-based  
 461 3D printing is that it allows the fabrication of multiple microfluidic chips contemporaneously with  
 462 high precision and accuracy. Walczak et al. presented the manufacturing of a series of microfluidic  
 463 chips (up to 170 chips) during a single 3D printing process. The chips with diameter dimensions of  
 464 400  $\mu\text{m}$  and semi-transparent features were used for capillarity gel electrophoresis. After  
 465 optimizing the printing parameters in terms of printing orientation, fluorescence detection of DNA  
 466 was possible [162].

467 In terms of optical transparency, highly transparent chips with intricate microchannels can also  
 468 be produced using Polyjet for fluid mixing and optical analysis. The fluid profile of microfluidic  
 469 systems is in a laminar flow; therefore, mixing different fluids efficiently and rapidly in this regime  
 470 is a fundamental aspect of microfluidic chips for biological and chemical applications [163–165].  
 471 Enders et al. produced different micro-passive mixers through Polyjet methods with great optical  
 472 features and sophisticated channel paths to study and compare the mixing performances between  
 473 each configuration (Fig. 5.d) [166]. The designs of the most diffused mixer types, e.g., Caterpillar,  
 474 enhanced Caterpillar, Tesla-like, and HC mixers, were produced using an acrylate-based material  
 475 (Visijet M2R-CL, 3D System). After a series of experimental and simulation comparison tests, they  
 476 observed that Tesla-like and especially HC chips were the most suitable for the rapid and efficient  
 477 mixing of fluids such as CHO-K1 (Chinese hamster ovary) cells.

478 The resolution of the i3Dp is generally higher than extrusion-based methods; however, it is still  
 479 challenging to obtain sub-100  $\mu\text{m}$  channels since this technique requires using a support material  
 480 to avoid filling the built microchannel during printing. The removal of the support material after  
 481 printing implies complex post-printing treatments [43,63,167]. This setback could become even  
 482 trickier when the microfluidic channel configuration increases the complexity and geometry. In this  
 483 context, Castiaux and collaborators proposed an interesting strategy: instead of using conventional

484 support material, the researchers stopped the printing process at a certain point to incorporate  
 485 either a thin polycarbonate membrane or a liquid (composed of glycerol/isopropanol 65:35 v:v) as  
 486 a physical barrier that can support the additional printed layers [103]. Both techniques  
 487 demonstrated to be useful for creating complex-shaped microfluidic chips with channels  
 488 dimensions as small as  $15 \times 250 \mu\text{m}$ , dimensions difficult to achieve by using conventional support  
 489 material. However, the results obtained appear difficult to reproduce since the  $250 \mu\text{m} \times 15 \mu\text{m}$   
 490 channel was initially intended to be  $125 \mu\text{m} \times 54 \mu\text{m}$  according to their CAD design. Besides, it must  
 491 be considered that stopping the printing procedure for placing extra material manually inevitably  
 492 introduces additional labor in the process. One advantage of the i3Dp is its multi-material  
 493 versatility by spraying various materials with different characteristics, e.g., mechanical or optical  
 494 properties, during the same printing process [52,168]. Taking advantage of this characteristic, S.  
 495 Keating et al. reported the 3D printing of multi-material valves using both rigid (VeroWhitePlus,  
 496 RGD835, Stratasys) and flexible (TangoPlus, FLX930, Stratasys) materials. They compared the  
 497 multi-material valves with single material valves observing that the former presents a more robust  
 498 capability to deformation, enabling better and precise control of fluids, leading to automated  
 499 production of microfluidic devices (Fig. 5.e) [169]. Keating and coworkers reported that such  
 500 multipurpose fluidic chips with channels  $800 \mu\text{m} \times 800 \mu\text{m}$  and programmable valves might be  
 501 used for various advanced biological applications such as DNA assembly and analysis, continuous  
 502 sampling sensing, and soft robotics.



503

504 Fig. 5. 3D printed milli- and microfluidic chips fabricated by photopolymer-based inkjet 3D printing  
 505 methods. (a) Scanning electron microscope (SEM) images of microchannels obtained by i3Dp (1-3)  
 506 compared to microchannels obtained by FFF (4-6), showing the surface roughness between both  
 507 techniques. Reprinted with permission from Ref. [151]. (b) 3D printed DNA-inspired fluidic devices are

508 composed of eight fluidic channels (750  $\mu\text{m}$  in diameter) filled with different dye-colored solutions.  
509 Adapted with permission from Ref. [160]. (c) Working principle representation of a finger-powered  
510 two-fluid FPA prototype for fluid mixing of two distinct dyed-colored solutions. Adapted with  
511 permission from Ref. [161]. (d) Photographs of the 3D printed microfluidic mixers: 1) Caterpillar mixer,  
512 2) enhanced Caterpillar mixer, 3) Tesla-like mixer, and 4) HC mixer. Next to each image is shown the  
513 calculated mixing performances (from simulation tests) as a mixer length function. Reprinted with  
514 permission from Ref. [166]. (e) 3D printed microfluidic multichannel valves made of 1) a single material  
515 and 2) a multi-material. Ref. [169].

516 Hence, the i3Dp techniques can be used for microfluidic chip fabrication with remarkable  
517 results, even if this technique requires a considerable post-printing process to clean the  
518 microchannels without damaging the microdevices correctly. Other aspects to consider are that  
519 i3Dp presents a relatively high initial cost in equipment and consumables. Besides, the window of  
520 available materials for i3Dp is limited since they are restrained by the range of viscosity and high  
521 curing rate other liquid properties (e.g., ink surface tension) requirements. Moreover, the printable  
522 materials are "regulated" formulations, developed only by the owners and therefore difficult to  
523 modify or adjust. Finally, more in-depth studies about the biocompatibility of the printable inks are  
524 still missing [58,102].

525

526

### 527 **2.3. Vat polymerization method**

528 Vat polymerization (VP) 3D printing is another photopolymerization-based technique that  
529 involves using a vat containing a liquid photopolymer [170]. This technique presents valuable  
530 features for microfluidic chips fabrication, e.g., high printing resolution and accuracy, faster  
531 printing times, and more flexibility in material tailoring and development than other polymeric 3D  
532 printing techniques (see Table 1) [90,170–174]. The VP-3D printing technique was introduced in  
533 the early '80s when the stereolithography (SL) method was developed by Hideo Kodama and  
534 Charles Hull works [175,176]. In the following years, various SL-based methods were developed,  
535 e.g., Digital Light Processing (DLP) [59,177], Micro-Stereolithography 3D printing ( $\mu\text{SL}$ ) [178],  
536 Continuous Liquid Interface Production (CLIP) [179,180], Two-Photon Polymerization(2PP) [181],  
537 and Computed Axial Lithography (CAL) [182]. The stereolithography (SL) method is based on the  
538 selective polymerization of photopolymers by using a laser beam focused on the liquid  
539 photopolymer, as represented in Fig. 2.f. The polymer is formed by moving the laser over the resin  
540 surface (usually using a galvanometric head to control the laser) to create the first layer [183]. This  
541 polymerized layer remains attached to the building platform that is lowered according to the layer  
542 slicing step. The subsequent layers are 'printed' following the same procedure until the complete  
543 fabrication of the object. The printed parts are subjected to post-curing processes to reach the  
544 highest chemical conversions possible [68]. SL machines can be configured either top-down (Fig  
545 2.f) or bottom-up approaches [172]. In the top-down configuration, the light comes from above,  
546 and the platform is submerged in the liquid as the part is created. While in the bottom-up, the laser  
547 beam hits the resin from the bottom of the vat through a transparent window, and the object  
548 remains attached to the platform that rises according to the formation of each layer. Generally, the  
549 bottom-up approach is preferred over the top-down since it is not dependent on the vat depth, and  
550 it requires less printable material (since it is not necessary to fill the entire vat to print).

551 With SL-3DP, printing features below 10  $\mu\text{m}$  can be achieved [184]. At the beginning of the 90s,  
552 a derived SL technology was created, the micro-stereolithography 3D printing (MSL or  $\mu\text{SL}$ ) with a

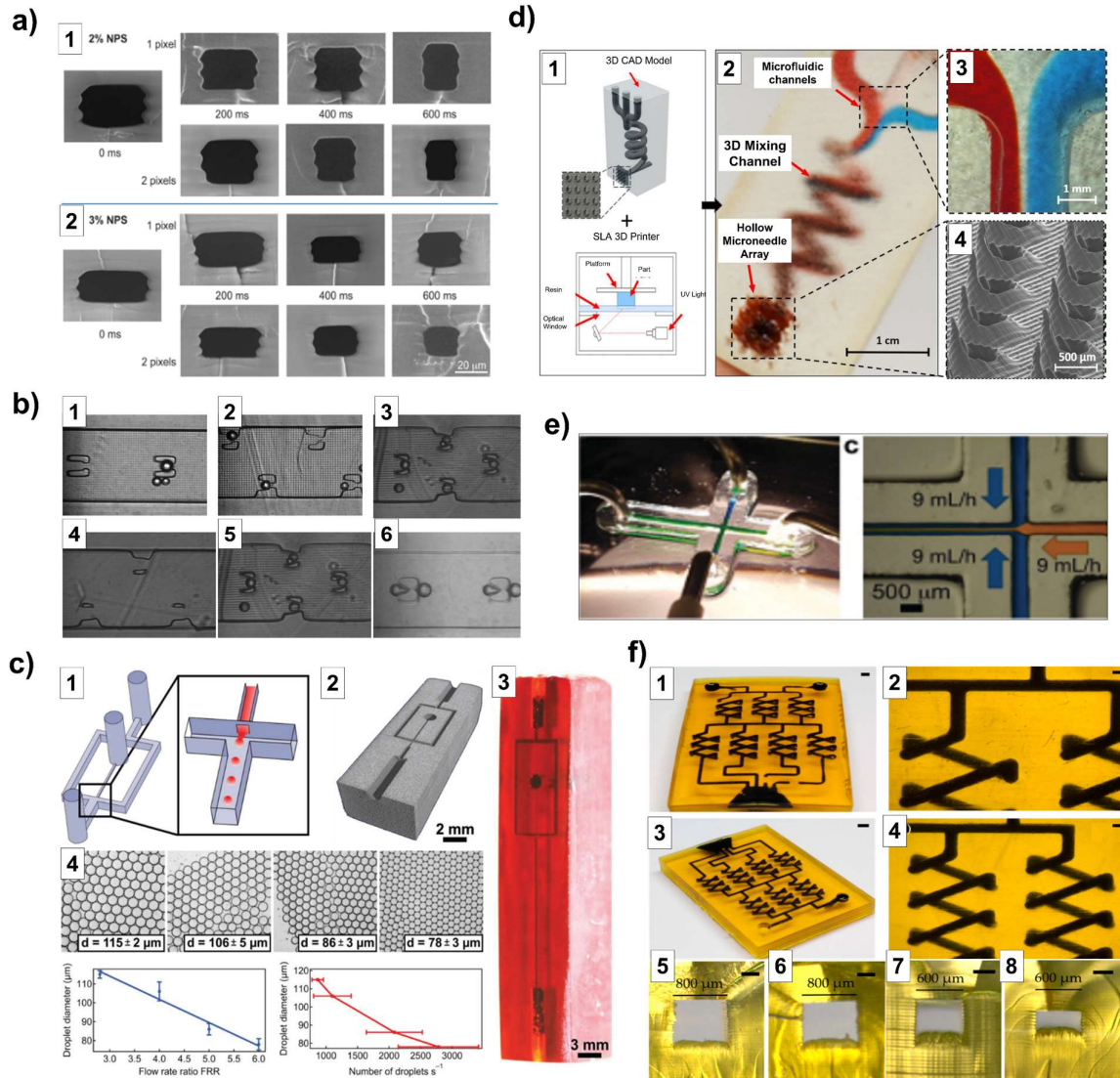
553 laser spot of about 5  $\mu\text{m}$  [178]. Through  $\mu\text{SL}$ -3D printing, structures with sub-1  $\mu\text{m}$  as a minimum  
554 feature size can be achieved [185]. Another SL-based is the Digital Light Processing 3D printing  
555 (DLP™). The DLP-based 3D printers are built by deformable mirror device (DMD) chips produced  
556 by Texas Instruments (see Fig. 2.g) [186,187]. In these configurations, each micromirror on the  
557 DMD represents one pixel in the digital image, which can drive to printing resolutions of 3 -5  $\mu\text{m}$  in  
558 the  $X$ - $Y$  plane according to the optical setup [188]. In the DLP-3D printing configurations, the parts  
559 are produced by projecting an entire cross-section of the object (plane-by-plane approach) rather  
560 than drawing it by a laser (line-by-line) as the case for SL methods. The photopolymerization of an  
561 entire cross-section of the object can significantly reduce printing times compared to SL  
562 techniques. Currently, commercial DLP-based printers present printing resolutions as small as 40  
563 x 40  $\mu\text{m}$  [177]. A variation of DLP-3D printing is the CLIP method which stands for Continuous  
564 Liquid Interface Production. CLIP-3D printing allows the continuous fabrication of objects by  
565 creating a thin interfacial layer of oxygen through an oxygen-permeable window. This thin oxygen  
566 layer (a dead zone) inhibits the free-radical polymerization only in the interface between the  
567 polymer film and the transparent window. Therefore, the just-built film does not adhere to the vat  
568 bottom; and the printing speed increases considerably up to hundreds of millimeters per hour.  
569 With the CLIP approach, large-scale and complex-shaped structures can be produced, maintaining  
570 high resolution [179,180]. Other light-based 3D printing methods have been developed in recent  
571 years, such as two-photon polymerization (2PP) or Computed Axial Lithography (CAL). The 2PP  
572 method is also based on a laser that scans a photopolymer [188]. The main peculiarity of the 2PP  
573 is that the process is activated by almost simultaneous absorption of two photons, which starts the  
574 free-radical polymerization, allowing polymerization control in the range of nanometer. [181,189]  
575 Some of the common drawbacks of 2PP are the limited dimensions of fabrication (no more than 1  
576 mm height) and the lower printing velocity, which is about 0.5-1 mm/s, compared to some SL  
577 techniques (200-300 mm/s) [190]. Besides, 2PP requires expensive equipment to set the optical  
578 arrangement [191]. Many researchers have been employed 2PP as a complementary tool to  
579 produce nanometric-scale structures, which can be integrated into microfluidic devices. The idea  
580 of producing a single microfluidic device that can be easily handled in laboratories using 2PP is still  
581 far from being a reality, so this technique will not be discussed in this review. Computed Axial  
582 Lithography (CAL) is a volumetric configuration developed as an alternative to the layer-by-layer  
583 3D printing approach [182]. CAL methods are based on computed tomography (CT) scans to  
584 generate a hologram within a controlled photopolymer volume, as shown in Fig. 2.h [192]. This  
585 hologram is created by the simultaneous projection of multiple 2D images while the vat container  
586 is rotating. The 2D images propagate through the liquid resin from different angles, resulting in a  
587 three-dimensional hologram with enough energy to photocuring, at once, a volume of  
588 photopolymer [193]. A fundamental parameter of CAL techniques is the rotation velocity that  
589 might directly influence the printing features when the rotary system is not in sync with the  
590 projected images. Another parameter of CAL is finding and adjusting the resins' viscosity since it  
591 must be high enough to avoid the relative shift between the 3D printed model and the rest of the  
592 liquid resin. CAL techniques' advantages are related to great production speed and surface  
593 definition, and these techniques can polymerize high viscosity resins (up to approximately 90 000  
594 cP) that are difficult to achieve with other techniques such as DLP or SL [194].

595 In all these SL-derived 3DP techniques, the printing part enters into contact with the liquid  
596 during the printing process. Hence, one crucial point is that the polymerized object is insoluble in  
597 the liquid resin, i.e., the cured structure remains dimensionally and mechanically invariable when  
598 contacting the liquid resin. Such a condition is achieved by using cross-linkable photopolymers and

599 supplying the system with sufficient light energy to reach the material's gel point (the point where  
600 the liquid system starts to show more solid-like mechanical features, becoming insoluble) [170].  
601 As for inks used in i3Dp, photopolymer for VP-3D printing combines, typically, three main chemical  
602 components: monomers/oligomers, photoinitiators, and additives. These formulations are mainly  
603 based on free-radically polymerizable resins, more frequently (meth)acrylate functionalities  
604 characterized by unsaturated C=C double bonds [195]. Such reactive groups are employed since  
605 they present high reactivity upon light irradiation, well-established mechanisms of reactions, and  
606 a wide range of (meth)acrylate-based are commercially available [196]. A few examples of the most  
607 used (meth)acrylate-based monomers and oligomers are depicted in Fig. 3. Other functionalities  
608 can also be employed, such as unsaturated polyester, vinyl, vinyl ether, thiol-ene/yne, and even  
609 cationic-based systems (in combination with free-radical systems) [197–200]. In general, the  
610 selection of suitable monomers or oligomers for vat polymerization is based on the specific  
611 application and the processing technology to be used. The main criteria are the resin functionality  
612 (mono-, di- or polyfunctional-), viscosity, reaction kinetic, hydrophobicity/hydrophilicity,  
613 shrinkage, costs, shelf life, volatility, toxicity, and the final mechanical and functional characteristic  
614 of the polymerized product [201]. As photoinitiators, different chemical compounds can be used  
615 and can operate in different electromagnetic spectrum wavelengths, e.g., UV, visible, and NIR [202–  
616 207]. These compounds can be divided into Type I (which directly generate the initiating species)  
617 and Type II (which needs a co-initiator to generate the initiating species) photoinitiators (see Table  
618 2) and have been widely explored in the literature, and most of them can be found commercially  
619 [208–218]. However, developing more efficient photoinitiators is still of great scientific interest  
620 nowadays [219–225]. Free-radical photoinitiators are the most common substances employed in  
621 light-based 3D printing. Selecting an appropriate photoinitiator is crucial for the correct production  
622 of structures by 3D printing. The absorption spectrum of the photoinitiator must match the  
623 emission light from the printer's light source [59]. Other additives can be added to the formulation,  
624 e.g., dyes, reactive diluents or fillers to improve features or functionalities of the printed parts  
625 [146,226–233]. Many researchers find VP-3D Printing a flexible technique since, being an open  
626 technique, it can be possible to modify or adjust the liquid resin willfully [59,68,234].

627 In the microfluidic field, VP-3DP found applications some years ago to fabricate templates for  
628 PDMS casting for photo-lithography procedures [235,236]. Although this approach led to  
629 interesting microfluidic parts, they still present a component of manual labor (not automated) that  
630 could introduce high levels of uncertainty or errors in microfluidic assays a posteriori. One of the  
631 reasons for using VP-3DP for microfluidic devices fabrication is the possibility of producing  
632 microchips in a single step of fabrication (or in the fewest possible steps) [237]. The printable  
633 materials used should satisfy some basic criteria in the microfluidic field, e.g., suitable mechanical  
634 characteristics, good optical transparency, water/gas permeability, and chemical resistance, and  
635 low cytotoxicity [201]. Fabricating polymeric 3D printed fluidic devices with all these features is a  
636 challenging task that has led to studying several types of printable photopolymers, ranging from  
637 commercially available photopolymers to custom-made formulations and performing adequate  
638 post-printing protocols on the parts [89,238]. Au et al., in 2014, presented one of the first attempts  
639 of using VP-3DP, producing single-step fluidic chips from a commercially available SL-3D printer  
640 (3D systems Viper) and the Somos® WaterShed XC 11122 resin (marketed as a suitable resin for  
641 obtaining biocompatible and transparent objects). [239]. The researchers produced microfluidic  
642 chips with channel dimensions down to 400  $\mu\text{m}$ . Another early try was presented by Prof.  
643 Breadmore in 2014 using commercial DLP-based Miicraft (Hsinchu, Taiwan) and a colorless  
644 acrylate-based resin (from the printer owner) to fabricate enclosed fluidic devices [240]. The

645 Miicraft is a bottom-up machine that allowed researchers to produce visible transparent  
646 microchips within a few minutes, with channel dimensions small as 250  $\mu\text{m}$  and averaging \$1 per  
647 chip. These early works probably provided the real starting signal for the effective production of  
648 microfluidic devices through VP-3D printing, even the technological limitations faced at that time.  
649 Gong et al. developed, in 2015, a mathematical model and performed optical characterization on a  
650 customized photopolymer to reach the smallest possible channel dimension into a microfluidic  
651 configuration [241]. In this case, the researchers developed their photopolymer based on a low-  
652 molecular PEGDA ( $M_n$  250 g/mol), the BAPO photoinitiator (see Table 2) and varying the dye  
653 concentration (the Solvent Yellow 14). By setting the appropriate experimental conditions (e.g.,  
654 light dose, build layer thickness, and resin composition), channel sizes as small as 60  $\mu\text{m}$  x 108  $\mu\text{m}$   
655 were successfully achieved. Later, in 2017, the same researcher group, led by Nordin G.P.,  
656 continued their studies, achieving flow channels as small as 18  $\mu\text{m}$  x 20  $\mu\text{m}$ , the smallest channel  
657 achieved to date (see Fig. 6.a) [41]. In this case, the researchers developed a 385 nm-UV-3D printer  
658 and a customized PEGDA-based photopolymer with 2-nitrophenyl phenyl sulfide (NPS) as a dye.  
659 The results obtained allowed the production of microfluidic chips for various applications such as  
660 entrapping microparticles (25  $\mu\text{m}$ ) inside microchannels built with pillars and ridged of  $\sim$  30  $\mu\text{m}$   
661 for instance, Fig. 6.b [242], or for the extraction and separation of preterm birth (PTB) biomarkers  
662 (ferritin) in a microchannel of 45  $\mu\text{m}$  x 50  $\mu\text{m}$  [243]. Parker et al. recently developed microfluidic  
663 devices with cross-section channel dimensions of  $\sim$  50  $\mu\text{m}$  for microchip electrophoresis ( $\mu\text{CE}$ )  
664 separation of various fluorescently labeled amino acids and biomarkers related to the risk of  
665 preterm birth (PTB) [244]. By optimizing the conditions of separations (e.g., devices layout,  
666 running buffer, and the voltages applied), the yield of separation of the printed devices was  
667 comparable to conventional material for microchip electrophoresis analysis with a limit of  
668 detection in the high picomolar (pM) to low nanomolar (nM) range; this was another example of  
669 how VP-3D printing could effectively be used for microfluidic chip fabrication.



670

671 Fig. 6. 3D printed microfluidic chips fabricated by VP-3D printing. (a) 3D printed microchannels (height  
 672  $\sim 18 \mu\text{m}$ ) using a custom-made photopolymer based on PEGDA and NPS. Reprinted with permission  
 673 from Ref. [41]. (b) Photograph showing the effect of the 3D printed particles trappers positioned at  
 674 different zones of a microchannel: traps positioned 1) in the center of the channels, 2) staggered along  
 675 the sides of the channel, 3) staggered along the sides, and in the middle of the channel, 4) traps partially  
 676 formed after 500 ms of light exposure with no bead capture, 5) particle captured in well-formed traps  
 677 after 750 ms of exposure, 6) overexposed traps after 1000 ms. Ref. [242]. (c) Nonplanar 3D printed  
 678 flow-focusing device: 1) representation of the microfluidic flow cell chip, 2) CAD image of the flow cell  
 679 model; 3) 3D printed chip using R11 resin, and 4) diameter of the droplet generated vs. flow rate ratio  
 680 (FRR) of dispersed and continuous water-oil phases. Reprinted with permission from Ref. [245]. (d) 3D  
 681 printed microfluidic-enabled hollow microneedle devices: 1) CAD design and representation of the  
 682 process, 2) device composed with 3) three inlets converging into a spiral mixing chamber and a 4)  
 683 hollow microneedle array outlet. Reprinted with permission from Ref. [246]. (e) Microfluidic devices  
 684 from a methacrylate-PDMS-based resin: 1) PDMS-based microfluidic device with  $500 \mu\text{m}$  wide channels  
 685 using a commercial 385 nm SL machine. 2) a central stream of yellow dye ( $9 \text{ mL/h}$ ) flanked by two  
 686 streams of blue dye ( $9 \text{ mL/h}$  each) produces a heterogeneous laminar flow ( $9 \text{ mL h}^{-1}$ ) in the fluidic  
 687 chip. Reprinted with permission from Ref. [247]. (f) 3D printed perfluoropolyether (PFEP) microfluidic  
 688 chip: 1) front view of the gradient mixing chip (scale bar:  $2 \text{ mm}$ ) with channel 2)  $800 \mu\text{m} \times 800 \mu\text{m}$  filled  
 689 with black ink (scale bar:  $500 \mu\text{m}$ ), 3) isometric view of the gradient mixing chip (scale bar:  $2 \text{ mm}$ )  
 690 with channel 4)  $600 \mu\text{m} \times 600 \mu\text{m}$  filled with black ink (scale bar:  $500 \mu\text{m}$ ), 5) lateral view of the  $800 \mu\text{m}$

691 channel width at the inlet and 6) in the middle (scale bar: 250 $\mu$ m), 7) lateral view of the 600  $\mu$ m channel  
692 width at the inlet and 8) in the middle (scale bar: 250 $\mu$ m). Ref. [248].

693 Other important components of microfluidic chips, such as microvalves, micropumps, and other  
694 actuators, can also be produced using VP-3D printing. These components can be used to program  
695 the fluid flow and create liquid mixtures and gradients during the analysis, sparing the human  
696 labor during the tests. Gong et al. (from the G. Nordin laboratory) demonstrated reported in 2015  
697 the production of 3D printed valves that can be driven pneumatically by willfully deflecting a thin  
698 membrane with compressed air and blocking the fluid flow [249]. These actuators were produced  
699 using a commercial 3D printer (the B9 Creator printer v1.1) and a lab-made resin based on a low-  
700 molecular PEGDA (Mn 250 g/mol), the BAPO photoinitiator and Sudan I dye. The same research  
701 group improved the stability over time of the valves and pumps, reaching performances up to 1  
702 million of actuation [250]. Besides, the authors optimized the valve's volume (to a tenth of the  
703 original design), allowing the production of multiplexers with high-density valves integrated into  
704 microfluidic devices. The Nordin research team has been working on miniaturizing membrane-  
705 based valves and pumps with active areas as small as 15  $\mu$ m  $\times$  15  $\mu$ m to be integrated into 3D  
706 printed microfluidic devices [251]. Au and coworkers reported an analogous work, presenting a  
707 fully 3D printed valve that could be integrated into microfluidic systems to allow fluids' proper  
708 distribution and mixing. The model was fabricated using a commercial rewin, the WaterShed XC  
709 11122 photopolymer (marketed as biocompatible and transparent) and the 3D systems Viper SL  
710 3D printer machine set in high-resolution mode. The printed valve consisted of two chambers  
711 separated by a thin film or membrane: a control chamber and a fluid chamber. By flushing  
712 compressed air in the control chamber, the thin membrane deflects and remains stable, blocking  
713 the liquids off with no leaking. As a proof of concept, the research team coupled four printed valves  
714 for routing four different liquids into a 3D-printed cell culture chamber, and in this way, CHO-K1  
715 cells were stimulated with ATP solutions, with the possibility to track their Ca<sup>2+</sup>-answer using a  
716 fluorescent dye (Fluo-4). The same group presented an article where transparent and  
717 biocompatible microfluidic chips arranged with a series of large arrays of valves were cost-  
718 affordable produced. In this case, the devices were produced using a customized photopolymer  
719 based on a low-molecular-weight (MW=258) monomer and using a commercial DLP-SL 3D printer  
720 from Asiga (Pico2-HD, 395 nm) [252].

721 Researchers have also been focusing more on studying the structure biocompatibility. Takenaga  
722 et al. used a commercial printer (PicoPlus 27) from Asiga and a commercial resin from the same  
723 company (PlasCLEAR) to 3D-print fluidic systems, presenting an innovative microfluidic assembly  
724 method in which the 3D printed fluidic chip is arranged on a light-addressable potentiometric  
725 sensor (LAPS) chip made from the same photopolymer. [253] The researchers used these types of  
726 assembled devices for Chinese hamster ovary (CHO)-cell growth yielding comparable results to  
727 standard cell-culture flasks and giving the possibility to monitor cells' reaction in the channels in  
728 real-time. Kuo et al. developed transparent and biocompatible microfluidic chips from a  
729 photocurable resin based on low-molecular-weight PEGDA (Mw 250), BAPO photoinitiator and the  
730 isopropyl thioxanthone (ITX) photosensitizer [254]. The ITX compound is a Type II photoinitiator  
731 that could start the polymerization process in the presence of a co-initiator. However, in Kuo et al.'s  
732 work, no co-initiators were added to the resin, and the ITX was used as a UV absorber due to the  
733 high molar absorption at 385 nm (the printer's light-emitting source). Besides, ITX neither affected  
734 the printed transparency of the microfluidic chips nor introduced unwanted coloration. The  
735 transparent chips were printed with the smallest channel width of 500  $\mu$ m and having surface  
736 pillars in the order of a single-pixel (27  $\mu$ m) and sub-pixel ( $\sim$  10  $\mu$ m). After a post-printing process,

737 the printed chips' biocompatibility was tested, testing the cell viability and proliferation of the  
738 Chinese hamster ovary (CHO-K1) with promising results.

739 Different and interesting works were published presenting 3D printed microfluidic devices  
740 production for diversified applications. For instance, Wang et al. presented multilayered 3D  
741 microfluidic devices for flow-focusing water/oil droplet generation employing a liquid crystal  
742 display (LCD)-based SLA 3D printer [255]. However, the chips were obtained from a commercial  
743 acrylate-based resin, Spot-LV from Spot-A. The researcher opted for adding up to 2 wt.% of a green  
744 dye into the commercial photopolymer to increase the light-absorbing effect, and thus the printing  
745 resolution. They performed various tests (e.g., curing times and printing resolution in each  
746 direction) to create microfluidic chips with microchannels of 400  $\mu\text{m}$  (*X-Y plane*) and 800  $\mu\text{m}$  (*Z-*  
747 *axis*), leading to obtaining 3D printed flow-focusing droplet generators that produced droplets with  
748 sizes between 50 and 185  $\mu\text{m}^2$ . Similar work was developed by Männel et al., presenting the  
749 production of nonplanar microfluidic flow cell devices for emulsion and polymeric  
750 hydrophilic/hydrophobic micro-particle formation [245]. The printed chips were produced  
751 through a commercial  $\mu\text{SL}$ -3DP (Perfactory P4 mini) and a commercial photopolymer (R11), both  
752 from *Envisiontec*. Printing settings such as object-resin vat separation distance, Z-axis building  
753 distance, and X-Y plane-light compensation at the edge's stages were adjusted to print precise  
754 microfluidic with closed channel sizes down to 75  $\mu\text{m}$  in a single-fabrication step (see Fig. 6.c). The  
755 3D printed microfluidic chips presented a similar drop-making yield to multi-step PDMS-based  
756 flow cell models fabricated by photo- and soft-lithography. Kotz et al. presented a simple method  
757 to 3D print microfluidic devices using a commercial printer (Asiga Pico 2) from a custom-made  
758 resin based on highly fluorinated (PFPE) methacrylate resin [248]. The authors selected the PFPE  
759 photocurable resin due to the high optical transparency and the polymerized parts' high chemical  
760 resistance. They opted to add into their resin two types of photoinitiator: TO and BAPO (See Table  
761 2), and various types of light absorbers: Sudan Orange G (SOG), Tinuvin 326 (T326), and Tinuvin  
762 384-2 (T384-2), to achieve the looked-for features. The researchers noted that the photopolymer  
763 stability was better using a SOG absorber, which also exhibits an intense absorption in the printer's  
764 light-emitting source (about 385 nm), leading to the 3D printing of embedded microfluidic chips  
765 (Fig. 6.f). As a result of the fine selection of materials, the 3D printed chips were produced with a  
766 channel width of 800  $\mu\text{m}$  and a height of 600  $\mu\text{m}$  as well as with high optical transparency. The  
767 printed chip presented excellent resistance toward organic solvents such as dichloromethane  
768 (DCM), N, N-dimethylformamide (DMF), tetrahydrofuran (THF) toluene, acetone, and n-heptane.  
769 In a curious work, Yeung et al. produced microfluidic chips made of an array of hollow microneedles  
770 positioned at the devices' outlet end (Fig. 6.d) [246]. The researchers employed a commercial SL-  
771 3D printer (Form2) and biocompatible material (Dental LT clear), both from FormLab. The devices  
772 were designed and printed with three separate inlet microfluidic channels that converge in one 3D  
773 spiral chamber. The incoming fluids are hydrodynamically mixed in this last chamber, emerging  
774 well-homogenized at the outlet where the microneedles (width between 800  $\mu\text{m}$  and 600  $\mu\text{m}$ ,  
775 height below 1 mm.) are positioned. Through the channels (2 mm roughly), three-fluorochrome  
776 model-drug solutions were injected, and it was observed by ex-vivo confocal microscopy analysis  
777 that the developed devices were able to achieve the transdermal drug delivery to porcine skin. The  
778 authors reported that such systems might be applied in preclinical drug therapy situations,  
779 allowing the in-situ mixing, and tuning of multiple drugs. Many works have also been reported  
780 utilizing custom-made photopolymers as alternatives to commercial printable materials.

781 Other interesting works have been reported using lab-made resin based on  
782 polydimethylsiloxane (PDMS) reagents as an alternative to conventional PDMS (the Sylgard 184),

783 which is typically used for producing microfluidic chips by casting. Bhattacharjee and coworkers  
784 created optically transparent PDMS-based microfluidic devices using a methacrylate-PDMS-based  
785 resin and a commercial desktop-SL 3D printer (see Fig. 6.e) [247]. The printed PDMS-based devices  
786 presented similar characteristics to the standard Sylgard 184 elastomer and produced chips with  
787 channel dimensions down to 500  $\mu\text{m}$ . Once the adequate post-printing washing steps were  
788 performed, these devices presented a promising cytocompatibility toward mammalian cell lines.  
789 More recently, Zips et al. presented silicone-hydrogel hybrid resins' preparation to produce flexible  
790 microfluidic devices with integrated valves, mixers, and chambers through a commercial  
791 stereolithography 3D printer [256]. The authors obtained microfluidic structures with internal  
792 channels of 450  $\mu\text{m}$  x 500  $\mu\text{m}$  when the printed chip was bonded (top and down) to a glass slide.  
793 As a proof of concept, the researchers used their 3D printed silicone-based microfluidic device to  
794 cultivate cardiac cells (cardiomyocyte-like HL-1) in a specifically designed chamber inside the  
795 printed chip, showing that the cardiac cells retained their electrophysiological activity inside the  
796 silicone-based chamber. Our group recently reported the production of complex-shaped PDMS-  
797 based fluidic devices by VP-3D printing [257]. The 3D printed chips were produced from a custom-  
798 made photopolymer based on acrylate-PDMS, a silicone soluble BAPO-derivate photoinitiator and  
799 DR1-MA as a dye, and a commercial DLP-3D printer emitting at 405 nm (Asiga PICO 2). The PDMS-  
800 based chips were obtained with good optical features, high chemical stability, good mechanical  
801 properties, and microchannels dimensions down to 400  $\mu\text{m}$  x 400  $\mu\text{m}$ . Besides, the microchannel's  
802 surfaces were successfully modified, exploiting the required UV-post-curing step by taking  
803 advantage of unreacted functional groups after the 3D printing step. In this way, the surface  
804 properties of the PDMS-based microdevices were effectively and selectively modified through UV-  
805 induced grafting polymerization techniques, giving an added value to the printed devices in terms  
806 of surface treatment compared to other methods. Using continuous liquid interface production  
807 (CLIP) methods, Berger and coworkers developed microfluidic devices for pathogen detection  
808 [258]. The microdevices were produced using RPU70 material and the CLIP-printer Carbon M2.  
809 Although with RPU70, one can produce only opaque materials, it is mechanically resistant,  
810 chemically stable and compatible with various common solvents, it presents low water  
811 absorptivity, and it is biocompatible (according to SO 10993-5/-10) [259]. The authors developed  
812 microfluidic devices with open microchannels (or grooves) widths and depth small as 400  $\mu\text{m}$ . The  
813 3D printed devices were covered with transparent biocompatible tape, allowing better  
814 visualization of the optical imaging during the filling. The printed chips were used to detect *E. Coli*  
815 bacteria from whole blood through a loop-mediated isothermal amplification (LAMP) assay with a  
816 50 cfu/ $\mu\text{L}$  limit of detection. The researchers reported a saponin-based lysing approach to process  
817 whole blood samples directly in the chip for amplification, which subsequently allowed the  
818 portable translation of the assay toward a point-of-a-care (POC) system using a smartphone.

### 819 **3. 3D printing microfluidic chips: key-points for future improvements**

820 Despite the inspiring and promising results obtained so far, there are still shortcomings that  
821 polymeric 3D printing should overcome to compete with well-established techniques for  
822 microchips fabrication, so to be considered a robust technology, and not just a promising  
823 alternative. The most looked-for characteristics in 3D printed fluidic chips are printing resolution  
824 and accuracy, optical transparency, and biocompatibility. Current commercial 3D printing  
825 resolution is still lower (or poorer) than conventional lithography methods. Most of the published  
826 works of 3D-printed microfluidics reported microchannels in the range of 0.5 - 1 mm. Researchers  
827 have been looking for novel methods to manufacture truly microfluidic devices (<100  $\mu\text{m}$ ). Some

828 researchers achieved sub-millimeter dimension channels using not-so-quite handy and replicable  
829 methods. The truth is that these strategies are still highly experimental, and even more  
830 technological and material development is needed to converge 3D printing and microfluidic  
831 systems entirely.

832 The FFF method is a 3D printing technique with a high printing speed and low initial cost. Using  
833 FFF, sacrificial masters can be produced, that can be dissolved in a post-3D printing step to develop  
834 truly sub-millimeters microfluidic chips (the smallest features 18  $\mu\text{m}$  using a nozzle of 30  $\mu\text{m}$  of  
835 diameter) [123,260]. However, for direct FFF 3D printing of microfluidic the precision remains  
836 quite above the sub-millimeter features. As discussed previously, photopolymer-based 3D printing  
837 methods are considered the best alternative for microfluidic chip manufacturing. Inkjet 3D printing  
838 (i3Dp) presents a better printing resolution than extrusion-based techniques. However, the correct  
839 fabrication of sub-microfluidic devices is limited by the supporting material used in the fabrication  
840 step. The supporting material can be trapped inside the channels, and it can be quite difficult to  
841 remove from the microchannels. In this view, an innovative strategy was presented based on the  
842 pausing-and-printing approach by introducing a thin sheet or liquid substances as a physical  
843 barrier rather than the conventional supporting material, leading researchers to reach sub-  
844 millimeter channel dimensions through i3Dp [103]. However, this method is rather manual and  
845 depends on the correct alignment of the physical barrier. With vat polymerization techniques,  
846 larger-scale and precise microfluidic chips can be produced faster, though the transversal  
847 resolution is still to be improved [258]. The printing resolution of stereolithography and digital  
848 light processing 3D printing techniques can reach a few micrometers, although they typically  
849 present a lower printing speed than FFF and i3Dp [54]. The stringent request for the future on this  
850 side is the improvement of printing resolution to a range similar to soft lithography. This can be  
851 reached with 2PP; however, this equipment is not suitable for mass production. It is thus necessary  
852 for a synergistic improvement of machines technology, which hopefully can gather multiple  
853 technologies, and materials.

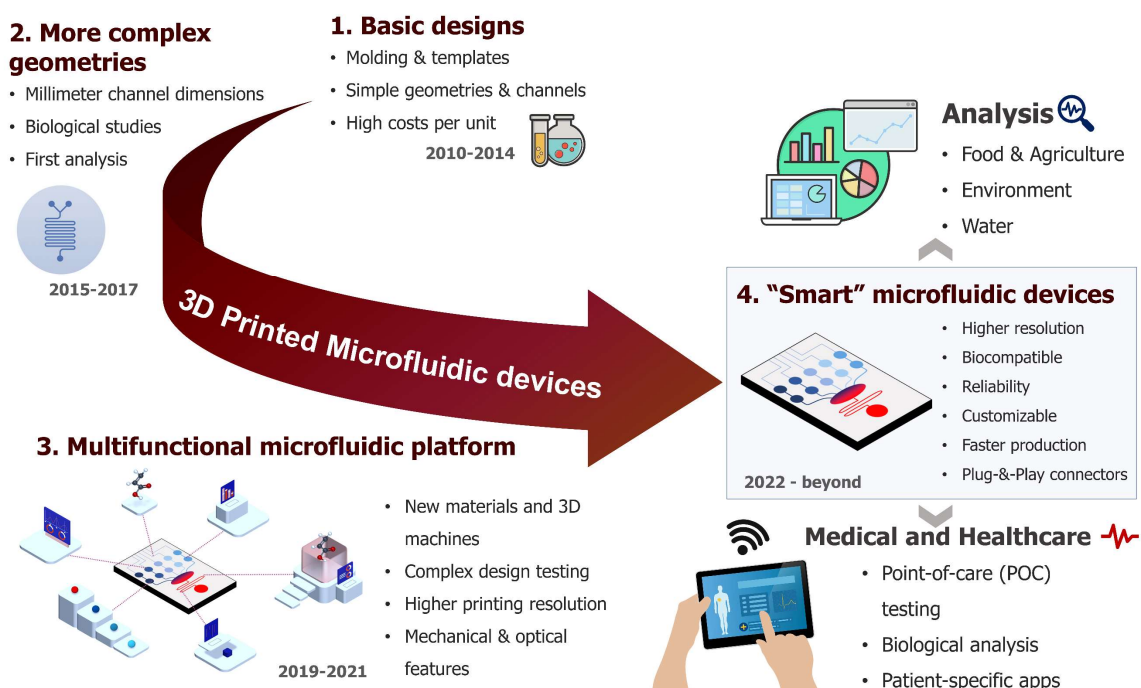
854 Beyond resolution, another crucial feature for the 3D printing of microfluidic chips is  
855 biocompatibility [261–263]. Among the 3D printed techniques discussed in this review, FFF is with  
856 the wider commercially available biocompatible materials, as shown in Table 1 [101,102], e.g.,  
857 polylactic acid (PLA), polymethylmethacrylate (PMMA), polycarbonate (PC), cyclic olefin  
858 copolymer (COC), polypropylene (PP), acrylonitrile-butadiene-styrene (ABS) and polyurethane  
859 (TPU). These materials can also be found in the market at good prices compared to other materials  
860 used for different polymeric 3D printing methods. The situation is slightly different for  
861 photopolymerization-based inkjet and Vat polymerization 3D printing. Considering the nature of  
862 printable photopolymers, the printed objects frequently contain unreacted chemical products  
863 (monomers, photoinitiators, and additives) after the printing step. Such unreacted chemicals can  
864 be toxic to biological entities, hindering the full potential application in the biomedical field  
865 [264,265]. Many researchers have reported novel formulations using hydrogels [120,266–269].  
866 Hydrogels' main characteristic is their great compatibility with biological entities since they are  
867 designed to uptake high water content ( $> 90 \text{ wt.}\%$ ) [270]. These features make hydrogels attractive  
868 for medical, biomedical and pharmaceuticals applications [271,272]. Though, their implementation  
869 for microfluidic devices' manufacturing has not been completely adopted because hydrogels could  
870 interact undesirably with the fluids flushing through the microchannels, leading to structural  
871 changes of the chips [267]. An aspect to consider is that the printed microfluidic devices need to  
872 operate with delicate aqueous-based analytes in cell culture or tissue engineering applications  
873 [273], which could be solved using hydrogels with partially hydrophobic characteristics [256]. On

874 the other hand, fluidic platforms made with more dimensionally stable and water-free polymers  
875 could enable better performance of microfluidic devices, even if the biocompatibility features are  
876 not so great as hydrogels. Recent studies have shown the importance of improving the  
877 biocompatibility of such water-free structures [273,274]. In this frame, diverse commercial  
878 photopolymers marketed as biocompatible have been reported [245,275]. However, as discussed  
879 in the review, only a few studies have been carried out related to the material-biological unit  
880 interactions. Most of the studies have been focused on Vat polymerization techniques; for instance,  
881 a detailed characterization of four commercial photopolymers (from Formlab) was carried out by  
882 Piironen et al., studying their compatibility toward cell lines [276]. The researchers concluded that  
883 even if a commercial resin is ISO-certified as biocompatible, it does not imply an adequate cell  
884 interaction of the produced parts. They observed that the most crucial point is performing a post-  
885 printing procedure on objects to remove the toxic component and improve biocompatibility. Other  
886 researchers reached a similar conclusion [277,278]. In all these previous works, the result was  
887 common: more attention must be paid to the post-printing procedures to reduce the leaching of  
888 toxic compounds from the printed parts.

889 Even following a post-printing procedure, the lack of detailed information from the supplier  
890 about the chemical composition of the resin further complicates the biological studies performance  
891 of the printed parts. Herein, the growing interest in developing custom-made photopolymers for  
892 3D printing with biocompatibility features [187,279]. In this line, the idea is to formulate resins to  
893 obtain printed parts with adequate biocompatibility and reduced cytotoxicity, which could be  
894 foreseen as biocompatible materials for advanced applications after standard treatment  
895 validations [68,280]. The development of in-lab and more biocompatible materials, however, could  
896 be achieved mainly using vat polymerization techniques owing to their versatility in material  
897 preparation (while for i3Dp, producing and implementing in-house materials is hindered by the  
898 restriction level of the machines' owners). A work from Nordin's group demonstrated that printed  
899 parts (based on PEGDA, Mn 250) were noncytotoxic toward endothelial cells (EA. hy926) even  
900 without any post-printing treatment [274]. Männel et al. evaluated the biocompatibility of  
901 (meth)acrylate resins toward human umbilical vein endothelial cells (HUVECs) [273]. They tested  
902 resins such as PEGMEMA (Mn 500 g/mol), TPGDA (Mn 300.55 g/mol), POEA (Mw 192.21 g/mol)  
903 and PEGDA (Mn 575 g/mol). They noticed that a combination of PEGDA and PEGMEMA was the  
904 most suitable composition, observing a cell proliferation after five (5) days of culture. Different  
905 researchers have explored how the biocompatibility of the printed parts can be increased by  
906 removing or reducing the unreacted and potential cytotoxic products by following the appropriate  
907 post-printing steps [170,281,282]. Though, the printed objects' bio-functionality can also be  
908 enhanced by performing particular post-3D printing protocols not to remove the potentially  
909 cytotoxic components from their surface (or "passivation") but by coupling bio-functional groups  
910 on their surfaces (or "activation"). These functional groups might be active biological molecules  
911 such as antibodies, peptides, nucleic acids, or biocompatible compounds to promote biological  
912 interactions like carboxylic acid groups or thiols. As proposed by Männel and coworkers in their  
913 work, the bioproperties of 3D printed parts might be significantly enhanced if RGD tripeptides are  
914 incorporated in the photosensitive resin rather than performing post-printing procedures [273].  
915 By adding Br-containing vinyl-terminated initiator into a commercial UV curable resin, 3D printed  
916 objects with modifiable surfaces can be obtained [283]. Such an approach promotes polymer  
917 brushes' growth via surface-initiated atom transfer radical polymerization (SI-ATRP) that can be  
918 potentially used in the biomedical field. This "activation" strategy could be an interesting path to

919 follow to introduce functional biomolecules that might enhance the biocompatibility or the bio-  
 920 interaction of the photopolymerized printed parts with specific biological entities [284].

921 As seen in this review, interesting use of 3D printed microfluidic chips has been reported. The  
 922 manufacturing of microfluidic devices by 3DP is still in a development phase, with some specific  
 923 works reporting the biomedical and pharmaceutical application of 3D printed chips [285–289].  
 924 Many expectations are still put on polymer 3D printing due to the flexibility and versatility to  
 925 simplify and decentralize the micro-manufacturing steps. We think that polymeric 3D printing will  
 926 soon meet the technological innovations and materials research necessary to bridge current gaps,  
 927 producing microfluidic devices for patient-specific treatment, more commonly known as Point-of-  
 928 a-care (POC) devices, as illustrated in Fig. 7. Many researchers have demonstrated the use of  
 929 polymeric 3D printing to produce microfluidic devices for the patient-specific detection of saliva,  
 930 urine, and other biological entities. This opens up a myriad of medical applications by combining  
 931 3D printing with real medical situations. Low-cost 3D printed microfluidic devices may provide a  
 932 new avenue for molecular detection at the point of care in resource-limited settings. Over time, it  
 933 is certainly possible to envision a future where these facilities are shared regionally or nationally,  
 934 supported by an on-call production team, to improve accessibility to these custom 3D printed and  
 935 POC devices.



936

937 Fig. 7. Past and projection of 3D printing for microfluidic chip fabrication. 1) Basic designs: initially,  
 938 3D printing was mainly used for the production of sacrificial molds for casting fabrication techniques;  
 939 2) More complex geometries: the development of new materials and 3D printing machines and  
 940 technology, more complex-shaped microfluidic chips were successfully fabricated, though most of the  
 941 application were proof-of-concepts based on preliminary biochemical analysis; 3) Multifunctional  
 942 microfluidic platforms: the growing interest for 3D printed microfluidic chips led researchers to  
 943 develop interesting works obtaining more performance microfluidic platforms with different  
 944 properties (e.g., biocompatibility and good mechanical and optical features) due to more advanced  
 945 materials and 3D printing methods; 4) "Smart" microfluidic devices: the future of 3D printed  
 946 microfluidic devices seems to be bright as more innovative materials and 3D printers are developed.  
 947 Based on our experience, we believe that the evolution of 3D printing in the microfluidic sector might

948 create a future scenario where one can produce rapidly microfluidic chips for the treatment of the  
949 specific analysis and patient situations, indeed, many researchers agree in a future where 3D printing,  
950 and the microfluidic world can contribute to the developing of precise and low-cost point-of-a-care  
951 devices.

#### 952 **4. Conclusions**

953 Polymeric 3D printing is a promising technology that can revolutionize the microfluidic field by  
954 introducing faster and cheaper ways to produce microdevices. These technologies, especially FFF,  
955 i3Dp and VP-3D printing, are also establishing new strategies for manufacturing such devices, new  
956 commercialization approaches, and fields of application. Although the expected potential of 3D  
957 printing, it still presents a few shortcomings that should be overcome to compete with well-  
958 established conventional techniques for microchips fabrication and thus be considered a valid  
959 technology and not just a promising alternative. In this review, an attempt was made to highlight  
960 the need to develop and improve the performance of current 3D printing materials and  
961 technologies to achieve the great potential of this technology.

962 In the next few years, we might expect that the progression of 3D printing will be establishing  
963 the pillars to appoint this technology as the best alternative for manufacturing microfluidic devices.  
964 To achieve such a goal, there is still so much to do in terms of materials and technology  
965 development to reach the greatest resolutions, the better precision as possible, the desired optical  
966 characteristics, and structures with higher biocompatible features. In recent years, most of the  
967 published works are more focused on presenting how polymeric 3D printing could be effectively  
968 used for microfluidic fabrication based on studying the characteristics of the machine or using or  
969 developing alternative materials. Now, it is time that the 3D printed microfluidics will be used in  
970 real microfluidic applications to start to comprehend the possible future scenarios that, in synergy  
971 with machines and software progress and material development, will lead to polymeric 3D printing  
972 the expected transformation in the field. Although the utilization of 3D printing has not yet become  
973 a central part of standard microfluidic chips today, we anticipate that given the prospects for 3D  
974 printing and continuous performance improvement, this technology will be adopted, and more  
975 opportunities will progressively emerge for companies and institutions to relevant applications in  
976 global health.

977

978 **5. References**

- 979 [1] P. Yager, T. Edwards, E. Fu, K. Helton, K. Nelson, M.R. Tam, B.H. Weigl,  
980 Microfluidic diagnostic technologies for global public health, *Nature*. 442 (2006)  
981 412–418. <https://doi.org/10.1038/nature05064>.
- 982 [2] E. Verpoorte, Microfluidic chips for clinical and forensic analysis,  
983 *Electrophoresis*. 23 (2002) 677–712. [https://doi.org/10.1002/1522-2683\(200203\)23:5<677::AID-ELPS677>3.0.CO;2-8](https://doi.org/10.1002/1522-2683(200203)23:5<677::AID-ELPS677>3.0.CO;2-8).
- 985 [3] C.Y. Lee, C.L. Chang, Y.N. Wang, L.M. Fu, Microfluidic mixing: A review,  
986 *International Journal of Molecular Sciences*. (2011).  
987 <https://doi.org/10.3390/ijms12053263>.
- 988 [4] M. Zhang, C. Xu, L. Jiang, J. Qin, A 3D human lung-on-a-chip model for  
989 nanotoxicity testing, *Toxicology Research*. 7 (2018) 1048–1060.  
990 <https://doi.org/10.1039/c8tx00156a>.
- 991 [5] D. Huh, A human breathing lung-on-a-chip, *Ann Am Thorac Soc*. 12 (2015) S42–  
992 S44. <https://doi.org/10.1513/AnnalsATS.201410-442MG>.
- 993 [6] D. Huh, Reconstituting Organ-Level Lung, *Science* (1979). (2010) 1662–1668.
- 994 [7] Y.-H.V. Ma, K. Middleton, L. You, Y. Sun, A review of microfluidic approaches  
995 for investigating cancer extravasation during metastasis, *Microsystems &*  
996 *Nanoengineering*. 4 (2018) 1–13. <https://doi.org/10.1038/micronano.2017.104>.
- 997 [8] A. Bohr, S. Colombo, H. Jensen, Chapter 15 - Future of microfluidics in research  
998 and in the market, in: H.A. Santos, D. Liu, H. Zhang (Eds.), *Microfluidics for*  
999 *Pharmaceutical Applications*, William Andrew Publishing, 2019: pp. 425–465.  
1000 <https://doi.org/https://doi.org/10.1016/B978-0-12-812659-2.00016-8>.
- 1001 [9] M. Lake, C. Arciso, K. Cowdrick, T. Storey, S. Zhang, J. Zartman, D. Hoelzle,  
1002 Microfluidic device design, fabrication, and testing protocols, *Protocol Exchange*.  
1003 (2015) 1–26. <https://doi.org/10.1038/protex.2015.069>.

- 1004 [10] M. Mehling, S. Tay, Microfluidic cell culture, *Current Opinion in Biotechnology*.  
1005 25 (2014) 95–102. <https://doi.org/10.1016/j.copbio.2013.10.005>.
- 1006 [11] C.Y. Lee, W.T. Wang, C.C. Liu, L.M. Fu, Passive mixers in microfluidic systems:  
1007 A review, *Chemical Engineering Journal*. (2016).  
1008 <https://doi.org/10.1016/j.cej.2015.10.122>.
- 1009 [12] E.A. Mansur, M. YE, Y. WANG, Y. DAI, A State-of-the-Art Review of Mixing in  
1010 Microfluidic Mixers, *Chinese Journal of Chemical Engineering*. (2008).  
1011 [https://doi.org/10.1016/S1004-9541\(08\)60114-7](https://doi.org/10.1016/S1004-9541(08)60114-7).
- 1012 [13] D. Di Carlo, Inertial microfluidics, *Lab on a Chip*. 9 (2009) 3038–3046.  
1013 <https://doi.org/10.1039/b912547g>.
- 1014 [14] B.M. Paegel, R.G. Blazej, R.A. Mathies, Microfluidic devices for DNA sequencing:  
1015 Sample preparation and electrophoretic analysis, *Current Opinion in*  
1016 *Biotechnology*. 14 (2003) 42–50. [https://doi.org/10.1016/S0958-1669\(02\)00004-6](https://doi.org/10.1016/S0958-1669(02)00004-6).
- 1017 [15] J. Scott Mellors, K. Jorabchi, L. M. Smith, J. Michael Ramsey, Integrated  
1018 Microfluidic Device for Automated Single Cell Analysis Using Electrophoretic  
1019 Separation and Electrospray Ionization Mass Spectrometry, *Analytical*  
1020 *Chemistry*. 82 (2010) 967–973. <https://doi.org/10.1021/ac902218y>.
- 1021 [16] S.K. Vashist, P.B. Lippa, L.Y. Yeo, A. Ozcan, J.H.T. Luong, Emerging  
1022 Technologies for Next-Generation Point-of-Care Testing, *Trends in*  
1023 *Biotechnology*. 33 (2015) 692–705. <https://doi.org/10.1016/j.tibtech.2015.09.001>.
- 1024 [17] G.A. Akceoglu, Y. Saylan, F. Inci, A Snapshot of Microfluidics in Point-of-Care  
1025 Diagnostics: Multifaceted Integrity with Materials and Sensors, *Advanced*  
1026 *Materials Technologies*. 2100049 (2021). <https://doi.org/10.1002/admt.202100049>.
- 1027 [18] S. Halldorsson, E. Lucumi, R. Gómez-Sjöberg, R.M.T. Fleming, Advantages and  
1028 challenges of microfluidic cell culture in polydimethylsiloxane devices,  
1029 *Biosensors and Bioelectronics*. 63 (2015) 218–231.  
1030 <https://doi.org/10.1016/j.bios.2014.07.029>.

- 1031 [19] A. Mata, A.J. Fleischman, S. Roy, Characterization of polydimethylsiloxane  
1032 (PDMS) properties for biomedical micro/nanosystems., *Biomed Microdevices*. 7  
1033 (2005) 281–293. <https://doi.org/10.1007/s10544-005-6070-2>.
- 1034 [20] I.D. Johnston, D.K. McCluskey, C.K.L. Tan, M.C. Tracey, Mechanical  
1035 characterization of bulk Sylgard 184 for microfluidics and microengineering,  
1036 *Journal of Micromechanics and Microengineering*. 24 (2014).  
1037 <https://doi.org/10.1088/0960-1317/24/3/035017>.
- 1038 [21] K. Ren, J. Zhou, H. Wu, Materials for microfluidic chip fabrication, *Accounts of*  
1039 *Chemical Research*. 46 (2013) 2396–2406. <https://doi.org/10.1021/ar300314s>.
- 1040 [22] L. Yu, C.M. Li, Y. Liu, J. Gao, W. Wang, Y. Gan, Flow-through functionalized  
1041 PDMS microfluidic channels with dextran derivative for ELISAs, *Lab on a Chip*.  
1042 9 (2009) 1243–1247. <https://doi.org/10.1039/b816018j>.
- 1043 [23] Z.L. Zhang, C. Crozatier, M. Le Berre, Y. Chen, In situ bio-functionalization and  
1044 cell adhesion in microfluidic devices, *Microelectronic Engineering*. 78–79 (2005)  
1045 556–562. <https://doi.org/10.1016/j.mee.2004.12.071>.
- 1046 [24] J. Xu, K.K. Gleason, Conformal, amine-functionalized thin films by initiated  
1047 chemical vapor deposition (iCVD) for hydrolytically stable microfluidic devices,  
1048 *Chemistry of Materials*. (2010). <https://doi.org/10.1021/cm903156a>.
- 1049 [25] X. Yu, J. Xiao, F. Dang, Surface modification of poly(dimethylsiloxane) using ionic  
1050 complementary peptides to minimize nonspecific protein adsorption, *Langmuir*.  
1051 31 (2015) 5891–5898. <https://doi.org/10.1021/acs.langmuir.5b01085>.
- 1052 [26] S. Hu, X. Ren, M. Bachman, C.E. Sims, G.P. Li, N. Allbritton, Surface modification  
1053 of poly(dimethylsiloxane) microfluidic devices by ultraviolet polymer grafting,  
1054 *Analytical Chemistry*. (2002). <https://doi.org/10.1021/ac025700w>.
- 1055 [27] B.T. Ginn, O. Steinbock, Polymer surface modification using microwave-oven-  
1056 generated plasma, *Langmuir*. (2003). <https://doi.org/10.1021/la034138h>.

- 1057 [28] A.Y.N. Hui, G. Wang, B. Lin, W.T. Chan, Microwave plasma treatment of  
1058 polymer surface for irreversible sealing of microfluidic devices, *Lab on a Chip*.  
1059 (2005). <https://doi.org/10.1039/b504271b>.
- 1060 [29] T. Goda, T. Konno, M. Takai, K. Ishihara, Synthesis and characterization on  
1061 polydimethylsiloxane grafted with poly(2-methacryloyloxyethyl  
1062 phosphorylcholine) by photo-induced radical polymerization, in: *Polymer*  
1063 *Preprints*, Japan, 2005.
- 1064 [30] M.D. Kurkuri, F. Al-Ejeh, J.Y. Shi, D. Palms, C. Prestidge, H.J. Griesser, M.P.  
1065 Brown, B. Thierry, Plasma functionalized PDMS microfluidic chips: Towards  
1066 point-of-care capture of circulating tumor cells, *Journal of Materials Chemistry*.  
1067 (2011). <https://doi.org/10.1039/c1jm10317b>.
- 1068 [31] J.C. McDonald, D.C. Duffy, J.R. Anderson, D.T. Chiu, H. Wu, O.J.A. Schueller,  
1069 G.M. Whitesides, Fabrication of microfluidic systems in poly(dimethylsiloxane),  
1070 *Electrophoresis*. 21 (2000) 27–40. [https://doi.org/10.1002/\(sici\)1522-  
1071 2683\(20000101\)21:1<27::aid-elps27>3.3.co;2-3](https://doi.org/10.1002/(sici)1522-2683(20000101)21:1<27::aid-elps27>3.3.co;2-3).
- 1072 [32] B.K. Gale, A.R. Jafek, C.J. Lambert, B.L. Goenner, H. Moghimifam, U.C. Nze, S.K.  
1073 Kamarapu, A review of current methods in microfluidic device fabrication and  
1074 future commercialization prospects, *Inventions*. 3 (2018).  
1075 <https://doi.org/10.3390/inventions3030060>.
- 1076 [33] A.G. Niculescu, C. Chircov, A.C. Bîrcă, A.M. Grumezescu, Fabrication and  
1077 applications of microfluidic devices: A review, *International Journal of Molecular*  
1078 *Sciences*. 22 (2021) 1–26. <https://doi.org/10.3390/ijms22042011>.
- 1079 [34] V.I. Vullev, J. Wan, V. Heinrich, P. Landsman, P.E. Bower, B. Xia, B. Millare, G.  
1080 Jones, Nonlithographic fabrication of microfluidic devices, *J Am Chem Soc*. 128  
1081 (2006) 16062–16072. <https://doi.org/10.1021/ja061776o>.
- 1082 [35] D. Mark, S. Haeberle, G. Roth, F. Von Stetten, R. Zengerle, Microfluidic Lab-on-  
1083 a-Chip Platforms: Requirements, Characteristics and Applications, in: S. Kakaç,

- 1084 B. Kosoy, D. Li, A. Pramuanjaroenkij (Eds.), *Microfluidics Based Microsystems*.  
1085 NATO Science for Peace and Security Series A: Chemistry and Biology, Springer,  
1086 Dordrecht, 2010.
- 1087 [36] C. Chen, B.T. Mehl, A.S. Munshi, A.D. Townsend, D.M. Spence, R.S. Martin, 3D-  
1088 printed microfluidic devices: fabrication, advantages and limitations - a mini  
1089 review, *Analytical Methods*. (2016). <https://doi.org/10.1039/c6ay01671e>.
- 1090 [37] V. Mehta, S.N. Rath, 3D printed microfluidic devices: a review focused on four  
1091 fundamental manufacturing approaches and implications on the field of  
1092 healthcare, *Bio-Design and Manufacturing*. (2021).  
1093 <https://doi.org/10.1007/s42242-020-00112-5>.
- 1094 [38] C. Su, Review of 3D-Printed functionalized devices for chemical and biochemical  
1095 analysis, *Analytica Chimica Acta*. (2021) 338348.  
1096 <https://doi.org/10.1016/j.aca.2021.338348>.
- 1097 [39] F. Zhu, A. Wigh, T. Friedrich, A. Devaux, S. Bony, D. Nugegoda, J. Kaslin, D.  
1098 Wlodkowic, Automated Lab-on-a-Chip Technology for Fish Embryo Toxicity  
1099 Tests Performed under Continuous Microperfusion ( $\mu$ FET), *Environmental*  
1100 *Science and Technology*. 49 (2015) 14570–14578.  
1101 <https://doi.org/10.1021/acs.est.5b03838>.
- 1102 [40] T.M. Valentin, E.M. Dubois, C.E. Machnicki, D. Bhaskar, F.R. Cui, I.Y. Wong, 3D  
1103 printed self-adhesive PEGDA-PAA hydrogels as modular components for soft  
1104 actuators and microfluidics, *Polymer Chemistry*. 10 (2019) 2015–2028.  
1105 <https://doi.org/10.1039/c9py00211a>.
- 1106 [41] H. Gong, B.P. Bickham, A.T. Woolley, G.P. Nordin, Custom 3D printer and resin  
1107 for  $18 \mu\text{m} \times 20 \mu\text{m}$  microfluidic flow channels, *Lab on a Chip*. (2017).  
1108 <https://doi.org/10.1039/C7LC00644F>.
- 1109 [42] K. Alessandri, M. Feyeux, B. Gurchenkov, C. Delgado, A. Trushko, K.H. Krause,  
1110 D. Vignjević, P. Nassoy, A. Roux, A 3D printed microfluidic device for production

- 1111 of functionalized hydrogel microcapsules for culture and differentiation of  
1112 human Neuronal Stem Cells (hNSC), *Lab on a Chip*. 16 (2016) 1593–1604.  
1113 <https://doi.org/10.1039/c6lc00133e>.
- 1114 [43] M.J. Beauchamp, G.P. Nordin, A.T. Woolley, Moving from millifluidic to truly  
1115 microfluidic sub-100- $\mu\text{m}$  cross-section 3D printed devices, *Analytical and*  
1116 *Bioanalytical Chemistry*. 409 (2017) 4311–4319. [https://doi.org/10.1007/s00216-](https://doi.org/10.1007/s00216-017-0398-3)  
1117 [017-0398-3](https://doi.org/10.1007/s00216-017-0398-3).
- 1118 [44] T.D. Ngo, A. Kashani, G. Imbalzano, K.T.Q. Nguyen, D. Hui, Additive  
1119 manufacturing (3D printing): A review of materials, methods, applications and  
1120 challenges, *Composites Part B: Engineering*. 143 (2018).  
1121 <https://doi.org/10.1016/j.compositesb.2018.02.012>.
- 1122 [45] G. Anglani, 3D printed capsules for self-healing concrete applications, (2019).  
1123 <https://doi.org/10.21012/fc10.235356>.
- 1124 [46] D.S. Thomas, S.W. Gilbert, Costs and cost effectiveness of additive  
1125 manufacturing: A literature review and discussion, in: *Additive Manufacturing:*  
1126 *Costs, Cost Effectiveness and Industry Economics*, 2015.
- 1127 [47] F. Matos, R. Godina, C. Jacinto, H. Carvalho, I. Ribeiro, P. Peças, Additive  
1128 manufacturing: Exploring the social changes and impacts, *Sustainability*  
1129 (Switzerland). (2019). <https://doi.org/10.3390/su11143757>.
- 1130 [48] M. Mehrpouya, A. Dehghanghadikolaei, B. Fotovvati, A. Vosooghnia, S.S.  
1131 Emamian, A. Gisario, The potential of additive manufacturing in the smart  
1132 factory industrial 4.0: A review, *Applied Sciences* (Switzerland). 9 (2019).  
1133 <https://doi.org/10.3390/app9183865>.
- 1134 [49] M. Gebler, A.J.M. Schoot Uiterkamp, C. Visser, A global sustainability  
1135 perspective on 3D printing technologies, *Energy Policy*. (2014).  
1136 <https://doi.org/10.1016/j.enpol.2014.08.033>.

- 1137 [50] S. Ford, M. Despeisse, Additive manufacturing and sustainability: an exploratory  
1138 study of the advantages and challenges, *Journal of Cleaner Production*. 137 (2016)  
1139 1573–1587. <https://doi.org/10.1016/j.jclepro.2016.04.150>.
- 1140 [51] D. Chen, S. Heyer, S. Ibbotson, K. Salonitis, J.G. Steingrímsson, S. Thiede, Direct  
1141 digital manufacturing: Definition, evolution, and sustainability implications,  
1142 *Journal of Cleaner Production*. (2015).  
1143 <https://doi.org/10.1016/j.jclepro.2015.05.009>.
- 1144 [52] M. Rafiee, R.D. Farahani, D. Therriault, Multi-Material 3D and 4D Printing: A  
1145 Survey, *Advanced Science*. 7 (2020) 1–26. <https://doi.org/10.1002/advs.201902307>.
- 1146 [53] D.T. Pham, R.S. Gault, A comparison of rapid prototyping technologies,  
1147 *International Journal of Machine Tools and Manufacture*. 38 (1998) 1257–1287.  
1148 [https://doi.org/10.1016/S0890-6955\(97\)00137-5](https://doi.org/10.1016/S0890-6955(97)00137-5).
- 1149 [54] L.Y. Zhou, J. Fu, Y. He, A Review of 3D Printing Technologies for Soft Polymer  
1150 Materials, *Advanced Functional Materials*. 2000187 (2020) 1–38.  
1151 <https://doi.org/10.1002/adfm.202000187>.
- 1152 [55] B.C. Gross, J.L. Erkal, S.Y. Lockwood, C. Chen, D.M. Spence, Evaluation of 3D  
1153 Printing and Its Potential Impact on Biotechnology and the Chemical Sciences,  
1154 (2014).
- 1155 [56] B. Berman, 3-D printing: The new industrial revolution, *Business Horizons*. 55  
1156 (2012) 155–162. <https://doi.org/10.1016/j.bushor.2011.11.003>.
- 1157 [57] J. Zhao, M. Hussain, M. Wang, Z. Li, N. He, Embedded 3D printing of multi-  
1158 internal surfaces of hydrogels, *Additive Manufacturing*. 32 (2020) 101097.  
1159 <https://doi.org/10.1016/j.addma.2020.101097>.
- 1160 [58] N. Bhattacharjee, A. Urrios, S. Kang, A. Folch, The upcoming 3D-printing  
1161 revolution in microfluidics, *Lab on a Chip*. 16 (2016) 1720–1742.  
1162 <https://doi.org/10.1039/C6LC00163G>.

- 1163 [59] J.W. Stansbury, M.J. Idacavage, 3D printing with polymers: Challenges among  
1164 expanding options and opportunities, *Dental Materials*. 32 (2016) 54–64.  
1165 <https://doi.org/10.1016/j.dental.2015.09.018>.
- 1166 [60] M. Hofmann, 3D printing gets a boost and opportunities with polymer materials,  
1167 *ACS Macro Letters*. (2014). <https://doi.org/10.1021/mz4006556>.
- 1168 [61] J. Ni, H. Ling, S. Zhang, Z. Wang, Z. Peng, C. Benyshek, R. Zan, A.K. Miri, Z. Li,  
1169 X. Zhang, J. Lee, K.J. Lee, H.J. Kim, P. Tebon, T. Hoffman, M.R. Dokmeci, N.  
1170 Ashammakhi, X. Li, A. Khademhosseini, Three-dimensional printing of metals  
1171 for biomedical applications, *Materials Today Bio*. 3 (2019).  
1172 <https://doi.org/10.1016/j.mtbio.2019.100024>.
- 1173 [62] R.D. Sochol, E. Sweet, C.C. Glick, S.Y. Wu, C. Yang, M. Restaino, L. Lin, 3D  
1174 printed microfluidics and microelectronics, *Microelectronic Engineering*. 189  
1175 (2018) 52–68. <https://doi.org/10.1016/j.mee.2017.12.010>.
- 1176 [63] S. Waheed, J.M. Cabot, N.P. Macdonald, T. Lewis, R.M. Guijt, B. Paull, M.C.  
1177 Breadmore, 3D printed microfluidic devices: enablers and barriers, *Lab on a Chip*.  
1178 16 (2016) 1993–2013. <https://doi.org/10.1039/C6LC00284F>.
- 1179 [64] R. Amin, S. Knowlton, A. Hart, B. Yenilmez, F. Ghaderinezhad, S. Katebifar, M.  
1180 Messina, A. Khademhosseini, S. Tasoglu, 3D-printed microfluidic devices,  
1181 *Biofabrication*. 8 (2016) 022001. <https://doi.org/10.1088/1758-5090/8/2/022001>.
- 1182 [65] C.M.B. Ho, S.H. Ng, K.H.H. Li, Y.-J. Yoon, 3D printed microfluidics for biological  
1183 applications, *Lab on a Chip*. 15 (2015) 3627–3637.  
1184 <https://doi.org/10.1039/C5LC00685F>.
- 1185 [66] Q. Yan, H. Dong, J. Su, J. Han, B. Song, Q. Wei, Y. Shi, A Review of 3D Printing  
1186 Technology for Medical Applications, *Engineering*. 4 (2018) 729–742.  
1187 <https://doi.org/10.1016/j.eng.2018.07.021>.
- 1188 [67] C. Lee Ventola, Medical applications for 3D printing: Current and projected uses,  
1189 *P and T*. 39 (2014) 704–711.

- 1190 [68] R.J. Mondschein, A. Kanitkar, C.B. Williams, S.S. Verbridge, T.E. Long, Polymer  
1191 structure-property requirements for stereolithographic 3D printing of soft tissue  
1192 engineering scaffolds, *Biomaterials*. 140 (2017) 170–188.  
1193 <https://doi.org/10.1016/j.biomaterials.2017.06.005>.
- 1194 [69] C.M. González-Henríquez, M.A. Sarabia-Vallejos, J. Rodríguez-Hernandez,  
1195 Polymers for additive manufacturing and 4D-printing: Materials, methodologies,  
1196 and biomedical applications, *Progress in Polymer Science*. 94 (2019) 57–116.  
1197 <https://doi.org/10.1016/j.progpolymsci.2019.03.001>.
- 1198 [70] S. V. Murphy, A. Atala, 3D bioprinting of tissues and organs, *Nature*  
1199 *Biotechnology*. 32 (2014) 773–785. <https://doi.org/10.1038/nbt.2958>.
- 1200 [71] S. Knowlton, B. Yenilmez, S. Tasoglu, Towards Single-Step Biofabrication of  
1201 Organs on a Chip via 3D Printing, *Trends in Biotechnology*. 34 (2016) 685–688.  
1202 <https://doi.org/10.1016/j.tibtech.2016.06.005>.
- 1203 [72] L. Cavallo, A. Marcianò, M. Cicciù, G. Oteri, 3D Printing beyond Dentistry during  
1204 COVID 19 Epidemic: A Technical Note for Producing Connectors to Breathing  
1205 Devices, *Prosthesis*. 2 (2020) 46–52. <https://doi.org/doi:10.3390/prosthesis2020005>.
- 1206 [73] R. Tino, R. Moore, S. Antoline, P. Ravi, N. Wake, C.N. Ionita, J.M. Morris, S.J.  
1207 Decker, A. Sheikh, F.J. Rybicki, L.L. Chepelev, COVID-19 and the role of 3D  
1208 printing in medicine, *3D Printing in Medicine*. (2020).  
1209 <https://doi.org/10.1186/s41205-020-00064-7>.
- 1210 [74] M. Salmi, J.S. Akmal, E. Pei, J. Wolff, A. Jaribion, S.H. Khajavi, 3D printing in  
1211 COVID-19: Productivity estimation of the most promising open source solutions  
1212 in emergency situations, *Applied Sciences (Switzerland)*. 10 (2020).  
1213 <https://doi.org/10.3390/app10114004>.
- 1214 [75] S. Ishack, S.R. Lipner, Applications of 3D Printing Technology to Address  
1215 COVID-19-Related Supply Shortages, *The American Journal of Medicine*. 133  
1216 (2020) 771–773. <https://doi.org/https://doi.org/10.1016/j.amjmed.2020.04.002>.

- 1217 [76] P. Prabhakar, R.K. Sen, N. Dwivedi, R. Khan, P.R. Solanki, A.K. Srivastava, C.  
1218 Dhand, 3D-Printed Microfluidics and Potential Biomedical Applications,  
1219 *Frontiers in Nanotechnology*. 3 (2021). <https://doi.org/10.3389/fnano.2021.609355>.
- 1220 [77] V. Mehta, S.N. Rath, 3D printed microfluidic devices: a review focused on four  
1221 fundamental manufacturing approaches and implications on the field of  
1222 healthcare, *Bio-Design and Manufacturing*. (2021).  
1223 <https://doi.org/10.1007/s42242-020-00112-5>.
- 1224 [78] C.M.B. Ho, S.H. Ng, K.H.H. Li, Y.-J. Yoon, 3D printed microfluidics for biological  
1225 applications, *Lab on a Chip*. 15 (2015) 3627–3637.  
1226 <https://doi.org/10.1039/C5LC00685F>.
- 1227 [79] H. Nazari, A. Heirani-Tabasi, S. Ghorbani, H. Eyni, S. Razavi Bazaz, M. Khayati,  
1228 F. Gheidari, K. Moradpour, M. Kehtari, S.M. Ahmadi Tafti, S.H. Ahmadi Tafti,  
1229 M.E. Warkiani, Microfluidic-Based Droplets for Advanced Regenerative  
1230 Medicine: Current Challenges and Future Trends, *Biosensors (Basel)*. 12 (2022).  
1231 <https://doi.org/10.3390/bios12010020>.
- 1232 [80] P. Prabhakar, R.K. Sen, N. Dwivedi, R. Khan, P.R. Solanki, A.K. Srivastava, C.  
1233 Dhand, 3D-Printed Microfluidics and Potential Biomedical Applications,  
1234 *Frontiers in Nanotechnology*. 3 (2021). <https://doi.org/10.3389/fnano.2021.609355>.
- 1235 [81] C. Heuer, J.A. Preuß, T. Habib, A. Enders, J. Bahnemann, 3D printing in  
1236 biotechnology—An insight into miniaturized and microfluidic systems for  
1237 applications from cell culture to bioanalytics, *Engineering in Life Sciences*. (2021).  
1238 <https://doi.org/10.1002/elsc.202100081>.
- 1239 [82] L. Wang, M. Pumera, Recent advances of 3D printing in analytical chemistry:  
1240 Focus on microfluidic, separation, and extraction devices, *TrAC - Trends in*  
1241 *Analytical Chemistry*. 135 (2021) 116151.  
1242 <https://doi.org/10.1016/j.trac.2020.116151>.

- 1243 [83] C. Chen, B.T. Mehl, A.S. Munshi, A.D. Townsend, D.M. Spence, R.S. Martin, 3D-  
1244 printed microfluidic devices: fabrication, advantages and limitations - a mini  
1245 review, *Analytical Methods*. 8 (2016) 6005–6012.  
1246 <https://doi.org/10.1039/c6ay01671e>.
- 1247 [84] H. Mea, J. Wan, Microfluidics-enabled functional 3D printing., *Biomicrofluidics*.  
1248 16 2 (2022) 021501.
- 1249 [85] A.K. Au, W. Huynh, L.F. Horowitz, A. Folch, 3D-Printed Microfluidics,  
1250 *Angewandte Chemie - International Edition*. (2016) 3862–3881.  
1251 <https://doi.org/10.1002/anie.201504382>.
- 1252 [86] C. Credi, G. Griffini, M. Levi, S. Turri, Biotinylated Photopolymers for 3D-Printed  
1253 Unibody Lab-on-a-Chip Optical Platforms, *Small*. 14 (2018) 1–8.  
1254 <https://doi.org/10.1002/sml.201702831>.
- 1255 [87] F. Zhu, N. Macdonald, J. Skommer, D. Wlodkowic, Biological implications of lab-  
1256 on-a-chip devices fabricated using multi-jet modelling and stereolithography  
1257 processes, *SPIE Microtechnologies*. 9518 (2015) 951808.  
1258 <https://doi.org/10.1117/12.2180743>.
- 1259 [88] P. Panjan, V. Virtanen, A.M. Sesay, Towards microbioprocess control: An  
1260 inexpensive 3D printed microreactor with integrated online real-Time glucose  
1261 monitoring, *Analyst*. 143 (2018) 3926–3933. <https://doi.org/10.1039/c8an00308d>.
- 1262 [89] G. Weisgrab, A. Ovsianikov, P.F. Costa, Functional 3D Printing for Microfluidic  
1263 Chips, *Advanced Materials Technologies*. 4 (2019).  
1264 <https://doi.org/10.1002/admt.201900275>.
- 1265 [90] N.P. Macdonald, J.M. Cabot, P. Smejkal, R.M. Guijt, B. Paull, M.C. Breadmore,  
1266 Comparing Microfluidic Performance of Three-Dimensional (3D) Printing  
1267 Platforms, *Analytical Chemistry*. 89 (2017) 3858–3866.  
1268 <https://doi.org/10.1021/acs.analchem.7b00136>.

- 1269 [91] M. Zeraatkar, D. Filippini, G. Percoco, On the impact of the fabrication method  
1270 on the performance of 3D printed mixers, *Micromachines (Basel)*. 10 (2019).  
1271 <https://doi.org/10.3390/mi10050298>.
- 1272 [92] R. Melnikova, A. Ehrmann, K. Finsterbusch, 3D printing of textile-based  
1273 structures by Fused Deposition Modelling (FDM) with different polymer  
1274 materials, *IOP Conference Series: Materials Science and Engineering*. 62 (2014).  
1275 <https://doi.org/10.1088/1757-899X/62/1/012018>.
- 1276 [93] J. Emmermacher, D. Spura, J. Cziommer, D. Kilian, T. Wollborn, U. Fritsching, J.  
1277 Steingroewer, T. Walther, M. Gelinsky, A. Lode, Engineering considerations on  
1278 extrusion-based bioprinting: interactions of material behavior, mechanical forces  
1279 and cells in the printing needle, *Biofabrication*. 12 (2020) 025022.  
1280 <https://doi.org/10.1088/1758-5090/ab7553>.
- 1281 [94] S. Vyavahare, S. Teraiya, D. Panghal, S. Kumar, Fused deposition modelling: a  
1282 review, *Rapid Prototyping Journal*. 26 (2020) 176–201.  
1283 <https://doi.org/10.1108/RPJ-04-2019-0106>.
- 1284 [95] S. Crump, Apparatus and method for creating three-dimensional objects - Patent,  
1285 1992. [https://doi.org/10.2116/bunsekikagaku.28.3\\_195](https://doi.org/10.2116/bunsekikagaku.28.3_195).
- 1286 [96] S. Singh, G. Singh, C. Prakash, S. Ramakrishna, Current status and future  
1287 directions of fused filament fabrication, *Journal of Manufacturing Processes*. 55  
1288 (2020) 288–306. <https://doi.org/10.1016/j.jmapro.2020.04.049>.
- 1289 [97] I.J. Solomon, P. Sevvel, J. Gunasekaran, A review on the various processing  
1290 parameters in FDM, *Materials Today: Proceedings*. 37 (2020) 509–514.  
1291 <https://doi.org/10.1016/j.matpr.2020.05.484>.
- 1292 [98] X. Wang, M. Jiang, Z. Zhou, J. Gou, D. Hui, 3D printing of polymer matrix  
1293 composites: A review and prospective, *Composites Part B: Engineering*. 110  
1294 (2017) 442–458. <https://doi.org/10.1016/j.compositesb.2016.11.034>.

- 1295 [99] Raise3D, Pro2 Dual Extruder 3D Printer, (2021). <https://www.raise3d.com/pro2/>  
1296 (accessed August 12, 2021).
- 1297 [100] Ultimaker, Ultimaker S3: Powerful, professional 3D printing, (n.d.).  
1298 <https://ultimaker.com/3d-printers/ultimaker-s3> (accessed August 16, 2021).
- 1299 [101] M.D. Nelson, N. Ramkumar, B.K. Gale, Flexible, transparent, sub-100  $\mu\text{m}$   
1300 microfluidic channels with fused deposition modeling 3D-printed thermoplastic  
1301 polyurethane, *Journal of Micromechanics and Microengineering*. 29 (2019).  
1302 <https://doi.org/10.1088/1361-6439/ab2f26>.
- 1303 [102] S.C. Ligon, R. Liska, J. Stampfl, M. Gurr, R. Mülhaupt, *Polymers for 3D Printing*  
1304 *and Customized Additive Manufacturing*, *Chemical Reviews*. 117 (2017) 10212–  
1305 10290. <https://doi.org/10.1021/acs.chemrev.7b00074>.
- 1306 [103] A.D. Castiaux, C.W. Pinger, E.A. Hayter, M.E. Bunn, R.S. Martin, D.M. Spence,  
1307 PolyJet 3D-Printed Enclosed Microfluidic Channels without Photocurable  
1308 Supports, *Analytical Chemistry*. (2019).  
1309 <https://doi.org/10.1021/acs.analchem.9b01302>.
- 1310 [104] BMF Materials Inc., Industrial Micro-Precision 3D Printers, (2020).  
1311 <https://bmf3d.com/>.
- 1312 [105] Q. Ge, Z. Li, Z. Wang, K. Kowsari, W. Zhang, X. He, J. Zhou, N.X. Fang, Projection  
1313 micro stereolithography based 3D printing and its applications, *International*  
1314 *Journal of Extreme Manufacturing*. 2 (2020). [https://doi.org/10.1088/2631-](https://doi.org/10.1088/2631-7990/ab8d9a)  
1315 [7990/ab8d9a](https://doi.org/10.1088/2631-7990/ab8d9a).
- 1316 [106] WASP, Delta WASP 2040 become PRO, (n.d.). [https://www.allthat3d.com/fastest-](https://www.allthat3d.com/fastest-3d-printers/)  
1317 [3d-printers/](https://www.allthat3d.com/fastest-3d-printers/) (accessed August 12, 2021).
- 1318 [107] D. Han, H. Lee, ScienceDirect Recent advances in multi-material additive  
1319 manufacturing: methods and applications, *Current Opinion in Chemical*  
1320 *Engineering*. 28 (2020) 158–166. <https://doi.org/10.1016/j.coche.2020.03.004>.

- 1321 [108] R.P. Rimington, A.J. Capel, S.D.R. Christie, M.P. Lewis, Biocompatible 3D printed  
1322 polymers: Via fused deposition modelling direct C2C12 cellular phenotype in  
1323 vitro, *Lab on a Chip*. 17 (2017) 2982–2993. <https://doi.org/10.1039/c7lc00577f>.
- 1324 [109] E. Nyberg, A. Rindone, A. Dorafshar, W.L. Grayson, Comparison of 3D-Printed  
1325 Poly- $\epsilon$ -Caprolactone Scaffolds Functionalized with Tricalcium Phosphate,  
1326 Hydroxyapatite, Bio-Oss, or Decellularized Bone Matrix, *Tissue Engineering -*  
1327 *Part A*. (2017). <https://doi.org/10.1089/ten.tea.2016.0418>.
- 1328 [110] V. Raeisdasteh Hokmabad, S. Davaran, A. Ramazani, R. Salehi, Design and  
1329 fabrication of porous biodegradable scaffolds: a strategy for tissue engineering,  
1330 *Journal of Biomaterials Science, Polymer Edition*. 28 (2017) 1797–1825.  
1331 <https://doi.org/10.1080/09205063.2017.1354674>.
- 1332 [111] X. Zhang, W. Fan, T. Liu, Fused deposition modeling 3D printing of polyamide-  
1333 based composites and its applications, *Composites Communications*. 21 (2020)  
1334 100413. <https://doi.org/10.1016/j.coco.2020.100413>.
- 1335 [112] J.A. Lewis, Direct ink writing of 3D functional materials, *Advanced Functional*  
1336 *Materials*. 16 (2006) 2193–2204. <https://doi.org/10.1002/adfm.200600434>.
- 1337 [113] X. Wan, L. Luo, Y. Liu, J. Leng, Direct Ink Writing Based 4D Printing of Materials  
1338 and Their Applications, *Advanced Science*. 7 (2020) 1–29.  
1339 <https://doi.org/10.1002/advs.202001000>.
- 1340 [114] Z. Liu, M. Zhang, B. Bhandari, Y. Wang, 3D printing: Printing precision and  
1341 application in food sector, *Trends in Food Science and Technology*. 69 (2017) 83–  
1342 94. <https://doi.org/10.1016/j.tifs.2017.08.018>.
- 1343 [115] L. Li, Q. Lin, M. Tang, A.J.E. Duncan, C. Ke, Advanced Polymer Designs for  
1344 Direct-Ink-Write 3D Printing, *Chemistry - A European Journal*. 25 (2019) 10768–  
1345 10781. <https://doi.org/10.1002/chem.201900975>.

- 1346 [116] Y. Jiang, J. Plog, A.L. Yarin, Y. Pan, Direct ink writing of surface-modified flax  
1347 elastomer composites, *Composites Part B: Engineering*. 194 (2020) 108061.  
1348 <https://doi.org/10.1016/j.compositesb.2020.108061>.
- 1349 [117] O.D. Yirmibesoglu, L.E. Simonsen, R. Manson, J. Davidson, K. Healy, Y. Menguc,  
1350 T. Wallin, Multi-material direct ink writing of photocurable elastomeric foams,  
1351 *Communications Materials*. 2 (2021). <https://doi.org/10.1038/s43246-021-00186-3>.
- 1352 [118] J.A. Lewis, J.E. Smay, J. Stuecker, J. Cesarano, Direct ink writing of three-  
1353 dimensional ceramic structures, *Journal of the American Ceramic Society*. 89  
1354 (2006) 3599–3609. <https://doi.org/10.1111/j.1551-2916.2006.01382.x>.
- 1355 [119] N.W.S. Pinargote, A. Smirnov, N. Peretyagin, A. Seleznev, P. Peretyagin, Direct  
1356 ink writing technology (3d printing) of graphene-based ceramic nanocomposites:  
1357 A review, *Nanomaterials*. 10 (2020) 1–48. <https://doi.org/10.3390/nano10071300>.
- 1358 [120] J. Li, C. Wu, P.K. Chu, M. Gelinsky, 3D printing of hydrogels: Rational design  
1359 strategies and emerging biomedical applications, *Materials Science and*  
1360 *Engineering R: Reports*. 140 (2020) 100543.  
1361 <https://doi.org/10.1016/j.mser.2020.100543>.
- 1362 [121] V.C.F. Li, C.K. Dunn, Z. Zhang, Y. Deng, H.J. Qi, Direct Ink Write (DIW) 3D  
1363 Printed Cellulose Nanocrystal Aerogel Structures, *Scientific Reports*. 7 (2017) 1–  
1364 8. <https://doi.org/10.1038/s41598-017-07771-y>.
- 1365 [122] S. Tagliaferri, A. Panagiotopoulos, C. Mattevi, Direct ink writing of energy  
1366 materials, *Materials Advances (RSC)*. 2 (2021) 540–563.  
1367 <https://doi.org/10.1039/d0ma00753f>.
- 1368 [123] V. Saggiomo, A.H. Velders, Simple 3D Printed Scaffold-Removal Method for the  
1369 Fabrication of Intricate Microfluidic Devices, *Advanced Science*. 2 (2015).  
1370 <https://doi.org/10.1002/advs.201500125>.
- 1371 [124] L.P. Bressan, T.M. Lima, G.D. da Silveira, J.A.F. da Silva, Low-cost and simple  
1372 FDM-based 3D-printed microfluidic device for the synthesis of metallic core–

- 1373 shell nanoparticles, SN Applied Sciences. 2 (2020) 1–8.  
1374 <https://doi.org/10.1007/s42452-020-2768-2>.
- 1375 [125] L.P. Bressan, J. Robles-Najar, C.B. Adamo, R.F. Quero, B.M.C. Costa, D.P. de  
1376 Jesus, J.A.F. da Silva, 3D-printed microfluidic device for the synthesis of silver  
1377 and gold nanoparticles, *Microchemical Journal*. 146 (2019) 1083–1089.  
1378 <https://doi.org/10.1016/j.microc.2019.02.043>.
- 1379 [126] M. Zeraatkar, M.D. de Tullio, A. Pricci, F. Pignatelli, G. Percoco, Exploiting  
1380 limitations of fused deposition modeling to enhance mixing in 3D printed  
1381 microfluidic devices, *Rapid Prototyping Journal*. 27 (2021) 1850–1859.  
1382 <https://doi.org/10.1108/RPJ-03-2021-0051>.
- 1383 [127] F. Li, N.P. Macdonald, R.M. Guijt, M.C. Breadmore, Using Printing Orientation  
1384 for Tuning Fluidic Behavior in Microfluidic Chips Made by Fused Deposition  
1385 Modeling 3D Printing, *Analytical Chemistry*. 89 (2017) 12805–12811.  
1386 <https://doi.org/10.1021/acs.analchem.7b03228>.
- 1387 [128] F. Kotz, M. Mader, N. Dellen, P. Risch, A. Kick, D. Helmer, B.E. Rapp, Fused  
1388 deposition modeling of microfluidic chips in polymethylmethacrylate,  
1389 *Micromachines (Basel)*. 11 (2020) 5–8. <https://doi.org/10.3390/mi11090873>.
- 1390 [129] L.P. Bressan, C.B. Adamo, R.F. Quero, D.P. de Jesus, J.A.F. da Silva, A simple  
1391 procedure to produce FDM-based 3D-printed microfluidic devices with an  
1392 integrated PMMA optical window, *Analytical Methods*. 11 (2019) 1014–1020.  
1393 <https://doi.org/10.1039/c8ay02092b>.
- 1394 [130] G. Gaal, M. Mendes, T.P. de Almeida, M.H.O. Piazzetta, Â.L. Gobbi, A. Riul, V.  
1395 Rodrigues, Simplified fabrication of integrated microfluidic devices using fused  
1396 deposition modeling 3D printing, *Sensors and Actuators, B: Chemical*. 242 (2017)  
1397 35–40. <https://doi.org/10.1016/j.snb.2016.10.110>.
- 1398 [131] V. Romanov, R. Samuel, M. Chaharlang, A.R. Jafek, A. Frost, B.K. Gale, FDM 3D  
1399 Printing of High-Pressure, Heat-Resistant, Transparent Microfluidic Devices,

1400 Analytical Chemistry. 90 (2018) 10450–10456.  
1401 <https://doi.org/10.1021/acs.analchem.8b02356>.

1402 [132] T. Ching, Y. Li, R. Karyappa, A. Ohno, Y.C. Toh, M. Hashimoto, Fabrication of  
1403 integrated microfluidic devices by direct ink writing (DIW) 3D printing, *Sensors*  
1404 and *Actuators*, B: Chemical. 297 (2019) 126609.  
1405 <https://doi.org/10.1016/j.snb.2019.05.086>.

1406 [133] M. Athanasiadis, A. Pak, D. Afanaskau, I.R. Mineev, Direct Writing of Elastic  
1407 Fibers with Optical, Electrical, and Microfluidic Functionality, *Advanced*  
1408 *Materials Technologies*. 4 (2019). <https://doi.org/10.1002/admt.201800659>.

1409 [134] D. Hur, M.G. Say, S.E. Diltemiz, F. Duman, A. Ersöz, R. Say, 3D Micropatterned  
1410 All-Flexible Microfluidic Platform for Microwave-Assisted Flow Organic  
1411 Synthesis, *Chempluschem*. 83 (2018) 42–46.  
1412 <https://doi.org/10.1002/cplu.201700440>.

1413 [135] Y. Alvarez-Braña, J. Etxebarria-Elezgarai, L. Ruiz de Larrinaga-Vicente, F. Benito-  
1414 Lopez, L. Basabe-Desmonts, Modular micropumps fabricated by 3D printed  
1415 technologies for polymeric microfluidic device applications, *Sensors and*  
1416 *Actuators*, B: Chemical. 342 (2021). <https://doi.org/10.1016/j.snb.2021.129991>.

1417 [136] F. Li, N.P. Macdonald, R.M. Guijt, M.C. Breadmore, Increasing the functionalities  
1418 of 3D printed microchemical devices by single material, multimaterial, and print-  
1419 pause-print 3D printing, *Lab on a Chip*. 19 (2019) 35–49.  
1420 <https://doi.org/10.1039/c8lc00826d>.

1421 [137] M. Kuang, L. Wang, Y. Song, Controllable Printing Droplets for High-Resolution  
1422 Patterns, *Advanced Materials*. 26 (2014) 6950–6958.  
1423 <https://doi.org/10.1002/adma.201305416>.

1424 [138] FacFox documents, PolyJet vs MultiJet Printing(MJP), (2019).  
1425 <https://facfox.com/docs/kb/polyjet-mjp-comparison> (accessed August 11, 2021).

- 1426 [139] H. Gudapati, M. Dey, I. Ozbolat, A comprehensive review on droplet-based  
1427 bioprinting: Past, present and future, *Biomaterials*. 102 (2016) 20–42.  
1428 <https://doi.org/10.1016/j.biomaterials.2016.06.012>.
- 1429 [140] W.L. Ng, W.Y. Yeong, M.W. Naing, Polyvinylpyrrolidone-based bio-ink  
1430 improves cell viability and homogeneity during drop-on-demand printing,  
1431 *Materials*. 10 (2017). <https://doi.org/10.3390/ma10020190>.
- 1432 [141] Y. Guo, H.S. Patanwala, B. Bognet, A.W.K. Ma, Inkjet and inkjet-based 3D  
1433 printing: Connecting fluid properties and printing performance, *Rapid*  
1434 *Prototyping Journal*. 23 (2017) 562–576. <https://doi.org/10.1108/RPJ-05-2016-0076>.
- 1435 [142] B. Derby, Bioprinting: Inkjet printing proteins and hybrid cell-containing  
1436 materials and structures, *Journal of Materials Chemistry*. 18 (2008) 5717–5721.  
1437 <https://doi.org/10.1039/b807560c>.
- 1438 [143] E.M. Kritchman, I. Zeytoun, RAPID PROTOTYPING APPARATUS (US 8.323.017  
1439 B2), 2011.
- 1440 [144] Y. Yagci, S. Jockusch, N.J. Turro, Photoinitiated polymerization: Advances,  
1441 challenges, and opportunities, *Macromolecules*. 43 (2010) 6245–6260.  
1442 <https://doi.org/10.1021/ma1007545>.
- 1443 [145] J. V Crivello, E. Reichmanis, *Photopolymer Materials and Processes for Advanced*  
1444 *Technologies*, (2014).
- 1445 [146] M. Gastaldi, F. Cardano, M. Zanetti, G. Viscardi, C. Barolo, S. Bordiga, S.  
1446 Magdassi, A. Fin, I. Roppolo, Functional Dyes in Polymeric 3D Printing:  
1447 Applications and Perspectives, (2021).  
1448 <https://doi.org/10.1021/acsmaterialslett.0c00455>.
- 1449 [147] F. Wang, Y. Chong, F.K. Wang, C. He, Photopolymer resins for luminescent three-  
1450 dimensional printing, *Journal of Applied Polymer Science*. 134 (2017) 1–8.  
1451 <https://doi.org/10.1002/app.44988>.

- 1452 [148] M. Schuster, C. Turecek, B. Kaiser, J. Stampfl, R. Liska, F. Varga, Evaluation of  
1453 biocompatible photopolymers I: Photoreactivity and mechanical properties of  
1454 reactive diluents, *Journal of Macromolecular Science, Part A: Pure and Applied*  
1455 *Chemistry*. 44 (2007) 547–557. <https://doi.org/10.1080/10601320701235958>.
- 1456 [149] M. Sugavaneswaran, G. Arumaikkannu, Analytical and experimental  
1457 investigation on elastic modulus of reinforced additive manufactured structure,  
1458 *Materials and Design*. 66 (2015) 29–36.  
1459 <https://doi.org/10.1016/j.matdes.2014.10.029>.
- 1460 [150] N. Vidakis, M. Petousis, N. Vaxevanidis, J. Kechagias, Surface Roughness  
1461 Investigation of Poly-Jet 3D Printing, *Mathematics*. 8 (2020) 1758.  
1462 <https://doi.org/10.3390/math8101758>.
- 1463 [151] J.M. Lee, M. Zhang, W.Y. Yeong, Characterization and evaluation of 3D printed  
1464 microfluidic chip for cell processing, *Microfluidics and Nanofluidics*. 20 (2016) 1–  
1465 15. <https://doi.org/10.1007/s10404-015-1688-8>.
- 1466 [152] N.F. Ayub, S. Hashim, J. Jamaluddin, N. Adrus, New UV LED curing approach  
1467 for polyacrylamide and poly(: N -isopropylacrylamide) hydrogels, *New Journal*  
1468 *of Chemistry*. (2017). <https://doi.org/10.1039/c7nj00176b>.
- 1469 [153] V. Mucci, C. Vallo, Efficiency of 2,2-dimethoxy-2-phenylacetophenone for the  
1470 photopolymerization of methacrylate monomers in thick sections, *Journal of*  
1471 *Applied Polymer Science*. (2012). <https://doi.org/10.1002/app.34473>.
- 1472 [154] B. Steyrer, P. Neubauer, R. Liska, J. Stampfl, Visible light photoinitiator for 3D-  
1473 printing of tough methacrylate resins, *Materials*. 10 (2017) 1–11.  
1474 <https://doi.org/10.3390/ma10121445>.
- 1475 [155] H.K. Park, M. Shin, B. Kim, J.W. Park, H. Lee, A visible light-curable yet visible  
1476 wavelength-transparent resin for stereolithography 3D printing, *NPG Asia*  
1477 *Materials*. 10 (2018) 82–89. <https://doi.org/10.1038/s41427-018-0021-x>.

- 1478 [156] B.D. Fairbanks, M.P. Schwartz, C.N. Bowman, K.S. Anseth, Photoinitiated  
1479 polymerization of PEG-diacrylate with lithium phenyl-2,4,6-  
1480 trimethylbenzoylphosphinate: polymerization rate and cytocompatibility,  
1481 *Biomaterials*. 30 (2009) 6702–6707.  
1482 <https://doi.org/10.1016/j.biomaterials.2009.08.055>.
- 1483 [157] K. Wang, K. Yang, Q. Yu, Novel polymeric photoinitiators with side-chain  
1484 benzophenone: Facile synthesis and photopolymerization properties without  
1485 coinitiator, *Progress in Organic Coatings*. (2014).  
1486 <https://doi.org/10.1016/j.porgcoat.2014.06.026>.
- 1487 [158] H. Matsushima, S. Hait, Q. Li, H. Zhou, M. Shirai, C.E. Hoyle, Non-extractable  
1488 photoinitiators based on thiol-functionalized benzophenones and thioxanthenes,  
1489 *European Polymer Journal*. (2010).  
1490 <https://doi.org/10.1016/j.eurpolymj.2010.03.003>.
- 1491 [159] Y.C. Chen, J.L. Ferracane, S.A. Prahl, Quantum yield of conversion of the  
1492 photoinitiator camphorquinone, *Dental Materials*. (2007).  
1493 <https://doi.org/10.1016/j.dental.2006.06.005>.
- 1494 [160] R.D. Sochol, E. Sweet, C.C. Glick, S. Venkatesh, A. Avetisyan, K.F. Ekman, A.  
1495 Raulinaitis, A. Tsai, A. Wienkers, K. Korner, K. Hanson, A. Long, B.J. Hightower,  
1496 G. Slatton, D.C. Burnett, T.L. Massey, K. Iwai, L.P. Lee, K.S.J. Pister, L. Lin, 3D  
1497 printed microfluidic circuitry via multijet-based additive manufacturing, *Lab on  
1498 a Chip*. 16 (2016) 668–678. <https://doi.org/10.1039/c5lc01389e>.
- 1499 [161] E. Sweet, R. Mehta, Y. Xu, R. Jew, R. Lin, L. Lin, Finger-powered fluidic actuation  
1500 and mixing: Via MultiJet 3D printing, *Lab on a Chip*. 20 (2020) 3375–3385.  
1501 <https://doi.org/10.1039/d0lc00488j>.
- 1502 [162] R. Walczak, K. Adamski, W. Kubicki, Inkjet 3D printed chip for capillary gel  
1503 electrophoresis, *Sensors and Actuators, B: Chemical*. 261 (2018) 474–480.  
1504 <https://doi.org/10.1016/j.snb.2018.01.174>.

- 1505 [163] E.A. Mansur, M. YE, Y. WANG, Y. DAI, A State-of-the-Art Review of Mixing in  
1506 Microfluidic Mixers, *Chinese Journal of Chemical Engineering*. (2008).  
1507 [https://doi.org/10.1016/S1004-9541\(08\)60114-7](https://doi.org/10.1016/S1004-9541(08)60114-7).
- 1508 [164] C.Y. Lee, C.L. Chang, Y.N. Wang, L.M. Fu, Microfluidic mixing: A review,  
1509 *International Journal of Molecular Sciences*. (2011).  
1510 <https://doi.org/10.3390/ijms12053263>.
- 1511 [165] C.Y. Lee, W.T. Wang, C.C. Liu, L.M. Fu, Passive mixers in microfluidic systems:  
1512 A review, *Chemical Engineering Journal*. (2016).  
1513 <https://doi.org/10.1016/j.cej.2015.10.122>.
- 1514 [166] A. Enders, I.G. Siller, K. Urmann, M.R. Hoffmann, J. Bahnemann, 3D Printed  
1515 Microfluidic Mixers—A Comparative Study on Mixing Unit Performances, *Small*.  
1516 15 (2019) 1–9. <https://doi.org/10.1002/sml.201804326>.
- 1517 [167] C. Chen, B.T. Mehl, A.S. Munshi, A.D. Townsend, D.M. Spence, R.S. Martin, 3D-  
1518 printed microfluidic devices: fabrication, advantages and limitations - a mini  
1519 review, *Analytical Methods*. (2016). <https://doi.org/10.1039/c6ay01671e>.
- 1520 [168] A.M. Tothill, M. Partridge, S.W. James, R.P. Tatam, Fabrication and optimisation  
1521 of a fused filament 3D-printed microfluidic platform, *Journal of Micromechanics  
1522 and Microengineering*. 27 (2017). <https://doi.org/10.1088/1361-6439/aa5ae3>.
- 1523 [169] S.J. Keating, M.I. Gariboldi, W.G. Patrick, S. Sharma, D.S. Kong, N. Oxman, 3D  
1524 printed multimaterial microfluidic valve, *PLoS ONE*. 11 (2016) 1–12.  
1525 <https://doi.org/10.1371/journal.pone.0160624>.
- 1526 [170] W.L. Ng, J.M. Lee, M. Zhou, Y.W. Chen, K.X.A. Lee, W.Y. Yeong, Y.F. Shen, Vat  
1527 polymerization-based bioprinting - process, materials, applications and  
1528 regulatory challenges, *Biofabrication*. 12 (2020). [https://doi.org/10.1088/1758-  
1529 5090/ab6034](https://doi.org/10.1088/1758-5090/ab6034).
- 1530 [171] W. Li, L.S. Mille, J.A. Robledo, T. Uribe, V. Huerta, Y.S. Zhang, Recent Advances  
1531 in Formulating and Processing Biomaterial Inks for Vat Polymerization-Based 3D

1532           Printing, *Advanced Healthcare Materials*. 9 (2020) 1–18.  
1533           <https://doi.org/10.1002/adhm.202000156>.

1534 [172] F.P.W. Melchels, J. Feijen, D.W. Grijpma, A review on stereolithography and its  
1535           applications in biomedical engineering, *Biomaterials*. 31 (2010) 6121–6130.  
1536           <https://doi.org/10.1016/j.biomaterials.2010.04.050>.

1537 [173] R.D. Farahani, M. Dubé, D. Therriault, Three-Dimensional Printing of  
1538           Multifunctional Nanocomposites: Manufacturing Techniques and Applications,  
1539           *Advanced Materials*. (2016) 5794–5821. <https://doi.org/10.1002/adma.201506215>.

1540 [174] M.G. Guerra, C. Volpone, L.M. Galantucci, G. Percoco, Photogrammetric  
1541           measurements of 3D printed microfluidic devices, *Additive Manufacturing*. 21  
1542           (2018) 53–62. <https://doi.org/10.1016/j.addma.2018.02.013>.

1543 [175] H. Kodama, Automatic method for fabricating a three-dimensional plastic model  
1544           with photo-hardening polymer, *Review of Scientific Instruments*. (1981).  
1545           <https://doi.org/10.1063/1.1136492>.

1546 [176] C.W. Hull, Apparatus for Production of Three-Dimensional Objects By  
1547           Stereolithography, Patent. (1984) 16.

1548 [177] A. Oesterreicher, J. Wiener, M. Roth, A. Moser, R. Gmeiner, M. Edler, G. Pinter,  
1549           T. Griesser, Tough and degradable photopolymers derived from alkyne  
1550           monomers for 3D printing of biomedical materials, *Polymer Chemistry*. (2016).  
1551           <https://doi.org/10.1039/c6py01132b>.

1552 [178] K. Ikuta, K. Hirowatari, Real three dimensional micro fabrication using stereo  
1553           lithography and metal molding, in: *Proceedings IEEE Micro Electro Mechanical*  
1554           *Systems*, Fort Lauderdale, FL, USA, 1993: pp. 42–27.  
1555           <https://doi.org/10.1109/MEMSYS.1993.296949>.

1556 [179] J. DeSimone, E. Sarnulski, A. Ermoshkin, P. DeSimone, Rapid 3D Continuous  
1557           Printing of Casting Molds for Metals and Other Materials, WO 2015/080888A2,  
1558           2015.

- 1559 [180] H. Quan, T. Zhang, H. Xu, S. Luo, J. Nie, X. Zhu, Photo-curing 3D printing  
1560 technique and its challenges, *Bioactive Materials*. (2020).  
1561 <https://doi.org/10.1016/j.bioactmat.2019.12.003>.
- 1562 [181] J.F. Xing, M.L. Zheng, X.M. Duan, Two-photon polymerization microfabrication  
1563 of hydrogels: an advanced 3D printing technology for tissue engineering and  
1564 drug delivery, *Chemical Society Reviews*. (2015).  
1565 <https://doi.org/10.1039/c5cs00278h>.
- 1566 [182] I. Bhattacharya, B. Kelly, M. Shusteff, C. Spadaccini, H. Taylor, Computed axial  
1567 lithography: volumetric 3D printing of arbitrary geometries (Conference  
1568 Presentation), in: 2018. <https://doi.org/10.1117/12.2307780>.
- 1569 [183] H. Li, W. Fan, X. Zhu, Three-dimensional printing: The potential technology  
1570 widely used in medical fields, *Journal of Biomedical Materials Research - Part A*.  
1571 (2020). <https://doi.org/10.1002/jbm.a.36979>.
- 1572 [184] P. Juskova, A. Ollitrault, M. Serra, J.L. Viovy, L. Malaquin, Resolution  
1573 improvement of 3D stereo-lithography through the direct laser trajectory  
1574 programming: Application to microfluidic deterministic lateral displacement  
1575 device, *Analytica Chimica Acta*. (2018). <https://doi.org/10.1016/j.aca.2017.11.062>.
- 1576 [185] Y. Liu, Q. Hu, F. Zhang, C. Tuck, D. Irvine, R. Hague, Y. He, M. Simonelli, G.A.  
1577 Rance, E.F. Smith, R.D. Wildman, Additive manufacture of three dimensional  
1578 nanocomposite based objects through multiphoton fabrication, *Polymers (Basel)*.  
1579 8 (2016) 325. <https://doi.org/10.3390/polym8090325>.
- 1580 [186] Y.-L. Cheng, H.-L. Kao, Study on visible-light-curable polycaprolactone and  
1581 poly(ethylene glycol) diacrylate for LCD-projected maskless additive  
1582 manufacturing system, in: *Light Manipulating Organic Materials and Devices II*,  
1583 2015. <https://doi.org/10.1117/12.2188047>.
- 1584 [187] S.H. Kim, Y.K. Yeon, J.M. Lee, J.R. Chao, Y.J. Lee, Y.B. Seo, M.T. Sultan, O.J. Lee,  
1585 J.S. Lee, S. Il Yoon, I.S. Hong, G. Khang, S.J. Lee, J.J. Yoo, C.H. Park, Precisely

1586 printable and biocompatible silk fibroin bioink for digital light processing 3D  
1587 printing, *Nature Communications*. 9 (2018) 1–14. [https://doi.org/10.1038/s41467-](https://doi.org/10.1038/s41467-018-03759-y)  
1588 [018-03759-y](https://doi.org/10.1038/s41467-018-03759-y).

1589 [188] C. Yu, J. Schimelman, P. Wang, K.L. Miller, X. Ma, S. You, J. Guan, B. Sun, W.  
1590 Zhu, S. Chen, Photopolymerizable Biomaterials and Light-Based 3D Printing  
1591 Strategies for Biomedical Applications, *Chemical Reviews*. (2020).  
1592 <https://doi.org/10.1021/acs.chemrev.9b00810>.

1593 [189] A.K. Nguyen, R.J. Narayan, Two-photon polymerization for biological  
1594 applications, *Materials Today*. (2017).  
1595 <https://doi.org/10.1016/j.mattod.2017.06.004>.

1596 [190] R. Infuehr, J. Stampfl, S. Krivec, R. Liska, H. Lichtenegger, V. Satzinger, V.  
1597 Schmidt, N. Matsko, W. Grogger, 3D-structuring of optical waveguides with two  
1598 photon polymerization, *MRS Proceedings*. 1179 (2009) 1179-BB01-07.  
1599 <https://doi.org/10.1557/PROC-1179-BB01-07>.

1600 [191] R. Whitby, Y. Ben-Tal, R. MacMillan, S. Janssens, S. Raymond, D. Clarke, J. Jin, A.  
1601 Kay, M.C. Simpson, Photoinitiators for two-photon polymerisation: effect of  
1602 branching and viscosity on polymerisation thresholds, *RSC Advances*. 7 (2017)  
1603 13232–13239. <https://doi.org/10.1039/c6ra27176f>.

1604 [192] B.E. Kelly, I. Bhattacharya, H. Heidari, M. Shusteff, C.M. Spadaccini, H.K. Taylor,  
1605 Volumetric additive manufacturing via tomographic reconstruction, *Science*  
1606 (1979). (2019). <https://doi.org/10.1126/science.aau7114>.

1607 [193] B.E. Kelly, I. Bhattacharya, M. Shusteff, H.K. Taylor, C.M. Spaddacini, Computed  
1608 axial lithography for rapid volumetric 3D additive manufacturing, in: *Solid*  
1609 *Freeform Fabrication 2017: Proceedings of the 28th Annual International Solid*  
1610 *Freeform Fabrication Symposium - An Additive Manufacturing Conference, SFF*  
1611 *2017, 2020*.

- 1612 [194] P.N. Bernal, P. Delrot, D. Loterie, Y. Li, J. Malda, C. Moser, R. Levato,  
1613 Biofabrication: Volumetric Bioprinting of Complex Living-Tissue Constructs  
1614 within Seconds (*Adv. Mater.* 42/2019), *Advanced Materials*. (2019).  
1615 <https://doi.org/10.1002/adma.201970302>.
- 1616 [195] J.P. Fouassier, J. Lalevée, *Photoinitiators for Polymer Synthesis*, 2012.  
1617 <https://doi.org/10.1002/9783527648245>.
- 1618 [196] B. Narupai, A. Nelson, 100th Anniversary of Macromolecular Science Viewpoint:  
1619 Macromolecular Materials for Additive Manufacturing, *ACS Macro Letters*.  
1620 (2020) 627–638. <https://doi.org/10.1021/acsmacrolett.0c00200>.
- 1621 [197] J. Lammel-Lindemann, I.A. Dourado, J. Shanklin, C.A. Rodriguez, L.H. Catalani,  
1622 D. Dean, Photocrosslinking-based 3D printing of unsaturated polyesters from  
1623 isosorbide: A new material for resorbable medical devices, *Bioprinting*. (2020).  
1624 <https://doi.org/10.1016/j.bprint.2019.e00062>.
- 1625 [198] P.J. Scott, V. Meenakshisundaram, M. Hegde, C.R. Kasprzak, C.R. Winkler, K.D.  
1626 Feller, C.B. Williams, T.E. Long, 3D Printing Latex: A Route to Complex  
1627 Geometries of High Molecular Weight Polymers, *ACS Applied Materials and*  
1628 *Interfaces*. (2020). <https://doi.org/10.1021/acсами.9b19986>.
- 1629 [199] H. Leonards, S. Engelhardt, A. Hoffmann, L. Pongratz, S. Schriever, J. Bläsius, M.  
1630 Wehner, A. Gillner, Advantages and drawbacks of Thiol-ene based resins for 3D-  
1631 printing, in: *Laser 3D Manufacturing II*, 2015. <https://doi.org/10.1117/12.2081169>.
- 1632 [200] T. Zhao, X. Li, R. Yu, Y. Zhang, X. Yang, X. Zhao, L. Wang, W. Huang, Silicone-  
1633 Epoxy-Based Hybrid Photopolymers for 3D Printing, *Macromolecular Chemistry*  
1634 *and Physics*. 219 (2018) 1–10. <https://doi.org/10.1002/macp.201700530>.
- 1635 [201] A. Bagheri, J. Jin, Photopolymerization in 3D Printing, *ACS Applied Polymer*  
1636 *Materials*. 1 (2019) 593–611. <https://doi.org/10.1021/acсаpm.8b00165>.

- 1637 [202] S. Shanmugam, J. Xu, C. Boyer, Light-regulated polymerization under near-  
1638 infrared/far-red irradiation catalyzed by bacteriochlorophyll a, *Angewandte*  
1639 *Chemie - International Edition*. (2016). <https://doi.org/10.1002/anie.201510037>.
- 1640 [203] N. Corrigan, J. Xu, C. Boyer, A Photoinitiation System for Conventional and  
1641 Controlled Radical Polymerization at Visible and NIR Wavelengths,  
1642 *Macromolecules*. (2016). <https://doi.org/10.1021/acs.macromol.6b00542>.
- 1643 [204] A. Al Mousawi, C. Poriel, F. Dumur, J. Toufaily, T. Hamieh, J.P. Fouassier, J.  
1644 Lalevée, Zinc Tetraphenylporphyrin as High Performance Visible Light  
1645 Photoinitiator of Cationic Photosensitive Resins for LED Projector 3D Printing  
1646 Applications, *Macromolecules*. (2017).  
1647 <https://doi.org/10.1021/acs.macromol.6b02596>.
- 1648 [205] J. Xu, S. Shanmugam, C. Fu, K.F. Aguey-Zinsou, C. Boyer, Selective  
1649 Photoactivation: From a Single Unit Monomer Insertion Reaction to Controlled  
1650 Polymer Architectures, *J Am Chem Soc*. (2016).  
1651 <https://doi.org/10.1021/jacs.5b12408>.
- 1652 [206] B.M. Hong, S.A. Park, W.H. Park, Effect of photoinitiator on chain degradation of  
1653 hyaluronic acid, *Biomaterials Research*. (2019). [https://doi.org/10.1186/s40824-](https://doi.org/10.1186/s40824-019-0170-1)  
1654 [019-0170-1](https://doi.org/10.1186/s40824-019-0170-1).
- 1655 [207] J. Zhang, J. Lalevée, J. Zhao, B. Graff, M.H. Stenzel, P. Xiao,  
1656 Dihydroxyanthraquinone derivatives: Natural dyes as blue-light-sensitive  
1657 versatile photoinitiators of photopolymerization, *Polymer Chemistry*. (2016).  
1658 <https://doi.org/10.1039/c6py01550f>.
- 1659 [208] F. Masson, C. Decker, S. Andre, X. Andrieu, UV-curable formulations for UV-  
1660 transparent optical fiber coatings: I. Acrylic resins, *Progress in Organic Coatings*.  
1661 49 (2004) 1–12. [https://doi.org/10.1016/S0300-9440\(03\)00122-X](https://doi.org/10.1016/S0300-9440(03)00122-X).
- 1662 [209] J.P. Fouassier, J. Lalevée, *Photoinitiators for Polymer Synthesis*, 2012.  
1663 <https://doi.org/10.1002/9783527648245>.

- 1664 [210] M. Stemmelen, F. Pessel, V. Lapinte, S. Caillol, J.P. Habas, J.J. Robin, A fully  
1665 biobased epoxy resin from vegetable oils: From the synthesis of the precursors by  
1666 thiol-ene reaction to the study of the final material, *Journal of Polymer Science,*  
1667 *Part A: Polymer Chemistry.* 49 (2011) 2434–2444.  
1668 <https://doi.org/10.1002/pola.24674>.
- 1669 [211] A. Ravve, *Light-Associated Reactions of Synthetic Polymers*, Springer US, 2006.
- 1670 [212] A. Santini, I.T. Gallegos, C.M. Felix, Photoinitiators in dentistry: a review., *Prim*  
1671 *Dent J.* (2013). <https://doi.org/10.1308/205016814809859563>.
- 1672 [213] I. Kunio, E. Takeshi, A review of the development of radical photopolymerization  
1673 initiators used for designing light-curing dental adhesives and resin composites,  
1674 *Dental Materials Journal.* (2010). <https://doi.org/10.4012/dmj.2009-137>.
- 1675 [214] J. Lalevée, F. Morlet-Savary, C. Dietlin, B. Graff, J.P. Fouassier, Photochemistry  
1676 and radical chemistry under low intensity visible light sources: Application to  
1677 photopolymerization reactions, *Molecules.* (2014).  
1678 <https://doi.org/10.3390/molecules190915026>.
- 1679 [215] M. Kaur, A.K. Srivastava, Photopolymerization: A review, *Journal of*  
1680 *Macromolecular Science - Polymer Reviews.* (2002). [https://doi.org/10.1081/MC-](https://doi.org/10.1081/MC-120015988)  
1681 [120015988](https://doi.org/10.1081/MC-120015988).
- 1682 [216] C. Kutall, P.A. Grutsch, D.B. Yang, A novel strategy for photoinitiated anionic-  
1683 polymerization, *Macromolecules.* 24 (1991) 6872–6873.  
1684 <https://doi.org/10.1021/ma00026a016>.
- 1685 [217] B.J. Palmer, C. Kutal, R. Billing, H. Hening, A new photoinitiator for anionic-  
1686 polymerization, *Macromolecules.* 28 (1995) 1328–1329.  
1687 <https://doi.org/10.1021/ma00108a078>.
- 1688 [218] Y.H. Wang, P. Wan, Ketoprofen as a photoinitiator for anionic polymerization,  
1689 *Photochemical and Photobiological Sciences.* (2015).  
1690 <https://doi.org/10.1039/c4pp00454j>.

- 1691 [219] M. Rahal, H. Mokbel, B. Gra, J. Toufaily, T. Hamieh, J. Lalev, Mono vs.  
1692 Difunctional Coumarin as Photoinitiators in Photocomposite Synthesis and 3D  
1693 Printing, *Catalysts*. 10 (2020) 1–18. <https://doi.org/doi:10.3390/catal10101202>.
- 1694 [220] A.K. Nguyen, P.L. Goering, R.K. Elespuru, S.S. Das, R.J. Narayan, The  
1695 photoinitiator lithium phenyl (2,4,6-Trimethylbenzoyl) phosphinate with  
1696 exposure to 405 nm light is cytotoxic to mammalian cells but not mutagenic in  
1697 bacterial reverse mutation assays, *Polymers (Basel)*. 12 (2020) 1–13.  
1698 <https://doi.org/10.3390/polym12071489>.
- 1699 [221] W. Tomal, J. Ortyl, Water-soluble photoinitiators in biomedical applications,  
1700 *Polymers (Basel)*. 12 (2020) 1–30. <https://doi.org/10.3390/POLYM12051073>.
- 1701 [222] T.N. Eren, T. Gencoglu, M. Abdallah, J. Lalevée, D. Avci, A water soluble and  
1702 highly reactive bisphosphonate functionalized thioxanthone-based  
1703 photoinitiator, *European Polymer Journal*. 135 (2020) 109906.  
1704 <https://doi.org/10.1016/j.eurpolymj.2020.109906>.
- 1705 [223] L. Breloy, C. Negrell, A.S. Mora, W.S.J. Li, V. Brezová, S. Caillol, D.L. Versace,  
1706 Vanillin derivative as performing type I photoinitiator, *European Polymer*  
1707 *Journal*. 132 (2020) 109727. <https://doi.org/10.1016/j.eurpolymj.2020.109727>.
- 1708 [224] D.M. Love, B.D. Fairbanks, C.N. Bowman, Evaluation of Aromatic Thiols as  
1709 Photoinitiators, *Macromolecules*. 53 (2020) 5237–5247.  
1710 <https://doi.org/10.1021/acs.macromol.0c00757>.
- 1711 [225] S. Liu, H. Chen, Y. Zhang, K. Sun, Y. Xu, F. Morlet-Savary, B. Graff, G. Noirbent,  
1712 C. Pigot, D. Brunel, M. Nechab, D. Gigmes, P. Xiao, F. Dumur, J. Lalevée,  
1713 Monocomponent photoinitiators based on benzophenone-carbazole structure for  
1714 LED photoinitiating systems and application on 3D printing, *Polymers (Basel)*. 12  
1715 (2020) 1–15. <https://doi.org/10.3390/polym12061394>.
- 1716 [226] R. Ni, B. Qian, C. Liu, X. Liu, J. Qiu, Three-dimensional printing of hybrid  
1717 organic/inorganic composites with long persistence luminescence, *Optical*

- 1718 Materials Express. 8 (2018) 2823–2831. <https://doi.org/10.1016/S0920->  
1719 9964(12)70638-2.
- 1720 [227] J. Palaganas, A.C. de Leon, J. Mangadlao, N. Palaganas, A. Mael, Y.J. Lee, H.Y.  
1721 Lai, R. Advincula, Facile Preparation of Photocurable Siloxane Composite for 3D  
1722 Printing, *Macromolecular Materials and Engineering*. 302 (2017) 1–9.  
1723 <https://doi.org/10.1002/mame.201600477>.
- 1724 [228] C.M. González-Henríquez, G. del C. Pizarro, M.A. Sarabia-Vallejos, C.A. Terraza,  
1725 Z.E. López-Cabaña, In situ-preparation and characterization of silver-  
1726 HEMA/PEGDA hydrogel matrix nanocomposites: Silver inclusion studies into  
1727 hydrogel matrix, *Arabian Journal of Chemistry*. (2014).  
1728 <https://doi.org/10.1016/j.arabjc.2014.11.012>.
- 1729 [229] E.T. Tenório-Neto, M.R. Guilherme, M.E.G. Winkler, L. Cardozo-Filho, S.C.  
1730 Beneti, A.F. Rubira, M.H. Kunita, Synthesis and characterization of silver  
1731 nanoparticle nanocomposite thin films with thermally induced surface  
1732 morphology changes, *Materials Letters*. 159 (2015) 118–121.  
1733 <https://doi.org/10.1016/j.matlet.2015.06.095>.
- 1734 [230] V. Jankauskaite, A. Lazauskas, E. Gri Konis, A. Lisauskaite, K. Ukiene, UV-  
1735 curable aliphatic silicone acrylate organic–inorganic hybrid coatings with  
1736 antibacterial activity, *Molecules*. 22 (2017).  
1737 <https://doi.org/10.3390/molecules22060964>.
- 1738 [231] Y.-C. Chen, T.-Y. Liu, Y.-H. Li, Photoreactivity study of photoinitiated free radical  
1739 polymerization using Type II photoinitiator containing thioxanthone initiator as  
1740 a hydrogen acceptor and various amine-type co-initiators as hydrogen donors,  
1741 *Journal of Coatings Technology and Research*. (2020).  
1742 <https://doi.org/10.1007/s11998-020-00401-9>.
- 1743 [232] G. Gonzalez, A. Chiappone, I. Roppolo, E. Fantino, V. Bertana, F. Perrucci, L.  
1744 Scaltrito, F. Pirri, M. Sangermano, Development of 3D printable formulations

1745 containing CNT with enhanced electrical properties, *Polymer (Guildf)*. 109 (2016)  
1746 246–253. <https://doi.org/10.1016/j.polymer.2016.12.051>.

1747 [233] J.S. Manzano, Z.B. Weinstein, A.D. Sadow, I.I. Slowing, Direct 3D Printing of  
1748 Catalytically Active Structures, *ACS Catalysis*. 7 (2017) 7567–7577.  
1749 <https://doi.org/10.1021/acscatal.7b02111>.

1750 [234] G.A. González Flores, V. Bertana, A. Chiappone, I. Roppolo, L. Scaltrito, S.L.  
1751 Marasso, M. Cocuzza, G. Massaglia, M. Quaglio, C.F. Pirri, S. Ferrero, Single-Step  
1752 3D Printing of Silver-Patterned Polymeric Devices for Bacteria Proliferation  
1753 Control, *Macromolecular Materials and Engineering*. 2100596 (2021) 2100596.  
1754 <https://doi.org/10.1002/mame.202100596>.

1755 [235] P.F. Costa, H.J. Albers, J.E.A. Linssen, H.H.T. Middelkamp, L. Van Der Hout, R.  
1756 Passier, A. Van Den Berg, J. Malda, A.D. Van Der Meer, Mimicking arterial  
1757 thrombosis in a 3D-printed microfluidic: In vitro vascular model based on  
1758 computed tomography angiography data, *Lab on a Chip*. 17 (2017) 2785–2792.  
1759 <https://doi.org/10.1039/c7lc00202e>.

1760 [236] P. Heo, S. Ramakrishnan, J. Coleman, J.E. Rothman, J.B. Fleury, F. Pincet, Highly  
1761 Reproducible Physiological Asymmetric Membrane with Freely Diffusing  
1762 Embedded Proteins in a 3D-Printed Microfluidic Setup, *Small*. 15 (2019) 1–13.  
1763 <https://doi.org/10.1002/smll.201900725>.

1764 [237] C.L. Manzanares Palenzuela, M. Pumera, (Bio)Analytical chemistry enabled by  
1765 3D printing: Sensors and biosensors, *TrAC - Trends in Analytical Chemistry*. 103  
1766 (2018) 110–118. <https://doi.org/10.1016/j.trac.2018.03.016>.

1767 [238] D.J. Wales, Q. Cao, K. Kastner, E. Karjalainen, G.N. Newton, V. Sans, 3D-Printable  
1768 Photochromic Molecular Materials for Reversible Information Storage, *Advanced  
1769 Materials*. 30 (2018) 1–7. <https://doi.org/10.1002/adma.201800159>.

- 1770 [239] A.K. Au, W. Lee, A. Folch, Mail-order microfluidics: Evaluation of  
1771 stereolithography for the production of microfluidic devices, *Lab on a Chip*. 14  
1772 (2014) 1294–1301. <https://doi.org/10.1039/c3lc51360b>.
- 1773 [240] A.I. Shallan, P. Smejkal, M. Corban, R.M. Guijt, M.C. Breadmore, Cost-effective  
1774 three-dimensional printing of visibly transparent microchips within minutes,  
1775 *Analytical Chemistry*. 86 (2014) 3124–3130. <https://doi.org/10.1021/ac4041857>.
- 1776 [241] H. Gong, M. Beauchamp, S. Perry, A. Woolley, G. Nordin, Optical Approach to  
1777 Resin Formulation for 3D Printed Microfluidics, *RSC Advances*. 5 (2015) 106621–  
1778 106632. <https://doi.org/10.1039/C5RA23855B>.
- 1779 [242] M.J. Beauchamp, H. Gong, A.T. Woolley, G.P. Nordin, 3D printed microfluidic  
1780 features using dose control in X, Y, and Z dimensions, *Micromachines (Basel)*. 9  
1781 (2018). <https://doi.org/10.3390/mi9070326>.
- 1782 [243] E.K. Parker, A. V. Nielsen, M.J. Beauchamp, H.M. Almughamsi, J.B. Nielsen, M.  
1783 Sonker, H. Gong, G.P. Nordin, A.T. Woolley, 3D printed microfluidic devices  
1784 with immunoaffinity monoliths for extraction of preterm birth biomarkers,  
1785 *Analytical and Bioanalytical Chemistry*. 411 (2019) 5405–5413.  
1786 <https://doi.org/10.1007/s00216-018-1440-9>.
- 1787 [244] M.J. Beauchamp, A. V. Nielsen, H. Gong, G.P. Nordin, A.T. Woolley, 3D Printed  
1788 Microfluidic Devices for Microchip Electrophoresis of Preterm Birth Biomarkers,  
1789 *Analytical Chemistry*. 91 (2019) 7418–7425.  
1790 <https://doi.org/10.1021/acs.analchem.9b01395>.
- 1791 [245] M.J. Männel, L. Selzer, R. Bernhardt, J. Thiele, Optimizing Process Parameters in  
1792 Commercial Micro-Stereolithography for Forming Emulsions and Polymer  
1793 Microparticles in Nonplanar Microfluidic Devices, *Advanced Materials*  
1794 *Technologies*. 4 (2019) 1–10. <https://doi.org/10.1002/admt.201800408>.
- 1795 [246] C. Yeung, S. Chen, B. King, H. Lin, K. King, F. Akhtar, G. Diaz, B. Wang, J. Zhu,  
1796 W. Sun, A. Khademhosseini, S. Emaminejad, A 3D-printed microfluidic-enabled

1797 hollow microneedle architecture for transdermal drug delivery, *Biomicrofluidics*.  
1798 13 (2019). <https://doi.org/10.1063/1.5127778>.

1799 [247] N. Bhattacharjee, C. Parra-Cabrera, Y.T. Kim, A.P. Kuo, A. Folch, Desktop-  
1800 Stereolithography 3D-Printing of a Poly(dimethylsiloxane)-Based Material with  
1801 Sylgard-184 Properties, *Advanced Materials*. 30 (2018) 1–7.  
1802 <https://doi.org/10.1002/adma.201800001>.

1803 [248] F. Kotz, P. Risch, D. Helmer, B.E. Rapp, Highly fluorinated methacrylates for  
1804 optical 3D printing of microfluidic devices, *Micromachines (Basel)*. 9 (2018).  
1805 <https://doi.org/10.3390/mi9030115>.

1806 [249] C.I. Rogers, K. Qaderi, A.T. Woolley, G.P. Nordin, 3D printed microfluidic  
1807 devices with integrated valves, *Biomicrofluidics*. 9 (2015) 1–9.  
1808 <https://doi.org/10.1063/1.4905840>.

1809 [250] H. Gong, A.T. Woolley, G.P. Nordin, High density 3D printed microfluidic  
1810 valves, pumps, and multiplexers, *Lab on a Chip*. 16 (2016) 2450–2458.  
1811 <https://doi.org/10.1039/c6lc00565a>.

1812 [251] J.L. Sanchez Noriega, N.A. Chartrand, J.C. Valdoz, C.G. Cribbs, D.A. Jacobs, D.  
1813 Poulson, M.S. Viglione, A.T. Woolley, P.M. van Ry, K.A. Christensen, G.P.  
1814 Nordin, Spatially and optically tailored 3D printing for highly miniaturized and  
1815 integrated microfluidics, *Nature Communications*. 12 (2021).  
1816 <https://doi.org/10.1038/s41467-021-25788-w>.

1817 [252] Y.S. Lee, N. Bhattacharjee, A. Folch, 3D-printed Quake-style microvalves and  
1818 micropumps, *Lab on a Chip*. 18 (2018) 1207–1214.  
1819 <https://doi.org/10.1039/c8lc00001h>.

1820 [253] S. Takenaga, B. Schneider, E. Erbay, M. Biselli, T. Schnitzler, M.J. Schöning, T.  
1821 Wagner, Fabrication of biocompatible lab-on-chip devices for biomedical  
1822 applications by means of a 3D-printing process, *Physica Status Solidi (A)*

1823 Applications and Materials Science. 212 (2015) 1347–1352.  
1824 <https://doi.org/10.1002/pssa.201532053>.

1825 [254] A.P. Kuo, N. Bhattacharjee, Y.S. Lee, K. Castro, Y.T. Kim, A. Folch, High-Precision  
1826 Stereolithography of Biomicrofluidic Devices, *Advanced Materials Technologies*.  
1827 1800395 (2019) 1–11. <https://doi.org/10.1002/admt.201800395>.

1828 [255] Z. Wang, N. Martin, D. Hini, B. Mills, K. Kim, Rapid fabrication of multilayer  
1829 microfluidic devices using the liquid crystal display-based stereolithography 3D  
1830 printing system, *3D Printing and Additive Manufacturing*. 4 (2017) 156–164.  
1831 <https://doi.org/10.1089/3dp.2017.0028>.

1832 [256] S. Zips, L. Hiendlmeier, L.J.K. Weiß, H. Url, T.F. Teshima, R. Schmid, M.  
1833 Eblenkamp, P. Mela, B. Wolfrum, Biocompatible, Flexible, and Oxygen-  
1834 Permeable Silicone-Hydrogel Material for Stereolithographic Printing of  
1835 Microfluidic Lab-On-A-Chip and Cell-Culture Devices, *ACS Applied Polymer*  
1836 *Materials*. (2020). <https://doi.org/10.1021/acsapm.0c01071>.

1837 [257] G. Gonzalez, A. Chiappone, K. Dietliker, C.F. Pirri, I. Roppolo, Fabrication and  
1838 Functionalization of 3D Printed Polydimethylsiloxane-Based Microfluidic  
1839 Devices Obtained through Digital Light Processing, *Advanced Materials*  
1840 *Technologies*. 5 (2020) 2000374. <https://doi.org/10.1002/admt.202000374>.

1841 [258] J. Berger, M.Y. Aydin, R. Stavins, J. Heredia, A. Mostafa, A. Ganguli, E. Valera, R.  
1842 Bashir, W.P. King, Portable Pathogen Diagnostics Using Microfluidic Cartridges  
1843 Made from Continuous Liquid Interface Production Additive Manufacturing,  
1844 *Analytical Chemistry*. 93 (2021) 10048–10055.  
1845 <https://doi.org/10.1021/acs.analchem.1c00654>.

1846 [259] Carbon3D, RPU 70, (2021). <https://www.carbon3d.com/materials/rpu-70/>  
1847 (accessed August 21, 2021).

- 1848 [260] W. Wu, A. Deconinck, J.A. Lewis, Omnidirectional printing of 3D microvascular  
1849 networks, *Advanced Materials*. 23 (2011) 178–183.  
1850 <https://doi.org/10.1002/adma.201004625>.
- 1851 [261] K.S. Lim, J.H. Galarraga, X. Cui, G.C.J. Lindberg, J.A. Burdick, T.B.F. Woodfield,  
1852 Fundamentals and Applications of Photo-Cross-Linking in Bioprinting, *Chemical*  
1853 *Reviews*. (2020). <https://doi.org/10.1021/acs.chemrev.9b00812>.
- 1854 [262] J.Y. Lee, J. An, C.K. Chua, Fundamentals and applications of 3D printing for novel  
1855 materials, *Applied Materials Today*. 7 (2017) 120–133.  
1856 <https://doi.org/10.1016/j.apmt.2017.02.004>.
- 1857 [263] M. Layani, X. Wang, S. Magdassi, Novel Materials for 3D Printing by  
1858 Photopolymerization, *Advanced Materials*. 30 (2018) 1–7.  
1859 <https://doi.org/10.1002/adma.201706344>.
- 1860 [264] L.S. Andrews, J.J. Clary, Review of the toxicity of multifunctional acrylates,  
1861 *Journal of Toxicology and Environmental Health*. (1986).  
1862 <https://doi.org/10.1080/15287398609530916>.
- 1863 [265] F. Zhu, J. Skommer, T. Friedrich, J. Kaslin, D. Wlodkovic, 3D printed polymers  
1864 toxicity profiling: A caution for biodevice applications, in: *SPIE Micro+Nano*  
1865 *Materials, Devices, and Applications Symposium*, Sidney, Australia, n.d.  
1866 <https://doi.org/10.1117/12.2202392>.
- 1867 [266] R. Zhang, N.B. Larsen, Stereolithographic hydrogel printing of 3D culture chips  
1868 with biofunctionalized complex 3D perfusion networks, *Lab on a Chip*. 17 (2017)  
1869 4273–4282. <https://doi.org/10.1039/c7lc00926g>.
- 1870 [267] A.D. Benjamin, R. Abbasi, M. Owens, R.J. Olsen, D.J. Walsh, T.B. Lefevre, J.N.  
1871 Wilking, Light-based 3D printing of hydrogels with high-resolution channels,  
1872 *Biomedical Physics and Engineering Express*. (2019).  
1873 <https://doi.org/10.1088/2057-1976/aad667>.

- 1874 [268] A.A. Pawar, G. Saada, I. Cooperstein, L. Larush, J.A. Jackman, S.R. Tabaei, N.J.  
1875 Cho, S. Magdassi, High-performance 3D printing of hydrogels by water-  
1876 dispersible photoinitiator nanoparticles, *Science Advances*. 2 (2016).  
1877 <https://doi.org/10.1126/sciadv.1501381>.
- 1878 [269] J.F. Xing, M.L. Zheng, X.M. Duan, Two-photon polymerization microfabrication  
1879 of hydrogels: an advanced 3D printing technology for tissue engineering and  
1880 drug delivery, *Chemical Society Reviews*. (2015).  
1881 <https://doi.org/10.1039/c5cs00278h>.
- 1882 [270] Y. Zhang, D. An, Y. Pardo, A. Chiu, W. Song, Q. Liu, F. Zhou, S.P. McDonough,  
1883 M. Ma, High-water-content and resilient PEG-containing hydrogels with low  
1884 fibrotic response, *Acta Biomaterialia*. 53 (2017) 100–108.  
1885 <https://doi.org/10.1016/j.actbio.2017.02.028>.
- 1886 [271] Y.S. Kim, K. Cho, H.J. Lee, S. Chang, H. Lee, J.H. Kim, W.G. Koh, Highly  
1887 conductive and hydrated PEG-based hydrogels for the potential application of a  
1888 tissue engineering scaffold, *Reactive and Functional Polymers*. 109 (2016) 15–22.  
1889 <https://doi.org/10.1016/j.reactfunctpolym.2016.09.003>.
- 1890 [272] C.M. González-Henríquez, F.E. Rodríguez-Umanzor, J. Almagro-Correa, M.A.  
1891 Sarabia-Vallejos, E. Martínez-Campos, M. Esteban-Lucía, A. del Campo-García, J.  
1892 Rodríguez-Hernández, Biocompatible fluorinated wrinkled hydrogel films with  
1893 antimicrobial activity, *Materials Science and Engineering C*. 114 (2020) 111031.  
1894 <https://doi.org/10.1016/j.msec.2020.111031>.
- 1895 [273] M.J. Männel, C. Fischer, J. Thiele, A Non-Cytotoxic Resin for Micro-  
1896 Stereolithography for Cell Cultures of HUVECs., *Micromachines* (Basel). 11  
1897 (2020). <https://doi.org/10.3390/mi11030246>.
- 1898 [274] C. Warr, J.C. Valdoz, B.P. Bickham, C.J. Knight, N.A. Franks, N. Chartrand, P.M.  
1899 Van Ry, K.A. Christensen, G.P. Nordin, A.D. Cook, Biocompatible PEGDA Resin

1900 for 3D Printing, ACS Applied Bio Materials. 3 (2020) 2239–2244.  
1901 <https://doi.org/10.1021/acsabm.0c00055>.

1902 [275] MicronInc, FDA Approved 3D Printer Resins, (2017).  
1903 [https://www.microndental.com/regulatory/fda-approved-cleared-3d-printer-](https://www.microndental.com/regulatory/fda-approved-cleared-3d-printer-resins)  
1904 [resins](https://www.microndental.com/regulatory/fda-approved-cleared-3d-printer-resins) (accessed October 30, 2019).

1905 [276] K. Piironen, M. Haapala, V. Talman, P. Järvinen, T. Sikanen, Cell adhesion and  
1906 proliferation on common 3D printing materials used in stereolithography of  
1907 microfluidic devices, Lab on a Chip. 20 (2020) 2372–2382.  
1908 <https://doi.org/10.1039/d0lc00114g>.

1909 [277] S. Kreß, R. Schaller-Ammann, J. Feiel, J. Priedl, C. Kasper, D. Egger, 3D printing  
1910 of cell culture devices: Assessment and prevention of the cytotoxicity of  
1911 photopolymers for stereolithography, Materials. 13 (2020).  
1912 <https://doi.org/10.3390/ma13133011>.

1913 [278] R.P. Rimington, A.J. Capel, D.J. Player, R.J. Bibb, S.D.R. Christie, M.P. Lewis,  
1914 Feasibility and Biocompatibility of 3D-Printed Photopolymerized and Laser  
1915 Sintered Polymers for Neuronal , Myogenic , and Hepatic Cell Types,  
1916 Macromolecular Bioscience. 1800113 (2018) 1–12.  
1917 <https://doi.org/10.1002/mabi.201800113>.

1918 [279] M. Schuster, C. Turecek, B. Kaiser, J. Stampfl, R. Liska, F. Varga, Evaluation of  
1919 biocompatible photopolymers I: Photoreactivity and mechanical properties of  
1920 reactive diluents, Journal of Macromolecular Science, Part A: Pure and Applied  
1921 Chemistry. 44 (2007) 547–557. <https://doi.org/10.1080/10601320701235958>.

1922 [280] C. Warr, J.C. Valdoz, B.P. Bickham, C.J. Knight, N.A. Franks, N. Chartrand, P.M.  
1923 Van Ry, K.A. Christensen, G.P. Nordin, A.D. Cook, Biocompatible PEGDA Resin  
1924 for 3D Printing, ACS Applied Bio Materials. 3 (2020) 2239–2244.  
1925 <https://doi.org/10.1021/acsabm.0c00055>.

- 1926 [281] Y. Zhang, Post-3D printing modification for improved biomedical applications,  
1927 International Journal of Bioprinting. 3 (2017).  
1928 <https://doi.org/10.18063/ijb.2017.02.001>.
- 1929 [282] G. Gonzalez, D. Baruffaldi, C. Martinengo, A. Angelini, A. Chiappone, I. Roppolo,  
1930 F.C. Pirri, F. Frascella, Materials Testing for the Development of Biocompatible  
1931 Devices through Vat-Polymerization 3D Printing, Nanomaterials. 10 (2020) 1788.  
1932 <https://doi.org/10.3390/nano10091788>.
- 1933 [283] X. Wang, X. Cai, Q. Guo, T. Zhang, B. Kobe, J. Yang, I3DP, a robust 3D printing  
1934 approach enabling genetic post-printing surface modification, Chemical  
1935 Communications. 49 (2013) 10064–10066. <https://doi.org/10.1039/c3cc45817b>.
- 1936 [284] A. Chiadò, G. Palmara, A. Chiappone, C. Tanzanu, C.F. Pirri, I. Roppolo, F.  
1937 Frascella, A modular 3D printed lab-on-a-chip for early cancer detection, Lab on  
1938 a Chip. 20 (2020) 665–674. <https://doi.org/10.1039/c9lc01108k>.
- 1939 [285] J.A. Calvo-Haro, J. Pascau, J.M. Asencio-Pascual, F. Calvo-Manuel, M.J. Cancho-  
1940 Gil, J.F. Del Cañizo López, M. Fanjul-Gómez, R. García-Leal, G. González-  
1941 Casaurrán, M. González-Leyte, J.A. León-Luis, L. Mediavilla-Santos, S.  
1942 Ochandiano-Caicoya, R. Pérez-Caballero, A. Ribed-Sánchez, J. Río-Gómez, E.  
1943 Sánchez-Pérez, J. Serrano-Andreu, M. Tousidonis-Rial, J. Vaquero-Martín, S.  
1944 García San José, R. Perez-Mañanes, Point-of-care manufacturing: a single  
1945 university hospital's initial experience, 3D Printing in Medicine. 7 (2021) 1–14.  
1946 <https://doi.org/10.1186/s41205-021-00101-z>.
- 1947 [286] H.N. Chan, M.J.A. Tan, H. Wu, Point-of-care testing: Applications of 3D printing,  
1948 Lab on a Chip. 17 (2017) 2713–2739. <https://doi.org/10.1039/c7lc00397h>.
- 1949 [287] D. Wang, H.N. Chan, Z. Liu, S. Micheal, L. Li, D.B. Baniani, M.J.A. Tan, L. Huang,  
1950 J. Wang, H. Wu, Recent Developments in Microfluidic -Based Point-of-care  
1951 Testing (POCT ) Diagnoses, 2020. <https://doi.org/10.1002/9783527818341.ch8>.

- 1952 [288] C. Tzivelekis, P. Sgardelis, K. Waldron, R. Whalley, D. Huo, K. Dalgarno,  
1953 Fabrication routes via projection stereolithography for 3D-printing of  
1954 microfluidic geometries for nucleic acid amplification, PLoS ONE. 15 (2020) 1–21.  
1955 <https://doi.org/10.1371/journal.pone.0240237>.
- 1956 [289] K. Kadimisetty, J. Song, A.M. Doto, Y. Hwang, J. Peng, M.G. Mauk, F.D.  
1957 Bushman, R. Gross, J.N. Jarvis, C. Liu, Fully 3D printed integrated reactor array  
1958 for point-of-care molecular diagnostics, Biosensors and Bioelectronics. 109 (2018)  
1959 156–163. <https://doi.org/10.1016/j.bios.2018.03.009>.
- 1960